Precisely Engineered Protein-Based PRINT® Particles for Delivery of Nucleic Acids

Jing Xu

A dissertation submitted to the faculty of the University of North Carolina at Chapel Hill in partial fulfillment of the requirements for the degree of Doctor of Philosophy in the Department of Chemistry

Chapel Hill
2012

Approved by

Joseph M. DeSimone

Valerie Ashby

Maurice Brookhart

Samuel Lai

Michael Rubinstein

Abstract

JING XU: Precisely Engineered Protein-Based PRINT® Particles for Delivery of Nucleic Acids
(Under the direction of Professor Joseph M. DeSimone)

RNA replicon (self-replicating RNA) has long been regarded as an important form of vaccines due to its remarkable immunogenicity and superior safety features. In this study, we report the first non-viral delivery of RNA replicons using protein-based PRINT particles. Cylindrical bovine serum albumin (BSA) particles (diameter (*d*) 1 μm, height (*h*) 1 μm) fabricated utilizing PRINT® technology were rendered transiently insoluble using a novel, reductively labile disulfide-based cross-linker. After being cross-linked, the protein particles retain their integrity in aqueous solution and dissolve preferentially under a reducing environment which is found in cytoplasm, the site of action for RNA replicons. Our data reveal that the cross-linker leaves no chemical residue on the amino group it reacts with after being cleaved, which represents a great advantage over traditionally used protein cross-linkers. The particles were loaded with RNA replicons encoding several different proteins including Chloramphenicol Acetyl Transferase (CAT), green fluorescent protein (GFP) and Luciferase protein. The PRINT process used to fabricate protein-based particles in this study is gentle and avoids the obvious degradation of RNA replicons. The disulfide cross-linker is RNA-friendly and can stabilize the particles without affecting the biological

performance of RNA replicons. Delivery of the particles to Vero cells was achieved by coating particles with a TransIT®-mRNA transfection reagent (TransIT) and cationic lipids (DOTAP and DOPE). Our data suggest that: 1) it is necessary to use a degradable cross-linker for successful delivery of RNA replicon via albumin-based PRINT particles and 2) this may be a promising system for delivery of RNA replicon-based vaccines.

ACKNOWLEDGEMENTS

First, I would like to express my deepest gratitude to my advisor Prof. Joseph DeSimone who took me into this unique research group where I grew tremendously both as a scientist and as a person. He offered me precious opportunities to work on projects with great significances and taught me how to move forward in accomplishing scientific goals while keeping the big picture in mind. Thank you for continued support and guidance throughout the years.

I would like to express my appreciation to those individuals who made significant contributions to this work: Dr. Mary Napier for all the scientific discussions, numerous help, support and encouragement; Dr. J. Christopher Luft, and Dr. Shaomin Tian for *in vitro* and *in vivo* work and being great support; Dr. Jin Wang for all the work he has done and all the help he offered me; Dr. Robert K. Pinschmidt, Jr. and Stuart Dunn for innumerable scientific discussions over the years; Dr. Benjamin W. Mayor, Dr. Gary Owen, Dr. Peter Berglund and Dr. Jonathan Smith for the generous help in particle fabrication, RNA replicon preparation and all the scientific discussions; Dr. Matthew C. Parrott and Dr. Stephanie E. A. Gratton for the training in organic synthesis and particle fabrication.

Many thanks go out to all the DeSimone group members, past and present. It was impossible to get any work done without everyone's effort to keep the lab running smoothly and efficiently. Special thanks go to Vicki Haithcock,

Crista Farrell, Dr. Ashish Pandya, Dr. Hanjun Zhang, Dr. Elizabeth Enlow, Dr. Yapei Wang, Dr. Timothy Merkel, Dr. Jieyu Wang, Dr. Warefta Hasan, Dr. Steve Blake, Dr. Kevin P. Herlihy, Dr. Christine Conwell, Kai Chen, Tammy Shen, Katie Moga, Dr. Charlie Bowerman, John Fain, Marc Kai, Kevin Chu, James Byrne, Dr. Adrian O'Neill and Luke Roode. Also I would like to thank Amar Kumbhar, Dr. Carrie Donley and Wallace Ambrose from UNC-CHANL for their assistance.

I would like to thank my family and friends especially my uncles Chuancai Xu and Chuanhe Xu, my sister Yan Xu, my brother-in-law Qiang Li, my brother Jibin Xu, and my dear nephew Hexuan Li (son of Yan and Qiang). Lastly and most importantly, I owe everything to my parents Chuanfa Xu and Xiaofeng Dai who have been supporting me throughout all my endeavors.

TABLE OF CONTENTS

LIST OF TABLES

LIST OF ILLUSTRATIONS

LIST OF ABREVIATIONS

APC — antigen presenting cell

BD — biodistribution

BSA — bovine serum albumin

CAT — chloramphenicol acetyl transferase

cBSA —Cationized BSA

CPP — Cell penetrating peptides

CTL — cytotoxic lymphocyte

DIC — dithio-bis(ethyl 1 H-imidazole-1-carboxylate)

DLS — dynamic light scattering

DOPE — 1,2-dioleoyl-sn-glycero-3-phosphoethanolamine

DOTAP — N-[1-(2,3-dioleoloxy)propyl]-N,N,N-trimethyl ammonium chloride

DOTMA — 1,2-di-O-octadecenyl-3-trimethylammonium propane

DSP — dithiobis[succinimidyl propionate]

DTT — dithiothreitol

EDC — 1-Ethyl-3-(3-dimethylaminopropyl)carbodiimide

ELISA — enzyme-linked immunosorbent assays

EtOAc — ethyl acetate

FBS — fetal bovine serum

GFP — green fluorescence protein

GMP — good manufacturing practice

GRAS — generally regarded as safe

GSH — reduced glutathione

LBL — layer-by-layer

MEM — Minimum Essential Medium

NHS — N-hydroxysuccinimide

OEDIC — 2,2'-oxybis(ethane-2,1-diyl) bis(1H-imidazole-1-carboxylate)

PBS — phosphate buffer saline

PDMS — poly(dimethyl siloxane)

PEI — poly (ethylene imine)

PET — polyethylene terephthatlate

PFPE — perfulorinated polyether

pI — Iso-electric point

PK — pharmacokinetics

PLGA — poly(lactic-co-glycolic acid)

PLL — poly(L-lysine)

PLLA — poly(lactic acid)

PRINT — Particle Replication In Non-wetting Templates

RES — reticuloendothelial system

SEM — scanning electron microscope

TEM — transmission electron microscopy

TGA — Thermal Gravimetric Analysis

TLC — thin layer chromatography

TransIT —TransIT®-mRNA transfection reagent

VRP — viral replicon particl

CHAPTER 1

INTRODUCTION TO RNA REPLICON AS NUCLEIC ACID VACCINE AND PRINT® AS A PLATFORM TECHNOLOGY FOR DRUG DELIVERY

1.1 RNA replicon: Nucleic Acid-Based Vaccine

At the end of eighteenth century, Edward Jenner showed that inoculation with cowpox can protect against smallpox, the “speckle monster” which, at that time, was the cause of 400,000 deaths per year in Europe.[1] This discovery has saved millions of lives and initiated vaccine development as one of the central topics in modern biomedical research. Vaccination is the way to prepare the immune system against potential attackers such as viruses and bacteria by giving it a “simulation of battle conditions” without exposing the vaccinated individual to real infections. Vaccines have been extremely useful in fighting a variety of viral and bacterial infectious diseases since its first discovery and the scientific advances in this field during the last two centuries have significantly contributed to increased human life expectancy.

1.1.1 Evolution of vaccines

1.1.1.1 Attenuated pathogens for vaccines

The initial effort for vaccine development is based on attenuated (live) or, inactivated (killed) pathogens. It was found that by growing pathogens in a cell type that is not its normal host, the pathogen would become weakened or

attenuated and this strategy results in pathogens that are still infectious but too weak to cause diseases. The vaccines currently used to protect against many diseases such as measles, mumps and rubella are in the form of attenuated pathogens.[2] Attenuated vaccines are very effective to trigger both humoral and cell-mediated immune responses due to the ability of the weakened pathogens to infect antigen presenting cells (APC) and stimulate the production of cytotoxic lymphocytes (CTLs) and memory killer T cells before the immune system eliminates the weakened potential attacker. The CTL memory will protect the vaccinated individual from future attacks against the real infections, in most cases, for a long time.

Although very efficient, however, attenuated pathogens as vaccines are inevitably accompanied by safety concerns. One safety concern is that the vaccinated individual may generate enough pathogens and spread it to people with weakened immune systems and cause harmful consequences. In addition, the attenuated pathogens may revert to their infectious forms and cause diseases in the vaccinated individual.

1.1.1.2 Killed pathogens for vaccines

Under these concerns, the vaccines based on killed pathogens which are inactivated through chemical, heat or radioactivity treatment have the advantages of being much safer than live, attenuated vaccines.[3] Since the vaccines in the form of inactivated viruses or bacteria bear the full spectrum of antigens of pathogens, they may effectively trigger the generation of memory helper T and B cells which will provide sufficient protection against the attack from many

pathogens. For example, vaccines against Salk polio and Japanese Encephalitis viruses in the inactivated pathogen forms are in wide use. In addition, in the case of influenza vaccines, the killed pathogens are easier to prepare in a time efficient way and are more widely used than live attenuated vaccines. For example, during the avian flu epidemic in 2005 and H1N1 epidemic in 2009, when there was a need to prepare vaccines in a short time for worldwide use, the inactivated vaccine was chosen as the best alternative.[4] However, the killed pathogens are less effective in triggering immune responses compared to their attenuated counterparts because they are not capable of replicating in the host and are thus quickly cleared from the body without stimulating production of CTLs. It is believed by many immunologists that to be effective, vaccines against many diseases must generate CTLs and memory killer T cells.[5]

1.1.1.3 Subunit vaccines

Vaccines have also been prepared by using only certain parts of a pathogen or isolated viral proteins. The idea is to retain the parts for the immune system needs to see to adopt protection against the real infections. And in the case of bacterial, the disease-causing toxins secreted by some bacteria have been used for generating effective vaccines. For subunit vaccines, there is no possibility of causing infection with the pathogen itself and safety is an apparent advantage. In addition, recent advances in genetic engineering can produce proteins used as antigens in large quantities and in pure forms and have opened up new opportunities for subunit vaccine development. However, there are a number of drawbacks, including low efficacy and short-term immunity because

the injected protein is quickly consumed in the immunogenic process and does not activate immune responses in a broad and robust manner. Frequently, an adjuvant is formulated together with the protein to increase the immune response by releasing the antigen over a longer period of time or eliciting inflammation that enhances antigen uptake and presentation by APCs. There have been many efforts to further improve the immune responses of the vaccines in the subunit forms by developing micro or nano particles for antigen delivery. The hypothesis behind is that APCs have evolved to effectively take up and process antigens bearing similar dimensions to pathogens, ranging from sub- 100 nm to microns.[6,7] So antigens in particulate forms have the potential to achieve enhanced uptake, processing and presentation by APCs.

1.1.1.4 Nucleic acid-based vaccination

A main challenge for vaccine development is to design and produce vaccines that are safe but also induce long-lasting and robust immune responses in both humoral and cellular branches. About two decades ago, immunologists found that injection of naked DNA containing a flu virus gene into muscles of mice, without any associated lipid, protein or carbohydrate, elicited production of memory killer T cells against an influenza infection.[8,9] The unexpected success was attributed to the gene being taken up by APCs which then generated the flu protein, processed the protein and activated CTLs. This result has initiated a whole new scientific field and has been regarded as one of the most important discoveries in the history of vaccinology by some scientists.

Nucleic acids offer a unique opportunity for vaccination and have emerged as excellent candidates for the treatment of cancers and infectious diseases.[10] Compared with traditional protein-based vaccination strategy, direct immunization with RNA or DNA has the advantages of the simplicity and purity with which they can be produced, as well as coding for only protein(s) of interest (i.e. an antigen) at high levels in a reproducible manner, potentially triggering strong immune response by producing CTLs and memory killer T cells. And because such vaccines only include part of the pathogen's total genes, this method will not cause real infections. The advancements in genetic engineering and molecular virology have made it possible to create genes that would not otherwise be found in biological organisms and the gene sequences can be added or subtracted to improve the immunogenicity of an antigen. To date, several DNA vaccine products have been approved by FDA in the area of veterinary medicine.

However, nucleic acid-based vaccines in the form of messenger RNA or plasmid DNA tested to date have had limited efficacy in humans, largely due to their inability to produce high dosages of antigen and for the duration required to trigger strong, durable immune responses. [11,12] To resolve the low efficacy issues of nucleic acid vaccines is currently the focus of many research groups and the potential resolution includes use of novel formulations, immune plasmid adjuvants and delivery systems to enhance immunogenicity etc.[13] The use of replicative RNA is one of the strategies under investigation.[12]

1.1.2 RNA replicon for vaccine applications

1.1.2.1 Introduction to RNA replicons

RNA replicon, also termed self-replicating RNA, is an important form of nucleic acid-based vaccines and is derived from either positive- or negative-strand RNA viruses such as Semliki Forest virus and Kunjin virus.[14] The RNA replicons can be produced in large quantities by *in vitro* transcription and capping using a variety of DNA templates. From these viruses, the gene sequences encoding structural proteins are replaced by mRNA encoding antigens of interest as well as the RNA polymerase for RNA replicon replication and transcription. RNA replicons can be regarded as “disabled” virus vectors that are capable of amplifying within the cytoplasm of host cells for a prolonged period but are unable to produce infectious progeny. Cells transfected with conventional RNA vaccines express widely varying amounts of antigen, due to the number of gene copies picked up by the cell. RNA replicon has the advantage of being able to generate large quantities of antigens with a single piece of the gene being introduced into the cell. Compared with DNA vaccines, which is also under active investigation, RNA replicon has several advantages: Firstly, RNA replicon is capable of replicating in the cytoplasm of host cells, thus avoiding the requirement of nucleus entry which represents a daunting hurdle in DNA delivery.[15] By eliminating the dependence on cellular transcription machinery and transport of nucleic acids to and from the nucleus, RNA replicon is potentially a more efficient form of nucleic acid vaccine.[16] Secondly, RNA replicon has superior biosafety features, which is crucial for vaccine purposes. Compared with DNA, RNA replicon can avoid the potential integration into the genome of host

cells and also prevent generation of anti-DNA antibodies, both of which may affect the host cell's gene expression in an uncontrollable manner and thus represent incalculable risks.[17] Also, RNA is self-adjuvanting. Diebold S. S. reported that single-stranded RNAs including both mouse mRNA and a wide range of synthetic RNAs can innate immune responses through TLR7-mediated recognition.[18] RNA replicon combines the safety characteristics of inactivated vaccines with the superior immunogenicity of live, attenuated vaccines and has the potential to trigger effective immune responses against a variety of diseases.

1.1.2.2 Initiation of immune response development

An immune response is primarily launched by dendritic cells (DCs), a specialized bone marrow (BM)-derived APC. DC as the most important APC can potentially capture antigens generated by RNA replicon through three routes:[19] Firstly, DC can capture soluble antigens secreted or released by transfected host cells. Secondly, DC can be directly infected with RNA replicons and immune response will be induced when the antigens encoded are endogenously processed by mature DCs. Thirdly, DC can take up the cells that have been killed or injured due to transfection of RNA replicons. The third route has been the focus of research investigation on the immunogenicity of RNA replicons.

RNA replicon vaccines can employ the host cells' machinery to replicate and encode desired antigens. Most research investigating initiation of immune responses by replicon vaccines has focused on two virus families: 1) alphaviruses, such as Semliki Forest virus and Sindbis virus; and 2) flaviviruses, such as Kunjin viruses and Yellow Fever viruses.[20] There is a major distinction in

their cytopathic nature between RNA replicons derived from these two families of viruses. Alphavirus-derived replicons are generally cytopathic and the “self-replicating” activity of these replicons can induce caspase-dependent apoptosis of transfected cells.[21] Flavivirus-derived replicons are generally non-cytopathic and the RNA replicon can maintain in high copy numbers in the cytoplasm of transfected cells without interfering with normal cellular functions.[22] In one regard, the non-cytopathic RNA replicons have the advantage of being able to produce antigens for prolonged periods of time, a feature that has been proved to be important in inducing effective immune responses. At the same time, cell damage or death triggered by replication of cytopathic RNA replicons can function as “danger signals” and effectively activate DCs and facilitate uptake of injured or killed cells by DCs, potentially enhancing immunogenicity.[19] Comparison of these two types of RNA replicon have been conducted and the influence of cytopathicity on the immunogenicity still remains controversial. Two groups used the anti-apoptotic molecule Bcl-X_L in alphavirus replicon plasmid vaccines to delay the apoptosis of transfected cells and compared the immunogenicity with and without Bcl-X_L. In one study, the immunogenicity of the plasmid vaccine was improved by prolonged survival of transfected cells,[23] while in another study the efficacy of alphaviral replicase-based vaccine was reduced by Bcl-X_L.[24] Racanelli V. et al. compared the immunity stimulated by DCs transfected with cytopathic and non-cytopathic RNA replicons and found that induction of cell death increased the DC-associated antigen.[22] Tannis L. L. et al. compared the cellular and humoral immunities elicited by RNA replicon based on

Semliki Forest virus (cytopathic) vs. Kunjin virus (non-cytopathic) RNA replicons and found that the two replicon systems elicited similar cellular responses while Semliki Forest virus elicited greater humoral responses.[20] Currently it still remains to be determined which RNA replicon system has more advantages for vaccine purposes and this may be an important factor to consider when designing RNA replicon-based vaccines.

1.1.3 Current approaches to administer RNA replicon

The initial effort to use RNA replicon for vaccination is based on their naked forms and *in vivo* immunity has been achieved in mice through direct intramuscular injection.[25] However, there are several drawbacks associated with this approach including the general liability of single strand RNA replicons and relatively low delivery efficiency without the protein coatings that protect the viral genome from degradation and facilitate entry into the host cell.

One solution is to administer RNA replicon in a DNA-layered form.[14] This approach resembles conventional DNA vaccines, but this DNA is transcribed in the nucleus into RNA replicon which is then exported from the nucleus and translated into polyproteins leading to the synthesis of RNA replicase and replication of RNA replicon. The DNA-layered form of RNA replicon can achieve high antigen expression due to the RNA replication but similar to conventional DNA vaccines, this process requires nucleus entry and is accompanied by a series of safety concerns such as the potential integration into the genome of host cells.

Another solution is to wrap the RNA replicon with viral replicon particles (VRP).[14, 26] A helper RNA encoding structural proteins is introduced into cells along with the RNA replicon encoding the antigen (Figure 1.1). The replicase generated by antigen RNA replicon catalyzes the replication of both the antigen RNA and helper RNA. The structural proteins expressed by the helper RNA can package the antigen RNA (not the helper RNA) into VRPs which are then released from the cell. The practical utility of this approach, however, is limited by cost-effectiveness and large-scale manufacturing considerations. In addition, the production has to be monitored to avoid RNA recombination and generation of propagation-competent RNA genomes which may cause adverse health effects.[27] A broadly applicable, scalable and cell-free vaccine fabrication platform for RNA replicon has the opportunity to fundamentally transform vaccine development.

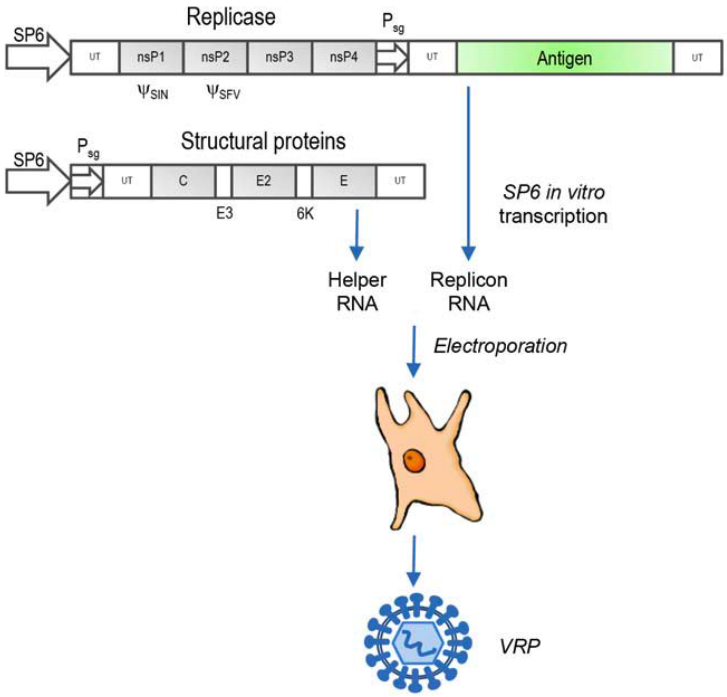

Figure 1.1 Generation of viral replicon particles (VRP). The replicon RNA

encodes for the foreign antigen (green) and the viral non-structural proteins nsP1- nsP4 that form the active viral replicase. Upon introduction of RNA replicon into the cell, RNA polymerase is generated and catalyzes the replication of both replicon and helper RNA as well as transcription from the subgenomic promoters (Psg). The helper RNA encodes for the three main structural proteins C, E2, and E1 and two minor proteins E3 and 6K. After viral structural proteins are expressed, the replicon RNA (but not the helper RNA) is packaged into VRPs which are released from the cell. UT, untranslated region. ψ_{SIN}, ψ_{SFV}, packaging signals of Sindbis virus and SFV, respectively. Adapted from [14].

1.2 PRINT: A Platform Technology for Drug Delivery

1.2.1 What is drug delivery

Conventionally, drugs are administered in forms of pills, eye drops, ointments, and solutions injected intramuscularly, subcutaneously, intranasally or intravenously.[28] Over the past few decades, there is a growing effort to address the problems associated with conventional forms of drugs such as low efficacy or harmful side effects with drug delivery systems. One approach is to take existing drugs and improve their biodistribution (BD, where the drug travels in the body) and pharmacokinetics (PK, the fate of the drug in the body), the major factors that directly affect the efficacy of the drug treatment.[29] One example that belongs to this category is chemotherapies which reach all tissues in the body and adversely affect healthy cells. This undesirable effect requires that patients be administered with the tolerable, lower-than-optimal amount of drugs, significantly reducing the effectiveness of the treatment. Another approach is to seek new therapeutics which are more effective in treating diseases or less harmful for the healthy tissues but rely more on drug delivery systems to be effective. This is

common for drugs with very poor solubility or biopharmaceuticals that may be unstable and degraded by the body such as RNA and peptides.

For the aforementioned reasons, numerous drug delivery carriers have been designed in different forms such as colloidal particles, patches, sutures and dressings etc. The mostly studied colloidal particles, for example, have been developed based on different techniques such as polymer particles,[30] liposomes,[31] micelles,[32] layer-by-layer (LBL) capsules[33] and dendrimers[34]. The advantages of using particles as drug delivery system include: 1) cargos can be incorporated into the particles and be protected from degradation or passive release into non-targeted tissues during the transportation in the body, 2) particles sizes and surface characteristics of particles can be designed to achieve biodistribution and targeting to specific tissues of treatment, as well as cellular internalization for drugs delivered intracellularly, 3) the controlled release of drug can be modulated to achieve the best efficacy, 4) the system can be administered through various routes including oral, nasal, parenteral, etc.

1.2.2 Introduction to PRINT

PRINT® (Particle Replication In Non-wetting Templates) is a platform technology that is an off-shoot of soft lithography that enables the molding of micro- and nano-particles having precisely controlled size, shape, chemical composition and surface functionality for broad applications in life sciences and material sciences.

PRINT was first developed in DeSimone group at University of North Carolina in Chapel Hill in 2005.[35] Silicon wafers patterned with different features

are fabricated using standard photolithographic techniques and used as masters in PRINT process. A photocurable perfulorinated polyether (PFPE) liquid polymer which has been trademarked Fluorocur® by Liquidia Technologies can completely wet the silicon wafer with micro- and nano-sized patterns due to its extremely low surface energy and can subsequently be photocured to form PFPE elastomer mold (Figure 1.2). The PFPE-based PRINT mold has extremely low surface energy, high gas permeability, high solvent resistance, high elastic recovery and good mechanical strength. This material demonstrated superior performance to poly(dimethyl siloxane) (PDMS), the most commonly used elastomer for the fabrication of microfluidic devices and its unique properties translate into a top-down approach of soft lithography that offers an engineering way to produce isolated micro- and nano-particles. The mold can now be manufactured on roll-to-roll machines and provided by Liquidia Technologies in 1000 ft rolls.

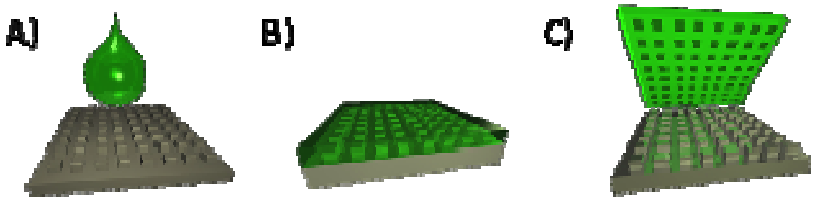

Figure 1.2 The PRINT mold fabrication. (A) Fluorocur (green) is poured onto a silicon wafer template (grey), (B) The Fluorocur completely wets the surface of the template and is then photochemically cured, (C) The mold is removed from the template and shows the inversed features of the template.

A typical PRINT process is schematically illustrated in Figure 1.3. Following generation of a PFPE mold (green) from the master template (grey), a liquid substance (red) is filled into the cavities with assistance from a piece of

high energy polyethylene terephthatlate (PET) and a roller applying pressure to the mold. The low surface energy of the PRINT mold enables the liquid to fill the cavities through capillary filling, but without wetting the landing area between the cavities and the excess liquid substance will adhere to the high energy PET. In this step, if a PDMS mold which has higher surface energy than PFPE, a flash layer of the liquid connecting the cavities which is termed “scum layer” will be formed and no isolated particles can be generated.[36] Once the liquid in the PFPE mold cavities is converted to a solid through photocuring, temperature change, solvent evaporation, etc., the array of particles (red) can be removed from the mold by bringing the mold in contact with an adhesive layer (yellow). The particles can now be easily freed from the surface by mechanical force or dissolving the adhesive layer.

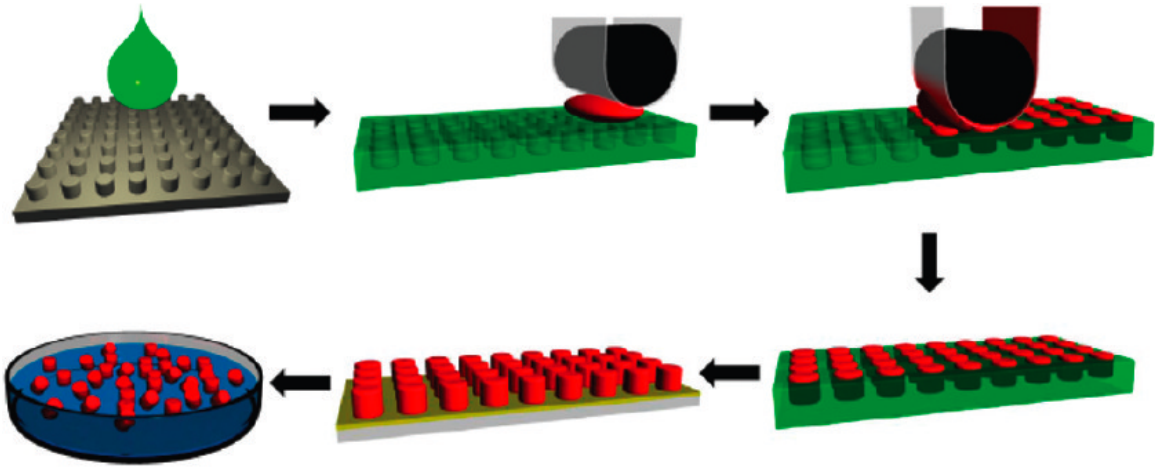

Figure 1.3 The PRINT particle fabrication process.

1.2.3 Control over all aspects of particle fabrication

1.2.3.1 Control over size and shape

To date, precise template fabrication has been achieved in electronics

industry due to the advancements in standard lithography and the PRINT process takes full advantage this state of the art technology to make uniform particles of unlimited sizes and shapes. The PRINT ensures replication of identical template features to afford particles that are truly monodisperse. PRINT allows for the precise control over particles size down to sub ~100 nm and PRINT mold with a 50 nm × 60 nm cylindrical feature can now be obtained from Liquidia Technologies. Shape features can be controlled through the choice of a template and geometries of particles such as spheres, cylinders, discs and toroids with different aspect ratios can be precisely defined. Figure 1.4 shows a selection of particles which have been fabricated using the PRINT process.

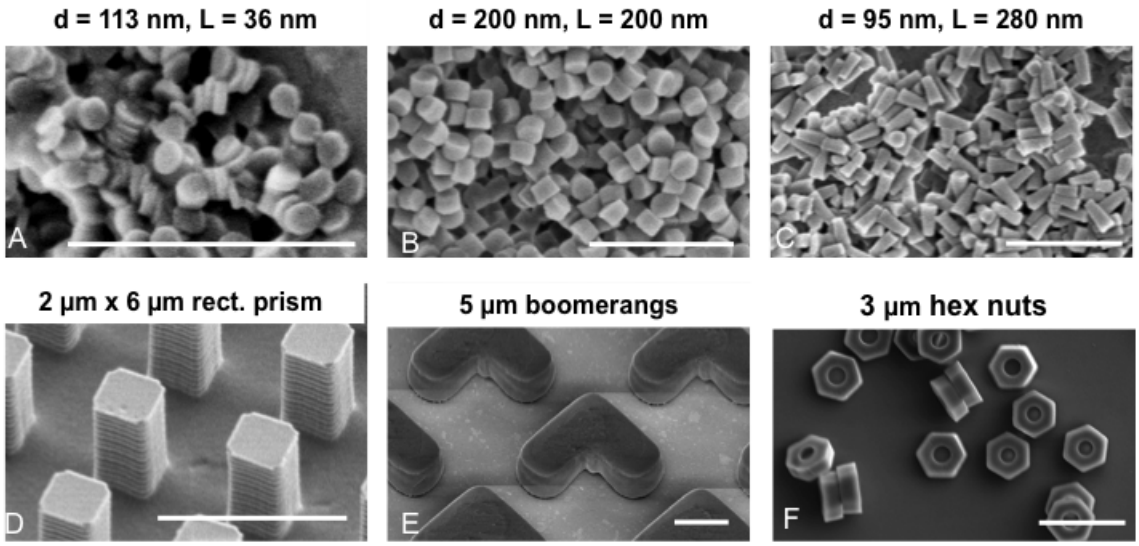

Figure 1.4 A variety of sizes and shapes generated using PRINT technology. Scale bars in (A), (B) and (C) represent 1 μm and scale bars in (D), (E) and (F) represent 5 μm.

Particle sizes and shapes could affect cellular internalization,[37] aerodynamics,[38, 39] circulation and biodistribution in the body[40] and drug release profiles[41]. PRINT can be used as an effective tool to study the role of size and

shape of the particles on all the biological processes mentioned above. Cellular internalization of PRINT particles has been studied by Gratton S.E. et al. and it was found that cell uptake exhibited a strong dependence on particle size and shape.[42] Interestingly, the internalization of the rod-like, high aspect ratio nanoparticles occurs much more rapidly and efficiently than would be expected based on size considerations alone, indicating a special role associated with the shape of the particles.

1.2.3.2 Control over composition

In addition to control over size and shape, the composition of particles fabricated from PRINT process is also readily tunable. The PRINT particles can now be fabricated from a variety of compositions (Figure 1.5): 1) Hydrogels such as cross-linked poly(ethylene glycol)s (PEG) and poly(silyl ether)s. PEG is a biocompatible polyether-based material and has wide applications in medicine and in the drug delivery field.[43] Parrot M. C. et al. developed a tunable silyl ether based acid-sensitive biomaterial and mold the material into medical devices including PRINT particles, sutures and stents.[44] These devices can preferentially degrade and release the model drug under acidic conditions known to exist in tumor tissue, inflammatory tissue, and diseased cells. 2) Polymers such as poly(lactic acid) (PLLA) and poly(lactic-co-glycolic acid) (PLGA).[45] PLLA and PLGA are both biocompatible, bioabsorbable materials and have shown great promise in medical applications. 3) Biologics such as insulin and albumin, etc.[46] Biologics such as protein and polypeptides have been extensively studied both

as integral components and as effective therapeutics in the development of novel drug delivery systems.

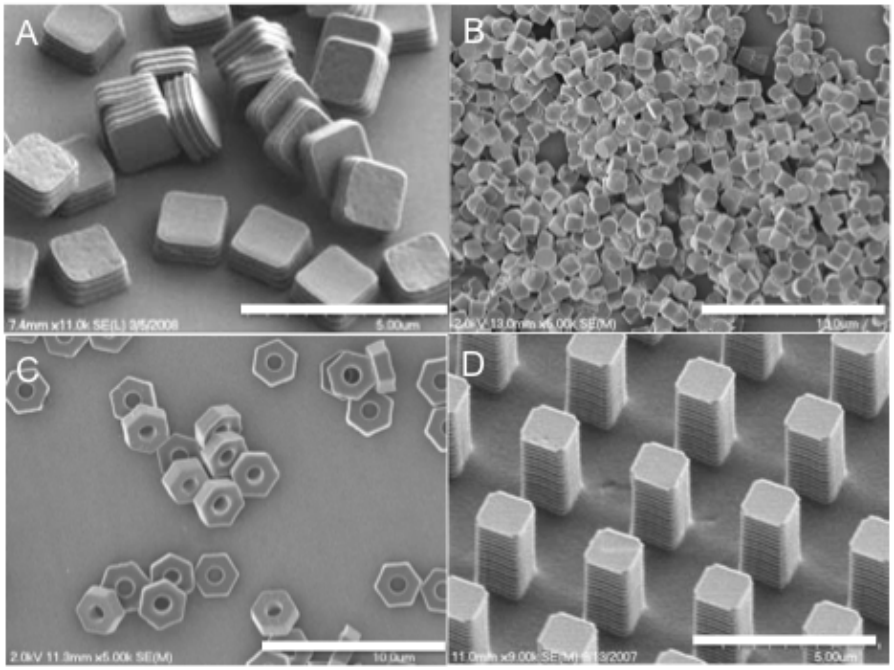

Figure 1.5 PRINT particles generated from different compositions. (A) Poly(ethylene glycol) 2 μm × 2 μm × 1 μm cubes, scale bar represents 5 μm, (B) PLGA, 1μm × 1μm cylinders, scale bar represents 10 μm, (C) poly(silyl ether), 3 μm × 1 μm hexnuts, scale bar represents 10 μm, (D) insulin, 2 μm × 4 μm cubes, scale bar represents 5 μm.

The unprecedented control over particle composition makes PRINT a platform technology in that a variety of cargos including hydrophilic or hydrophobic therapeutic molecules, biologicals, peptides, proteins, contrast agents, radiotracers et al. can be accommodated through inclusion in the particle matrices of choice. In addition, the porosity, texture and modulus of the particles can be altered through careful design of matrices formulation for different applications. For example, Merkel T. J. et al. reported that the modulus of microparticles could be decreased by decreasing the cross-linking density of the

hydrogel matrices, resulting in increasingly longer circulation times for these particles.[47] These long-circulating particles can potentially be used to generate mimic red blood cells. Interestingly, multiphasic and regio-specifically functionalized particles can also be fabricated using PRINT. Zhang H. et al. developed a strategy to prepare end-labeled particles, biphasic Janus particles and multiphasic shape-specific particles by integrating two compositionally different chemistries into a single particle.[48]

1.2.3.3 Control over surface properties

The surface properties of the PRINT particles including charges and functional groups can also be modulated. One approach is to accommodate molecules with chemistry reaction handles in the PRINT particles and then post-functionalization through chemical reactions after PRINT process can be used to effectively tailor the surface properties. For example, Gratton S. E. et al. treated surface amine groups on the PEG-based particles with acetic anhydride, converting the zeta potential of nanoparticles from positive to negative.[42] The results indicated that positively charged nanoparticles were readily internalized whereas the identically shaped negatively charged particles showed minimal cell internalization. Wang J. et al. developed strategies to modify the surface functional groups of the PEG-based PRINT nanoparticles through conjugation with human transferring or transferring receptor monoclonal antibody (Figure 1.6).[49] The 200 nm $\times$ 200 nm cylindrical PRINT nanoparticles labeled with transferrin receptor antibody or human transferrin showed highly specific Transferin-mediated uptake by all human tumor cell lines tested, while negative

controls (IgG1 and bovine transferring) showed minimal internalization. Another approach is to modify the surface properties of the PRINT particles through physical absorption. Hasan W. et al. developed a PLGA-lipid system to deliver siRNA. The lipids were absorbed onto the surface of the PLGA nanoparticles through hydrophobic-hydrophobic interaction (Figure 1.7) and facilitated cell uptake as well as endosomal escape of the particles.[50] PRINT allows for the control over surface properties which greatly affect cell internalization and biodistribution of particles and is a platform for targeted drug delivery.

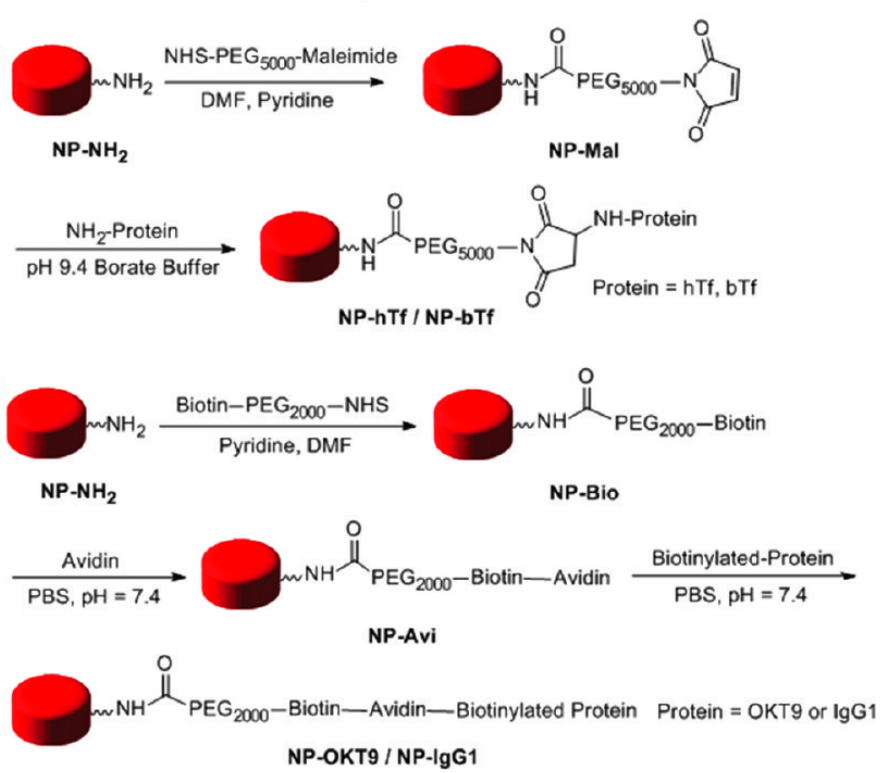

Figure 1.6 Post-functionalizations of PRINT nanoparticles. Top: with human/bovine transferrin through lysine-maleimide reactions, bottom: with transferrin receptor monoclonal antibody OKT9 and its isotype control IgG1 through biotin-avidin strategies. Adapted from [41].

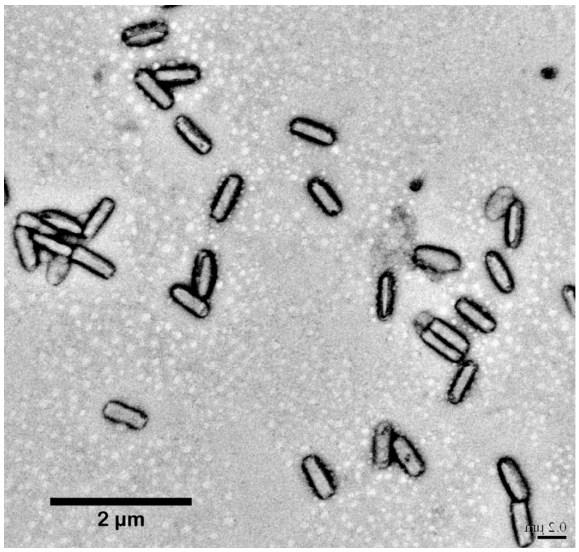

Figure 1.7 TEM image of lipid coated PRINT PLGA-siRNA nanoparticles. Adapted from [49].

1.2.4 PRINT particles for delivery of therapeutics

In addition to the fact that PRINT is compatible with a wide range of chemistry composition and the gentle nature the particles can be fabricated, this technology also has the advantage of a straightforward incorporation of a variety of cargos. Based on the nature of the cargo, the appropriate particle matrices can be selected and the cargo encapsulation can be achieved through mixing the two components and any other additives, if there is any, to form a pre-particle material, followed by filling the cavities with the pre-particle material.

1.2.4.1 PRINT particles for delivery of chemotherapeutics

Enlow E. M. et al. reported the delivery of a chemotherapeutic drug, docetaxel, with PLGA PRINT nanoparticles.[45] Docetaxel is a highly hydrophobic drug and has very limited solubility in water. PLGA and docetaxel can be evenly mixed in an organic solvent mixture (DMF:DMSO=4:1) and the one-phase pre-particle material can be molded into nanoparticles using PRINT technology.

Compared with other methods to fabricate PLGA-docetaxel particles, PRINT enjoys exceptionally high loadings of the drug in the particles up to 40% (w/w) with encapsulation efficiencies > 90%. In addition, the particles with different drug loadings possessed exactly the same particle size and shape and were fabricated without the necessity of adjustments to the process. The PLGA particles without drug showed minimal toxicity on the cell lines investigated and drug-loaded particles showed high toxicity *in vitro*. The commercially available formulation of docetaxel, Taxotere®, was outperformed by the 30% and 40% drug loading PLGA-docetaxel PRINT particles in toxicity. The *in vivo* efficacy of the PLGA-docetaxel particles bearing different sizes and shapes is currently being investigated.

1.2.4.2 PRINT particles for gene delivery

The PLGA particles were also investigated as delivery vehicles for siRNA. Hasan W. et al. developed a simple two-component PLGA-siRNA nano-particle system which allows for protection of siRNA from degradation as well as controlled release of the cargo.[50] Similar to the loading of docetaxel, siRNA and PLGA were mixed evenly to form pre-particle material which was then filled into the cavities of PRINT mold. Lipids were coated on the surface of the particles at the time of particle harvesting to facilitate cell uptake as well as particle transfection. The internalization of the lipid-coated PLGA/siRNA nanoparticles was achieved on multiple cancer cell lines and the particles have successfully shown *in vitro* knockdown of therapeutic genes relevant to prostate cancer. The *in vivo* efficacy of lipid/PLGA/siRNA nanoparticle system is currently under

investigation.

1.3 Summary

In summary, RNA replicon is highly effective for generating cellular and protective immune responses and has shown great promise to treat and protect against a variety of diseases, but it is essential to find a method to effectively deliver the RNA replicon molecule. PRINT technique developed in our lab is a platform that allows for the precise and simultaneous control over all the parameters that are essential to protect and deliver the delicate biological cargos. PRINT is also amenable to continuous roll-to-roll fabrication techniques that enable the scale-up of the particle fabrication under good manufacturing practice (GMP) compliance. PRINT has the straightforward incorporation of a variety of cargos which can be accommodated through inclusion in the particle matrices in a “plug-and-play” manner. This broadly applicable and readily tunable platform has the potential to fundamentally revolutionize vaccine development. The goal of the research here is to develop a particle system based on PRINT to effectively deliver RNA replicon *in vitro* and *in vivo* and ultimately initiate effective protection against diseases.

REFERENCES

1. Riedel, S., Edward Jenner and the history of smallpox and vaccination. BUMC Proceedings 2005, 18, 21-25.

2. Singh, M.; Srivastava, I. K., Development of Vaccines: From Discovery to Clinical Testing. 2011.

3. Badgett, M. R.; Auer, A.; Carmichael, L. E.; Parrish, C. R.; Bull, J. J., Evolutionary Dynamics of Viral Attenuation. Journal of Virology 2002, 76 (20), 10524-10529.

4. Rappuoli, R.; Bagnoli, F., Vaccine Design: Innovative Approaches and Novel Strategies. 2011.

5. Sompayrac, L., How the Immune System Works. 2008.

6. Bachmann, M. F.; Jennings, G. T., Vaccine delivery: a matter of size, geometry, kinetics and molecular patterns. Nature Reviews Immunology 2010, 10 (11), 787-796.

7. O'Hagan, D. T.; Singh, M.; Ulmer, J. B., Microparticle-based technologies for vaccines. Methods 2006, 40 (1), 10-19.

8. Ulmer, J. B.; Donnelly, J. J.; Parker, S. E.; Rhodes, G. H.; Felgner, P. L.; Dwarki, V. J.; Gromkowski, S. H.; Deck, R. R.; DeWitt, C. M.; Friedman, A.; et al., Heterologous protection against influenza by injection of DNA encoding a viral protein. Science 1993, 259 (5102), 1745-9.

9. Tang, D. C.; DeVit, M.; Johnston, S. A., Genetic immunization is a simple method for eliciting an immune response. Nature 1992, 356 (6365), 152-4.

10. Weide, B.; Garbe, C.; Rammensee, H.-G.; Pascolo, S., Plasmid DNA- and messenger RNA-based anti-cancer vaccination. Immunology Letters 2008, 115 (1), 33-42.

11. Kutzler, M. A.; Weiner, D. B., DNA vaccines: ready for prime time? Nature Reviews Genetics 2008, 9 (10), 776-788.

12. Cannon, G.; Weissman, D., RNA based vaccines. DNA Cell Biol 2002, 21 (12), 953-61.

13. Vajdy, M.; Srivastava, I.; Polo, J.; Donnelly, J.; O'Hagan, D.; Singh, M., Mucosal adjuvants and delivery systems for protein-, DNA- and RNA-based vaccines. Immunology and Cell Biology 2004, 82 (6), 617-627.

14. Zimmer, G., RNA Replicons - A New Approach for Influenza Virus Immunoprophylaxis. Viruses 2010, 2 (2), 413-434.

15. Lechardeur, D.; Sohn, K. J.; Haardt, M.; Joshi, P. B.; Monck, M.; Graham, R. W.; Beatty, B.; Squire, J.; O'Brodovich, H.; Lukacs, G. L., Metabolic instability of plasmid DNA in the cytosol: a potential barrier to gene transfer. Gene Ther 1999, 6 (4), 482-97.

16. Nishimura, K.; Segawa, H.; Goto, T.; Morishita, M.; Masago, A.; Takahashi, H.; Ohmiya, Y.; Sakaguchi, T.; Asada, M.; Imamura, T.; Shimotono, K.; Takayama, K.; Yoshida, T.; Nakanishi, M., Persistent and Stable Gene Expression by a Cytoplasmic RNA Replicon Based on a Noncytopathic Variant Sendai Virus. Journal of Biological Chemistry 2007, 282 (37), 27383-27391.

17. Wang, Z.; Troilo, P. J.; Wang, X.; Griffiths, T. G.; Pacchione, S. J.; Barnum, A. B.; Harper, L. B.; Pauley, C. J.; Niu, Z.; Denisova, L.; Follmer, T. T.; Rizzuto, G.; Ciliberto, G.; Fattori, E.; Monica, N. L.; Manam, S.; Ledwith, B. J., Detection of integration of plasmid DNA into host genomic DNA following intramuscular injection and electroporation. Gene Therapy 2004, 11 (8), 711-721.

18. Diebold, S. S.; Kaisho, T.; Hemmi, H.; Akira, S.; Reis e Sousa, C., Innate antiviral responses by means of TLR7-mediated recognition of single-stranded RNA. Science 2004, 303 (5663), 1529-31.

19. Restifo, N. P.; Ying, H.; Hwang, L.; Leitner, W. W., The promise of nucleic acid vaccines. Gene Therapy 2000, 7, 89-92.

20. Tannis, L.; Gauthier, A.; Evelegh, C.; Parsons, R.; Nyholt, D.; Khromykh, A.; Bramson, J., Semliki Forest virus and Kunjin virus RNA replicons elicit comparable cellular immunity but distinct humoral immunity. Vaccine 2005, 23 (33), 4189-4194.

21. Ying, H.; Zaks, T. Z.; Wang, R. F.; Irvine, K. R.; Kammula, U. S.; Marincola, F. M.; Leitner, W. W.; Restifo, N. P., Cancer therapy using a self-replicating RNA vaccine. Nat Med 1999, 5 (7), 823-7.

22. Racanelli, V.; Behrens, S.-E.; Aliberti, J.; Rehermann, B., Dendritic Cells Transfected with Cytopathic Self-Replicating RNA Induce Crosspriming of CD8 T Cells and Antiviral Immunity. Immunity 2004, 20, 47-58.

23. Kim, T. W.; Hung, C. F.; Juang, J.; He, L.; Hardwick, J. M.; Wu, T. C., Enhancement of suicidal DNA vaccine potency by delaying suicidal DNA-induced cell death. Gene Ther 2004, 11 (3), 336-42.

24. Leitner, W. W.; Hwang, L. N.; Bergmann-Leitner, E. S.; Finkelstein, S. E.; Frank, S.; Restifo, N. P., Apoptosis is essential for the increased efficacy of alphaviral replicase-based DNA vaccines. Vaccine 2004, 22 (11-12), 1537-44.

25. Vignuzzi, M.; Gerbaud, S.; van der Werf, S.; Escriou, N., Naked RNA immunization with replicons derived from poliovirus and Semliki Forest virus genomes for the generation of a cytotoxic T cell response against the influenza A virus nucleoprotein. J Gen Virol 2001, 82 (Pt 7), 1737-47.

26. Schleiss, M. R.; Lacayo, J. C.; Belkaid, Y.; McGregor, A.; Stroup, G.; Rayner, J.; Alterson, K.; Chulay, J. D.; Smith, J. F., Preconceptual administration of an alphavirus replicon UL83 (pp65 homolog) vaccine induces humoral and cellular immunity and improves pregnancy outcome in the guinea pig model of congenital cytomegalovirus infection. J Infect Dis 2007, 195 (6), 789-98.

27. Grgacic, E. V. L.; Anderson, D. A., Virus-like particles: Passport to immune recognition. Methods 2006, 40 (1), 60-65.

28. Langer, R., New methods of drug delivery. Science 1990, 249 (4976), 1527-33.

29. Johnston, A. P. R.; Such, G. K.; Ng, S. L.; Caruso, F., Challenges facing colloidal delivery systems: From synthesis to the clinic. Current Opinion in Colloid & Interface Science 2011, 16 (3), 171-181.

30. Laurencin, C. T.; Langer, R., Polymeric controlled release systems: new methods for drug delivery. Clin Lab Med 1987, 7 (2), 301-23.

31. Bhattacharya, S.; Bajaj, A., Advances in gene delivery through molecular design of cationic lipids. Chemical Communications 2009, (31), 4632.

32. Rapoport, N., Physical stimuli-responsive polymeric micelles for anti-cancer drug delivery. Progress in Polymer Science 2007, 32 (8-9), 962-990.

33. Tong, W.; Gao, C.; Möhwald, H., Stable Weak Polyelectrolyte Microcapsules with pH-Responsive Permeability. Macromolecules 2006, 39 (1), 335-340.

34. Ganta, S.; Devalapally, H.; Shahiwala, A.; Amiji, M., A review of stimuli-responsive nanocarriers for drug and gene delivery. Journal of Controlled Release 2008, 126 (3), 187-204.

35. Rolland, J. P.; Maynor, B. W.; Euliss, L. E.; Exner, A. E.; Denison, G. M.;

DeSimone, J. M., Direct fabrication and harvesting of monodisperse, shape-specific nanobiomaterials. J Am Chem Soc 2005, 127 (28), 10096-100.

36. Euliss, L. E.; DuPont, J. A.; Gratton, S.; DeSimone, J., Imparting size, shape, and composition control of materials for nanomedicine. Chemical Society Reviews 2006, 35 (11), 1095.

37. Champion, J. A.; Mitragotri, S., Role of target geometry in phagocytosis. Proc Natl Acad Sci U S A 2006, 103 (13), 4930-4.

38. Boshhiha, A. M.; Urbanetz, N. A., Influence of carrier surface fines on dry powder inhalation formulations. Drug Dev Ind Pharm 2009, 35 (8), 904-16.

39. Hassan, M. S.; Lau, R. W., Effect of particle shape on dry particle inhalation: study of flowability, aerosolization, and deposition properties. AAPS PharmSciTech 2009, 10 (4), 1252-62.

40. Geng, Y.; Dalhaimer, P.; Cai, S.; Tsai, R.; Tewari, M.; Minko, T.; Discher, D. E., Shape effects of filaments versus spherical particles in flow and drug delivery. Nat Nanotechnol 2007, 2 (4), 249-55.

41. Galli, C., Experimental determination of the diffusion boundary layer width of micron and submicron particles. Int J Pharm 2006, 313 (1-2), 114-22.

42. Gratton, S. E. A.; Ropp, P. A.; Pohlhaus, P. D.; Luft, J. C.; Madden, V. J.; Napier, M. E.; DeSimone, J. M., The effect of particle design on cellular internalization pathways. Proceedings of the National Academy of Sciences 2008, 105 (33), 11613-11618.

43. Petros, R. A.; Ropp, P. A.; DeSimone, J. M., Reductively labile PRINT particles for the delivery of doxorubicin to HeLa cells. J Am Chem Soc 2008, 130 (15), 5008-9.

44. Parrott, M. C.; Luft, J. C.; Byrne, J. D.; Fain, J. H.; Napier, M. E.; Desimone, J. M., Tunable bifunctional silyl ether cross-linkers for the design of acid-sensitive biomaterials. J Am Chem Soc 2010, 132 (50), 17928-32.

45. Enlow, E. M.; Luft, J. C.; Napier, M. E.; DeSimone, J. M., Potent Engineered PLGA Nanoparticles by Virtue of Exceptionally High Chemotherapeutic Loadings. Nano Letters 2011, 11 (2), 808-813.

46. Kelly, J. Y.; DeSimone, J. M., Shape-specific, monodisperse nano-molding of protein particles. J Am Chem Soc 2008, 130 (16), 5438-9.

47. Merkel, T. J.; Jones, S. W.; Herlihy, K. P.; Kersey, F. R.; Shields, A. R.;

Napier, M.; Luft, J. C.; Wu, H.; Zamboni, W. C.; Wang, A. Z.; Bear, J. E.; DeSimone, J. M., Using mechanobiological mimicry of red blood cells to extend circulation times of hydrogel microparticles. Proc Natl Acad Sci U S A 2011, 108 (2), 586-91.

48. Zhang, H.; Nunes, J. K.; Gratton, S. E. A.; Herlihy, K. P.; Pohlhaus, P. D.; DeSimone, J. M., Fabrication of multiphasic and regio-specifically functionalized PRINT® particles of controlled size and shape. New Journal of Physics 2009, 11, 075018,16pp.

49. Wang, J.; Tian, S.; Petros, R. A.; Napier, M. E.; Desimone, J. M., The complex role of multivalency in nanoparticles targeting the transferrin receptor for cancer therapies. J Am Chem Soc 2010, 132 (32), 11306-13.

50. Hasan, W.; Chu, K.; Gullapalli, A.; Dunn, S. S.; Enlow, E. M.; Luft, J. C.; Tian, S.; Napier, M. E.; Pohlhaus, P. D.; Rolland, J. P.; DeSimone, J. M., Delivery of multiple siRNAs using lipid-coated PLGA nanoparticles for treatment of prostate cancer. Nano Lett 2012, 12 (1), 287-92.

CHAPTER 2

NOVEL DISULFIDE-BASED CROSS-LINKER RENDERING PROTEIN-BASED PARTICLES TRANSIENTLY INSOLUBLE FOR THERAPEUTIC APPLICATIONS

2.1 Introduction

Delivering promising biological therapeutics like RNA replicons to the desired location in the body in a safe and effective fashion is one of the key challenges in medicine. A protein matrix was chosen for the delivery of RNA replicons based on the fact that both RNA replicon and protein are highly hydrophilic and dissolve readily in aqueous solutions in which RNA replicons and proteins can be evenly mixed together and subsequently molded into particles utilizing PRINT technology.

Drug carriers using proteins as matrices for the delivery of small molecule drugs and biological cargos, such as plasmid DNA and siRNA, are being extensively studied. In addition, protein-based therapies, which involve the delivery of therapeutic proteins or polypeptides, such as tumor necrosis factor, and monoclonal antibodies, are considered a safe and effective approach to treat many diseases. Each of these applications would benefit from having protein-based particles that dissolve slowly in a controlled and desirable manner.

2.2 Protein-based Particles for Drug Delivery and Conventional Fabrication Methods

2.2.1 Protein-based particles for drug delivery

Proteins as the matrices for drug delivery particles have many advantages including biodegradability, biocompatibility and amenability to surface modification.[1] There are over 30 therapeutics compounds that have been investigated with protein-based drug delivery systems including chemotherapies, e.g., doxorubicin, docetaxel, paclitaxel, and gemcitabine, and biopharmaceuticals such as plasmid DNA, siRNA, etc. [2] The proteins under active investigation nowadays include gelatin [3], albumin [4], collagen [5], gliadin etc. Table 2.1 shows a list of proteins that have been used to prepare drug delivery systems, their properties and examples of the therapeutics that have been delivered by these systems.

Table 2.1 List of proteins investigated as matrices for drug delivery systems, partially adapted from [2].

Protein	Properties	Drugs investigated
Albumin	1. Mw of 66.5 kDa, highly soluble in water, moderately soluble in concentrated salt solutions 2. Iso-electric point (pI) is 4.75, slightly negative charged in physiological condition 3. Robust to various conditions	Doxorubicin, paclitaxel, plasmid DNA[6], siRNA[7]
Collagen	1. Has a three dimensional helical structure and is neutral-salt soluble or acid soluble 2. Poor mechanical strength 3. Contains carboxyl groups and secondary amino groups with possible cross-linking function	Glucocorticosteroids, all-trans retinol
Gelatin	1. Hydrolyzed form of collagen, possesses a random coil structure and many carboxyl	Colchicine, thrombocidin (rTC-

	groups, soluble in water at above 35-40°C, gels below 35-40°C 2. Type A pI 7.0-9.0, type B pI 4.8-5.0 3. Widely used as an capsule ingredient in drug formulations	1), lysozyme
Gliadin	1. Protein of vegetarian source 2. Highly soluble in water and slightly soluble in ethanol 3. Can fuse with sensitive enzymes and protect them from breaking down in contact with stomach acids	Superoxide dismutase
Silk-elastin-like polypeptide	1. Processes a pentapeptide repeatable unit as Val-Pro-Gly-Xaa-Gly 2. Structure and properties can be engineered	Insulin[8], doxorubicin, plasmid DNA
Ferritin/ apoferritin	1. A globular protein complex consisting of 24 protein subunits, has a Mw of 450 kDa 2. Stores and releases iron in a controlled fashion 3. Found intracellularly in all cell types	RGD4C peptide
Whey protein	1. A mixture of globular proteins and soluble in water, independent of pH 2. Widely used in food products because of their high nutritional value and their ability to form gels, emulsions, or foams	riboflavin, caffeine, retinol
Viral capsid	1. Protects the nucleic acid of a virus 2. Composed of capsomers, the individual morphological units 3. Can form Virus-like particles through self-assembly with RNA molecules	Protein, RNA eplicon[9]
Zein	1. Used to deliver hydrophobic drugs 2. Has antibacterial activity, 3. Protects ivermecin from photodegradation 4. Cost-effectiveness	Ivermectin
Heat shock proteins	1. Involved in the folding and unfolding of other proteins when cells are under the stress of high temperature, etc. 2. Uniform cage sizes with 12 nm exterior and 6.5 nm interior 3. Large pores (3 nm) between interior and exterior for easy cargo exchange 4. Used as scaffold for chemical reactions and material synthesis	RGD 4C peptide, anti-CD4 antibody, doxorubicin
Casein	1. Consists of proline peptides and no disulfide bridges	Progesterone, doxorubicin,

	2. Used to incorporate hydrophobic drugs 3. Robust under various conditions	theophylline

2.2.2 Conventional methods to prepare protein-based particles

Conventionally, the micro- and nano-sized protein particles are often made through processes which include solvent evaporation, micro-emulsion, spray-freeze-drying methods etc. Much effort has been dedicated to investigating the effects of numerous protein processing parameters such as temperature, humidity, composition, and fabrication method in order to retain the protein's native state and biological function.

Protein particles can be prepared through a solvent evaporation (desolvation) technique.[10] Typically, the aqueous solution of protein is added to an excess of the stabilizing solvent (e.g. ethanol) wherein the aqueous phase is subjected to evaporation and protein particles grow in size as the reaction continues.

Micro-emulsion is another important fabrication method used for protein particles, which involves the use of a dispersing oil phase.[11] In the process, the aqueous protein solution is dispersed in an immiscible liquid (oil phase, e.g. cottonseed oil) and the mixture is then shaken and sonicated vigorously to create an emulsion. The emulsion formation step determines the size and size distribution the resulting micro-particles. The dispersed droplets of protein solution are usually further stabilized by heat or chemical cross-linking to form hardened protein particles.

In the process of spray-freeze-drying, a liquid feed containing dissolved protein is first broken into tiny droplets by an ultrasonic atomizer and the resulting droplets are frozen in contact with cold gas (or cryogenic liquid).[12] Solid protein particles are obtained after the frozen droplets solidify at low temperature and pressure. The stress imposed on proteins in the atomization step and the extremely rapid freezing of droplets differentiates spray-freeze-drying from lyophilization which is normally used to prepare protein powders.

Other protein particle fabrication methods include a supercritical fluid method[13], the isoelectric point precipitation method (pH-coacercation)[14] and templating mesoporous silica spheres[15] etc. Frequently, these procedures result in highly heterogeneous spherical or granular particles and don't allow for control over particle size or shape, resulting in particle populations of significant heterogeneity. Moreover, many of these processes are not compatible with optimal production of biological particles, as denaturation and aggregation of proteins tend to occur during processing. Another disadvantage associated with these methods is the costly and complicated processes which limit their ability to manufacture in bulk quantities.

2.3 Fabrication of Protein Particles Using PRINT Technology

2.3.1 Introduction

Fabrication of PRINT protein particles has been achieved by a solvent evaporation strategy. [16] PRINT protein particles were prepared by filling 25 wt% protein solution in water into the PRINT mold and removing excess solution through multiple delamination steps. Then the filled mold containing aqueous

protein solution was frozen and lyophilized overnight to remove the water. Particles were harvested using medical adhesive layer poly(cyano acrylate) or Providone (poly(vinyl pyrrolidinone)). Figure 2.1 shows the SEM images of the PRINT protein particles. Fluorescent dye was introduced into the particles and dissolution of the particles was monitored using microscope. The results indicated that molding process did not change the dissolution characteristics of the protein particles (Figure 2.2).

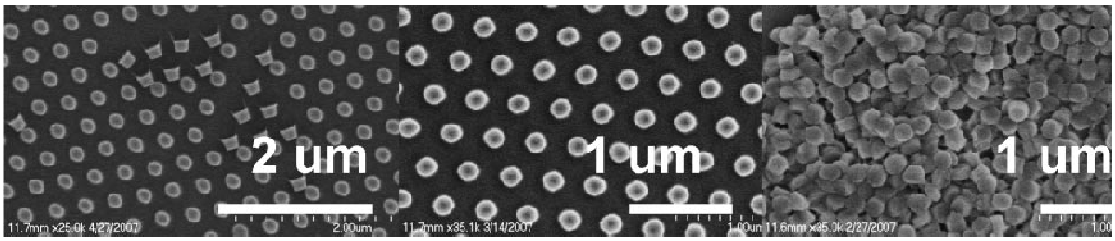

Figure 2.1 SEM images of PRINT protein particles. Left: 200 nm Abraxane particles harvested on medical adhesive layer, middle: 200 nm albumin with siRNA particles harvested on medical adhesive layer, right: harvested and dispersed 200 nm albumin particles.

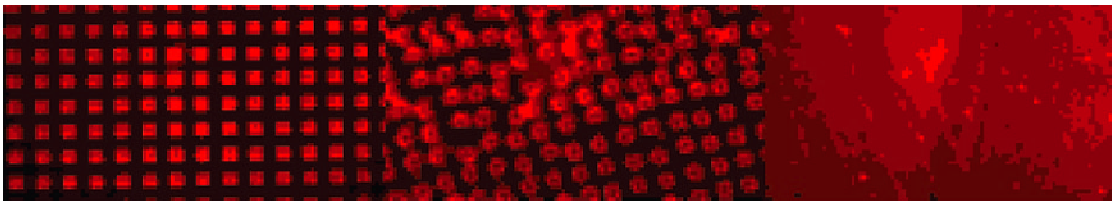

Figure 2.2 Fluorescent images of 5 μm albumin particles with dye harvested onto Povidone (left) after adding water to watch dissolution (middle) and after full dissolution (right).

There are several disadvantages associated with this method that limit the particle fabrication efficiency especially in bulk quantities. Firstly, the filling process requires multiple delaminating steps to remove the excess protein solution that may form a scum layer connecting the particles together. Secondly, the lyophilization step is time-consuming and requires demanding instrument

setups. Thirdly, the particle harvesting with adhesive only allows for particles to be harvest on centimeter-square scales. Having found the limitations of the solvent evaporation PRINT method, a new method was sought with the ability to fabricate PRINT protein particles on a scale that is practical for therapeutic application studies. Scientists at Liquidia Technologies developed a protein particle fabrication method based on the previous success in the fabrication of protein particles and poly (lactic-co-glycolic acid) particles. In this method, diluents or plasticizers based on lactose and glycerol can be mixed with the protein of choice to form the pre-particle material that "flows" when heated. Herein, the strategy is further optimized to increase gentleness toward protein and other biologic cargos. Serum albumin was chosen in this study for two reasons. As the most abundant blood plasma protein it is essential for the transport of many physiological molecules and it also has the advantage of being readily available. Abraxane®, an albumin based paclitaxel containing nanomedicine, has achieved tremendous success as an approved treatment for metastatic breast cancer.[17] In particular, bovine serum albumin (BSA) was used in this study due to its easy accessibility, cost effectiveness and availability in RNAse-free grade for our proof-of-concept study.

2.3.2 Fabrication of albumin particles using PRINT technology

2.3.2.1 Materials

Bovine serum albumin was from Calbiochem. BCA protein assay reagent was from Thermo Scientific. Alexa fluor 555® labeled Bovine serum albumin was purchased from invitrogen. Lactose assay kit was purchased from Abcam. α-D-

Lactose, glycerol and anhydrous isopropanol were purchased from Acros. Pre-fabricated molds with 200 nm × 200 nm (mold # MMM-369-070) and 1 μm × 1 μm (mold # MMM-262-090A, MMM-369-070) cylindrical features and poly(ethylene terephthalate) (PET) sheets coated with Plasdone films were obtained from Liquidia Technologies.

2.3.2.2 PRINT albumin particle preparation

The bovine serum albumin (BSA) PRINT particles (1μm × 1μm, cylindrical) were derived from a mixture composed of 37.5 wt % of BSA, 37.5 wt % of D-lactose and 25 wt % of glycerol. A 7.8 wt% solution of this mixture in water was prepared and then cast a film onto a PET sheet with a #7 Mayer rod (R.D Specialties) (Figure 2.3 A). Water was removed with a heat gun moving back and forth. The film was optically transparent and was laminated onto a piece of PRINT mold (1 × 1 inch, cylindrical, d =1μm, h = 1μm), forming a sandwich structure with the film in the middle (Figure 2.3 B and C). This laminating step was carried out under a humidity level of 30-35% (based on 11-661-8 humidity meter, purchased from Control Company, TX 77546). The mold and the PET were passed through a heated laminator with a temperature of 60 °C on the heated roller and a pressure of 80 psi between the rollers and split (Figure 2.3 D and E). In this step, the PET and mold were passed through the heated laminator with the PET sheet facing the heated roller. The filled mold was relaminated onto a sheet of Plasdone covered PET (Figure 2.3 F and G). The laminated mold and PET were passed through the heated laminator again (Figure 2.3 H). After the filled mold cooled down (placed at room temperature for 1 minute), the mold and

the PET were separated gently and all the PRINT particles were transferred from the mold to the Plasdone film (Figure 2.3 I). The particles were harvested from the PET by dissolving Plasdone with isopropanol (Figure 2.3 J). The harvested particles were washed with isopropanol for three times by centrifugation to remove Plasdone.

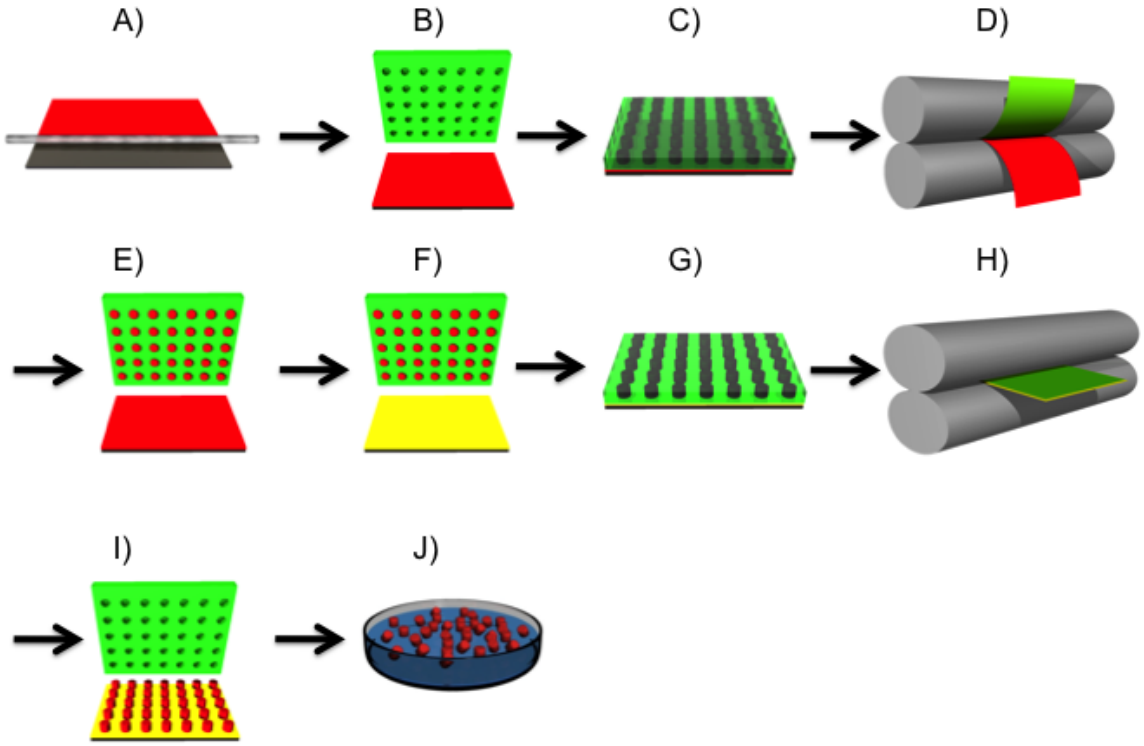

Figure 2.3 The fabrication process for protein-based PRINT particles. BSA, lactose and glycerol were dissolved in water to create a solution (red). (A) A mayer rod is then used to draw a film from this solution on a PET sheet. Water is removed and a solid film is generated. (B) A PRINT mold (green) is laminated onto the film. (C) The mold with pre-particle film. (D) The mold is passed through a heated pressured nip (grey) and split. (E) The cavities of the mold are filled. (F) The filled mold is laminated onto a sacrificial adhesive layer (Plasdone film on PET sheet, yellow). (G) The mold with the sacrificial adhesive layer. (H) The mold is passed through the nip again without splitting. (I) After the mold cools down, the mold is peeled off and particles are transferred to the adhesive layer. (J) The sacrificial adhesive layer was dissolved to free the particles.

Particles with a 200 nm × 200 nm cylindrical feature were fabricated following the same procedures with adjusted parameters. The particles were

derived from a pre-particle mixture composed of 54 wt% of BSA, 30 wt% of D-lactose and 16 wt% of glycerol. A 5.0 wt% solution of this mixture in water was cast a film onto a PET sheet with a #5 Mayer rod (R.D Specialties). PRINT mold (1 × 1 inch, cylindrical, d =200 nm, h = 200 nm) was laminated onto the pre-particle material film under a humidity level of 40-45%. The mold was filled by passing the mold and the PET through a heated laminator with a temperature of 93 °C on the top roller and a pressure of 80 psi between the rollers. The particles were then transferred onto Plasdone film and harvested using isopropanol.

2.3.2.3 Scanning electron microscopy (SEM)

For visualization samples were coated with 2 nm gold palladium alloy using a Cressington 108 auto sputter coater. Images were taken at an accelerating voltage of 2 kV using a Hitachi model S-4700 scanning electron microscope (SEM).

2.3.2.4 Particle composition analysis

Particles were dispersed in water. The amount of BSA was measured using HPLC (Agilent Technologies 1260) with a C18 rapid resolution column (Zorbax Eclipse plus, 4.6 × 100 mm, 3.5 micron). A mobile phase of water and acetonitrile on a gradient from 85% of water to pure acetonitrile over 15 minutes with a flow rate of 0.6 mL/min was employed with a detection temperature of 50 °C on the ELSD (Agilent Technologies 1260). The BSA peak appeared at 8.2 minutes and the peak area was compared to the BSA standard curve to determine the concentration of BSA in the particle solution. The particle solution was filtered with centrifugal filters (Amicon ultra, 0.5 mL, MWCO 30K) to remove

BSA. The filtered solution was analyzed using HPLC with a Hi-plex Ca column (Agilent, 300 × 7.7 mm, 8 micron). A mobile phase of pure water over 25 minutes with a flow rate of 0.6 mL/min was employed with a detection temperature of 26 °C on the ELSD. The lactose peak appeared at 9.3 minutes and the glycerol peak appeared at 16.3 minutes. The concentrations of lactose and glycerol in the particle solution were calculated based on lactose and glycerol standard curves.

2.3.2.5 Dissolution test in water

The cylindrical particles (1μm × 1μm) were labeled with Alexa fluor 555® and the particle stability in water was visualized with fluorescence microscope. The particles were derived from a mixture composed of 37.0 wt% of BSA, 37.0 wt% of lactose, 25.0 wt% of glycerol and 1.0 wt% of Alexa fluro 555® labeled BSA. The particles were transferred onto the sacrificial adhesive layer and visualized with fluorescence microscope before and after addition of water.

2.3.3 Results and discussion

This thermal fill method has the ability to fabricate protein particles on a large scale in a convenient and efficient way, a benefit over the solvent evaporation method. For example, fabrication of 1 mg of 1μm × 1μm cylindrical particles using the solvent evaporation method and particle purification take several hours of bench work and also requires an overnight lyophilization procedure. As a comparison, fabricating and purifying the same amount of particles takes approximately half an hour with the new method. Figure 2.4

shows the successful fabrication of 1μm × 1μm (A) and 200 nm × 200 nm (B) cylindrical particles using the thermal fill method.

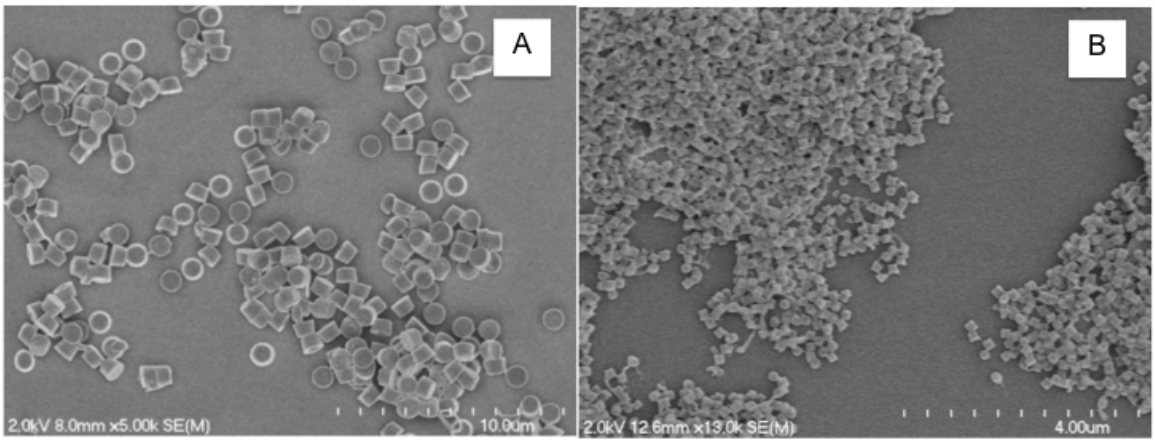

Figure 2.4 1μm × 1μm (A) and 200 nm × 200 nm (B) cylindrical BSA particles.

The thermal fill method is based on the heating pre-particle material above its T_g and reaching a state of flow. BSA in a lyophilized form can be significantly denatured even heated to an unsoftened state and can not fill the mold without addition of plasticizing agents. Lactose and glycerol are both regarded as GRAS materials (generally regarded as safe) by FDA and have been commonly used as plasticizers in food and pharmaceutical industries. Introducing these two components into the formulation significantly dropped the T_g of the pre-particle material and the temperature used to make this material flow can be as low as 60 °C for 1μm × 1μm cylindrical particle fabrication, which avoids the obvious degradation of the protein and delicate biological therapeutics that we are looking at.

There are two main factors that affect the mold filling of a pre-particle formulation:

1) Contact angle of the pre-particle mixture on the PRINT mold. The filling of the PRINT mold happens when the capillary force pulls the pre-particle material into the nano-scale or micron-scale cavities. At the same time, the pre-particle material has to be non-wetting on the surface of the mold, preventing the generation of flash layers between the particles. The surface tension of the pre-particle material and the contact angle on the patterned mold surface determine the "PRINT-ability" of certain formulations. This explains the fact that certain protein-lactose-glycerol formulations can fill the mold under a flow state but can not generate isolated particles. Fabrication of 200 nm × 200 nm cylindrical using a pre-particle mixture of 40 wt% of BSA, 30 wt% of lactose and 30 wt% of glycerol under a humidity level of 40-45% resulted in some isolated particles and a significant amount of scum (Figure 2.5 A).

2) Humidity level. In the process of pre-particle film preparation, most water is removed but certain amount of water still exists in the pre-particle material, reaching a state of equilibrium with the water in the air. Water is also widely used as a plasticizer for hydrophilic polymers and the amount of water in the pre-particle material strongly affects the property of the film. For example, Figure 2.5 (B) showed particles derived from the same formulation as for the particles shown in Figure 2.2 (B), but under a higher humidity (55%). In this case, the particles appeared to be significantly interconnected with a flash layer. As a comparison, the same pre-particle material was filled under a humidity level of 20%, which generated very minimal mold filling. The result indicated that the

humidity level in the air has to be strictly controlled so that particle fabrication can be reproducible using a particular formulation.

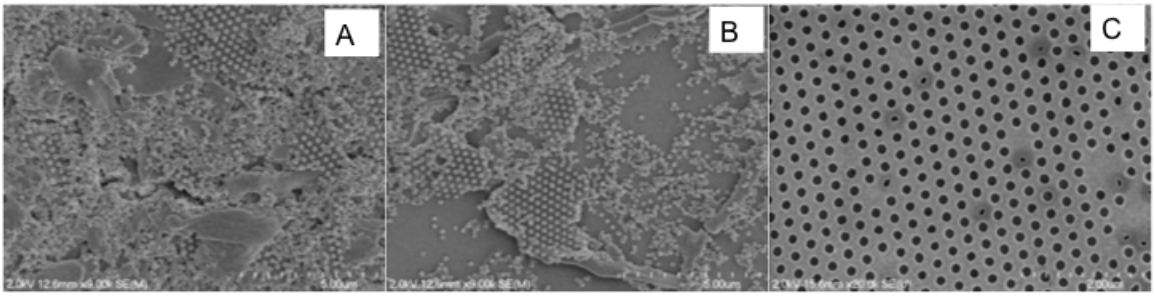

Figure 2.5 (A) 200 nm × 200 nm cylindrical particles derived from a mixture of 40 wt% of BSA, 30 wt% of lactose and 30 wt% of glycerol under the humidity level of 40-45%, (B) 200 nm × 200 nm cylindrical particles derived from a mixture composed of 54 wt% of BSA, 30 wt% of D-lactose and 16 wt% of glycerol under the humidity level of 55%, (C) 200 nm × 200 nm cylindrical mold filled with a mixture composed of 54 wt% of BSA, 30 wt% of D-lactose and 16 wt% of glycerol under the humidity level of 20%.

Images were taken of the 1μm × 1μm cylindrical particles labeled with Alexa Fluor 555® on the sacrificial adhesive layer before and after addition of water (Figure 2.6). The particles dissolved instantaneously after exposure to water, which also illustrated that the molding process didn't change the dissolution properties of albumin and indicated the necessity for a cross-linker to stabilize the albumin particles transiently.

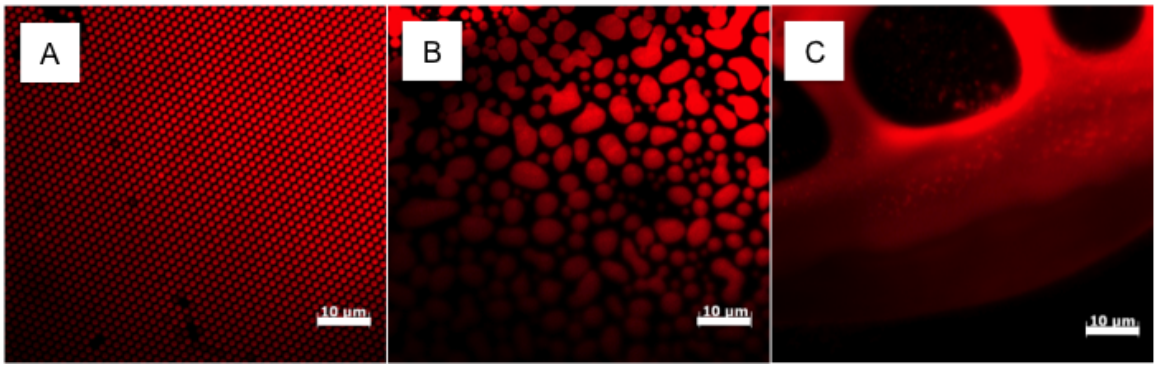

Figure 2.6 BSA particle dissolution imaged by fluorescence microscopy. (A) Particles transferred on to Plasdone PET sheet (B) Particles with water added after 10 s, (C) Particles with water added after 5 min.

2.4 Synthesis of Novel Disulfide-based Cross-linker

2.4.1 Introduction

Dry microspheres or nanospheres composed of proteins are usually instantaneously soluble when placed into aqueous solutions. A couple of strategies have been reported that maintains the stability of protein-based particles: i) thermal cross-linking, which causes the formation of intermolecular disulfide bridges between free thiol groups;[18] ii) the use of non-reversible chemical cross-linkers, such as 1-Ethyl-3-(3-dimethylaminopropyl)carbodiimide (EDC), glutaraldehyde, formaldehyde etc.; [11, 19] and iii) the use of reversible cross-linkers like Lomant's reagent, dithiobis[succinimidyl propionate] (DSP), which can be cleaved upon exposure to certain biologic conditions. Thermal cross-linking involves the thermal denaturation of a given protein at high temperature and cannot be applied to the delivery of functional therapeutic proteins. The use of non-reversible chemical cross-linkers introduces permanent cross-linkages between individual protein molecules which limit the release of free protein molecules. Such an approach has limited utility for the delivery of therapeutic proteins and biological cargos. Reversible cross-linkers can be cleaved upon exposure to certain biologic conditions but leaves a chemical residue —a potential neo-epitope—on the protein after cleavage of the disulfide bond (Scheme 2.1 a).[20, 21] If the released protein from the particles has molecular pendants attached, it may elicit undesirable immune responses towards foreign antigens, which may induce adverse health effects. In addition, for therapeutic proteins, very often, lysine residues are also involved in the active sites and

modifying lysine residues with molecular pendants, if DSP is used, may abolish the protein activity.

In order to utilize protein-based particles for therapeutic applications like RNA replicon delivery, they are usually stabilized with cross-linkers, which can be cleaved under certain physiological stimuli.[22] The site of action for RNA replicon is cytoplasm of cells which is known for its high concentration of reduced glutathione (GSH) compared to the extracellular environment (GSH concentration differs by 1000 folds intracellularly and extracellularly).[23] In this study, we take advantage of the reducing environment in the cytoplasm of cells by introducing a disulfide-based cross-linker that should trigger the intracellular dissolution of our protein particles and release of RNA replicon from the particles. Our initial studies using DSP to cross-link BSA particles indicated that di-N-hydroxysuccinimide (NHS) ester is highly reactive towards lysine residues on BSA and it is very difficult to control the cross-linking density of BSA particles, which is essential to achieve desired dissolution profiles. In addition, even though DSP is advertised as a reversible cross-linker, it is not a "truly" reversible cross-linker as it will leave molecular pendants after disulfide cleavage under reducing environment (Scheme 2.1a).

All the aforementioned concerns motivated us to develop a truly reversible disulfide cross-linker with well-controlled reactivity. Wender et al. developed a disulfide based pro-drug linker, which contains a carbonate group instead of conventionally used ester linkage, to release the drug in its original state.[24, 25] This chemistry has also been applied to develop a fluorogenic probe for thiol

detection and a pro-drug for intracellular delivery.[26, 27, 28] Inspired by previous work, we substituted the ester moieties in DSP with carbonate groups and developed a novel cross-linker dithio-bis(ethyl 1 H-imidazole-1-carboxylate) (DIC) for this study (Scheme 2.1b).

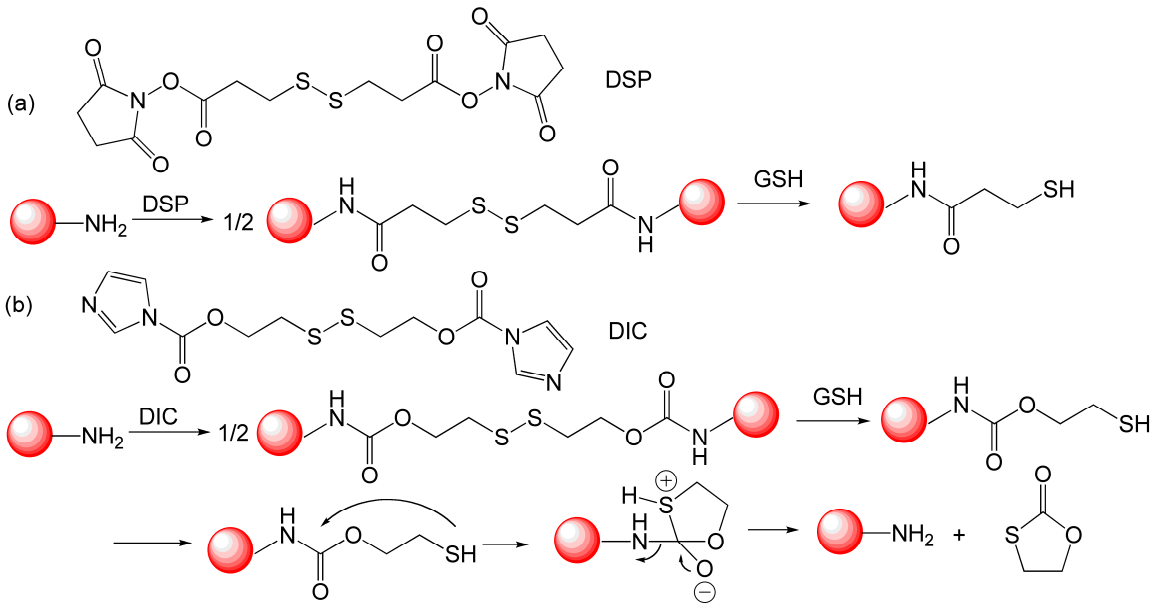

Scheme 2.1 (a) Structure of DSP and reaction scheme for protein crosslinking and dissolution; (b) Structure of DIC and reaction scheme for protein crosslinking and dissolution

2.4.2 Experiment section

2.4.2.1 Materials

Tyramine and 1'-Carbonyldiimidazole was purchased from Sigma Aldrich. DSP (Dithiobis[succinimidyl propionate]) were from Thermo Scientific. bis(2-hydroxyethyl)ether and 2-hydroxyethyl disulfide were purchased from Acros.

2.4.2.2 Synthesis of cross-linker dithio-bis(ethyl 1 H-imidazole-1-carboxylate) (DIC) and 2,2'-oxybis(ethane-2,1-diyl) bis(1H-imidazole-1-carboxylate) (OEDIC)

A solution of 2-hydroxyethyl disulfide (1g, 6.48mmol) in chloroform (50 mL) was added dropwise to a solution of 1,1'-Carbonyldiimidazole (10g, 61.67 mmol) in chloroform (300 mL) under reflux (Scheme 2.2 A). The reaction mixture was stirred for 24 hours. The mixture was washed with cold water three times and the organic layer was dried with magnesium sulfate, filtered, concentrated and purified by column chromatography (EtOAc/chloroform=95:5) to give DIC (0.85g) as clear oil, which turned to white solid upon cooling. The reaction of Bis(2-hydroxyethyl)ether (0.69g, 6.48mmol) with 1,1'-Carbonyldiimidazole (10g, 61.67mmol) gave OEDIC (0.73g) as clear oil, which turned to white solid upon cooling (Scheme 2.2 B). The synthesis and purification followed procedures described above for DIC.

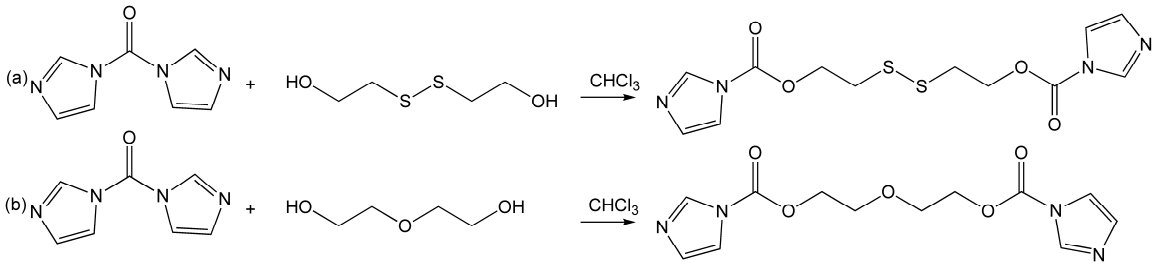

Scheme 2.2 Synthesis of cross-linker DIC (A) and OEDIC (B)

2.4.2.3 Characterization of cross-linkers

The compounds were dissolved in $CDCl_3$ and their structures were characterized by NMR spectrometry (^{1}H and ^{13}C). High-resolution mass spectrometry (Agilent technologies 6210 LC-TOF) was used to characterize the mass of the compounds.

2.4.2.4 Synthesis of tyramine-cross-linker compounds

Tyramine (0.24g, 1.75mmol) was added to a solution of DIC (0.12g, 0.35mmol) in isopropanol (15mL) (Scheme 2.3). The reaction mixture was stirred for 24 h at 40°C. The mixture was concentrated and purified by column chromatography (EtOAc) to give tyramine-DIC (0.10g) as light yellow solid. Tyramine (0.24g, 1.75mmol) was added to a solution of DSP (0.14g, 0.35mmol) in DMF (4mL). The reaction mixture was stirred for 24 h at 40°C. The reaction was stopped by adding water (15 mL) to the reaction mixture. Then the product was filtered and washed with water (10 mL) three times. The product tyramine-DSP (light yellow solid) was then dried and weighed (0.11g).

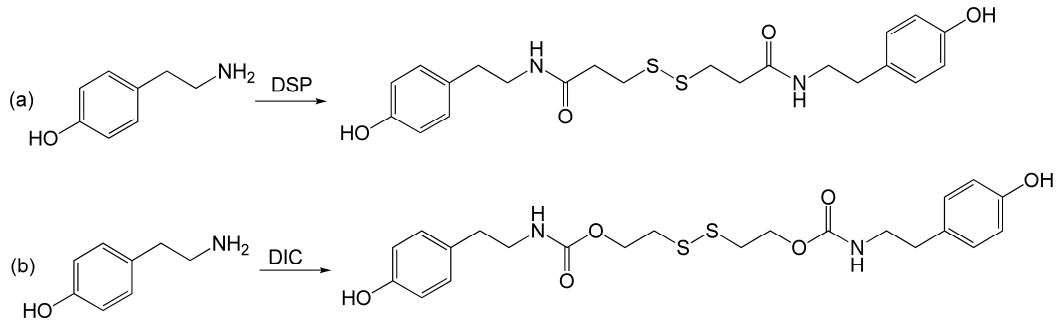

Scheme 2.3 Synthesis of tyramine-DIC (a) and tyramine-DSP (b)

2.4.2.4 Characterization of tyramine-cross-linker compounds

The compounds were dissolved in acetone-D6 and their structures were characterized by NMR spectrometry (^{1}H and ^{13}C). High-resolution mass spectrometry (Agilent technologies 6210 LC-TOF) was used to characterize the mass of the compounds.

2.4.2.5 Degradation of tyramine-cross-linker compounds

The products tyramine-DSP and tyramine-DIC were added to dithiothreitol solution (50 mM, PBS) at 37 °C and stirred for 24 h. Then the solutions were

lyophilized. Isopropanol (1 mL) was added to the powder acquired and bath sonicated for 15 min. The supernatants from the solutions were collected and analyzed by gas chromatography-mass spectrometry (Alilent Technologies 5975 series MSD, 7820A GC system) and untreated tyramine was used as standard.

Tyramine generated from tyramine-DIC was purified through thin layer chromatography (TLC) (EtOAc 90%, methanol 10%). ^{1}H NMR and mass spectrometry (Agilent technologies 6210 LC-TOF) were used to confirm the structure of the compound.

2.4.3 Results and discussion

The successful synthesis of cross-linkers (DIC, OEDIC) and tyramine-cross-linker compounds were confirmed by ^{1}H NMR, ^{13}CNMR and high-resolution mass spectrometry (Table 2.2, 2.3).

Table 2.2 Characterization of compounds by NMR

Compound	NMR Condition	Peak information
DIC	^{1}H, 400 MHz, $CDCl_3$	δ 8.18 (s, 2H), 7.45 (s, 2H), 7.11 (s, 2H), 4.71 (t, J = 6.8Hz, 4H), 3.11 (t, J = 6.4Hz, 4H)
DIC	^{13}C, 150 MHz, $CDCl_3$	δ 36.3, 65.6, 117.2, 130.8, 137.1, 148.4
OEDIC	^{1}H, 600 MHz, $CDCl_3$	δ 8.17 (s, 2H), 7.43 (s, 2H), 7.10 (s, 2H), 4.61 (t, J = 6.6Hz, 4H), 3.89 (t, J = 7.2Hz, 4H)
OEDIC	^{13}C, 150 MHz, $CDCl_3$	δ 66.5, 68.4, 115.9, 130.5, 137.0, 148.4
Tyramine-DIC	^{1}H, 400 MHz, actone-D6	δ 7.07 (d, J=8.4Hz, 4H), 6.78 (d, J=8Hz, 4H), 4.28(t, J=7.6Hz, 4H), 3.33 (q, J = 6.4Hz, 4H), 2.98 (t, J = 6.4Hz, 4H), 2.74(t, J=7.2Hz, 4H)
Tyramine-DIC	^{13}C, 100 MHz, actone-D6	δ 155.8, 130.1, 129.6, 115.2, 115.1, 62.0, 42.6, 37.8, 35.1

Tyramine-DSP	^{1}H, 400 MHz, actone-D6	δ 7.08 (d, J=8.4Hz, 4H), 6.78 (d, J=8.8Hz, 4H), 3.41(q, J=7.6Hz, 4H), 2.98 (t, J = 7.2Hz, 4H), 2.73(t, J=7.2Hz, 4H), 2.57(t, J=6.8Hz, 4H)
Tyramine-DSP	^{13}C, 100 MHz, actone-D6	δ170.4, 156.0, 130.0, 129.6, 115.3, 41.0, 35.4, 34.7, 34.4

Table 2.3 Characterization of compounds by high-resolution mass spectrometry

Compound	m/z	m/z (calculated)
DIC	365.0346 (M+Na)+	365.0354 (M+Na)+
OEDIC	317.0859 (M+Na)+	317.0862 (M+Na)+
Tyramine-DIC	503.1274 (M+Na)+	503.1287 (M+Na)+
Tyramine-DSP	471.1388 (M+Na)+	471.1388 (M+Na)+

Compared to DSP, DIC has several advantages. Imidazoles were introduced as the leaving groups in DIC to replace the highly reactive NHS as in DSP in order to better control the rate of the cross-linking reaction and the cross-linking density on the particle surface. Furthermore, DIC is a “traceless” reversible cross-linker, which does not leave any molecular pendants after disulfide cleavage (Scheme 2.1b). Losing a stable five-membered ring structure is the driving force for this reaction cascade.

To demonstrate the ability of DIC to release the amino group in its original form after cleavage of the disulfide, we utilized tyramine as a model, a small molecule with only one amino group. Two tyramine molecules were reacted with DIC in isopropanol, which completely simulates the cross-linking conditions for protein-based particles (Scheme 2.3). To prove this unique property of DIC, the commercially available disulfide cross-linker DSP was used as a control in this

study. The dimer products were denoted as tyramine-DIC and tyramine-DSP, respectively. Both compounds were treated with 50 mM of dithiothreitol (DTT) in phosphate buffer saline (PBS) to cleave the disulfide bond. Gas chromatography mass spectrum (GC-MS) results indicated that after cleavage of the disulfide bond, tyramine was regenerated from tyramine-DIC. No peak of tyramine was observed with tyramine-DSP (Figure 2.7). In addition, ^{1}H-NMR and high-resolution mass spectrometry confirmed the structure of tyramine recovered after DTT treatment of tyramine-DIC. (Table 2.4) Therefore, all the aforementioned results support the successful design of the novel DIC cross-linker.

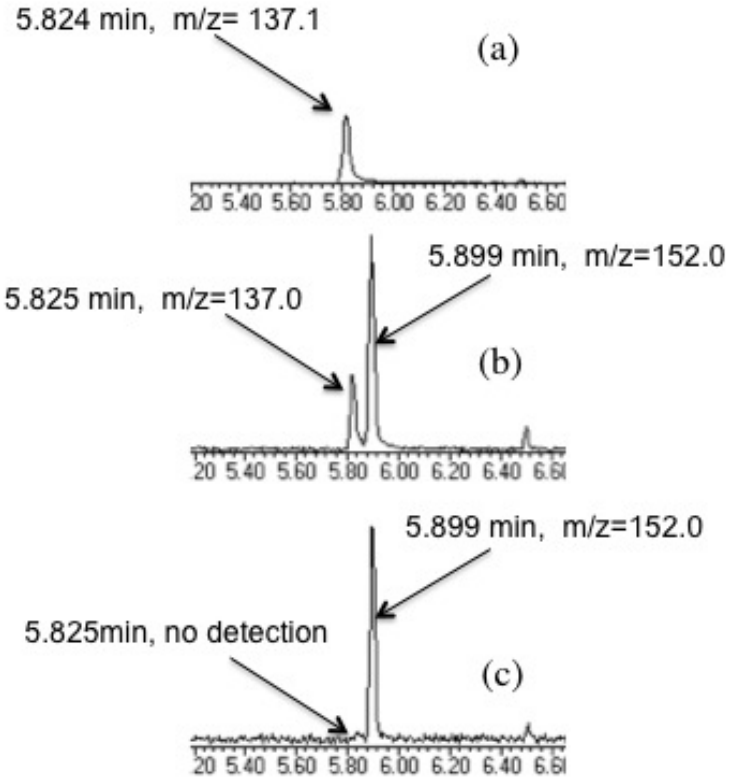

Figure 2.7 GC-MS characterization of tyramine-DIC and tyramine-DSP after treatment with DTT, (a) standardard tyramine, (b) tyramine-DIC, (c) tyramine-DSP. The peak at 5.899 min (m/z=152.0) in (b) and (c) represents oxidized DTT.

Table 2.4 Characterization of tyramine by ^{1}H NMR and high-resolution mass spectrometry

Compound	^{1}H NMR (400 MHz, MeOD)	MS (m/z) [a]
Tyramine standard	δ 7.02 (d, J=4.2 Hz, 2H), 6.71 (d, J=4.2 Hz, 2H), 2.81 (t, J = 7.2 Hz, 2H), 2.65(t, J=7.2 Hz, 2H)	138.0914 (M+H)+
Tyramine generated from tyramine-DIC	δ 7.02 (d, J=4.2 Hz, 2H), 6.71 (d, J=4.2 Hz, 2H), 2.82 (t, J = 7.2 Hz, 2H), 2.65(t, J=7.2 Hz, 2H)	138.0916 (M+H)+

[a] m/z calculated for tyramine $[M+H]^{+}$=138.0919

2.4.4 Conclusions

A novel disulfide-based cross-linker was synthesized and the structure was confirmed by ^{1}H-NMR, ^{13}C-NMR and MS. By using tyramine as a model molecule, DIC demonstrated the ability to release the amino group in its original form after cleavage of the disulfide, a benefit over commercially available protein cross-linker DSP.

2.5 Stabilization of Protein Particles with Cross-linker DIC

2.5.1 Introduction

Having successfully fabricated protein-based particles using PRINT technology and synthesized the disulfide-based cross-linker DIC, the cross-linker was applied to stabilize the protein-based particles transiently. This method is ideal for utilizing the protein-based particles for therapeutic applications especially for RNA replicon delivery.

2.5.2 Experimental section

2.5.2.1 Materials

Bovine serum albumin was from Calbiochem. Alexa fluor 555® labeled bovine serum albumin was purchased from invitrogen. Bovine albumin ELISA quantitation set was purchased from Bethyl Laboratories, Inc. α-D-Lactose, glutathione and glycerol, were purchased from Acros. Cross-linkers DIC and OEDIC were synthesized as previously described.

2.5.2.2 Prepartion of cross-linked protein particles

The Alexa fluor 555® labeled protein particles (1μm × 1μm, cylindrical) were prepared as previously described in section 2.3.2.2. The particle concentration in isopropanol was determined by Thermal Gravimetric Analysis (TGA) (TA Q5000). Based on the TGA results, an appropriate amount of isopropanol was added to the particle dispersion to achieve a particle concentration of 1mg/mL. To 850 μL of particle dispersion, cross-linkers (1.275 mg, 1.913 mg, 2.869 mg of DIC, corresponding to 4.4 mM, 6.6 mM and 9.9 mM in the final solution, 1.096 mg of OEDIC corresponding to 4.4 mM in the final solution) was added. The resulting dispersion was shaken on a vortex machine for 24 h at 40 °C. The reaction was terminated by centrifuging particles down for 3 minutes, followed by removal of the supernatant containing the cross-linker and adding 850μL of isopropanol. The particles were washed three times with isopropanol by centrifugation to remove the excess cross-linkers and then resuspended in water.

2.5.2.3 Characterization of cross-linked particles using SEM, DLS and Zeta-sizer

The PRINT particles were imaged by a scanning electron microscopy (Hitachi modelS-4700) and the hydrodynamic diameters of the PRINT particles were measured by dynamic light scattering (Brookhaven Instruments Inc., 90Plus). For zeta potential measurements, the particles were dispersed in 1 mM potassium chloride at a concentration of 20 μg/ml and tested by a Zetasizer Nano Analyzer (Malvern Instruments Inc., Nano Zetasizer).

2.5.2.4 Particle dissolution profile measurements

The release of Alexa Fluor® 555-conjugated BSA was used to characterize the dissolution rate of the particles. The cross-linked particles were resuspended in water to achieve a particle concentration of 1.33 mg/mL. To each mini dialysis unit (purchased from Fisher Scientific, MWCO 20K), 75 μL of particle solution was added. Typically, 24 units were dialyzed against 1 L of Phosphate Buffers Saline solution (PBS) containing 5 mM glutathione with a magnetic bar stirring gently at the bottom of the beaker. Another 24 units were dialyzed against 1 L of PBS buffer without glutathione as controls. The dialysis process was carried out in a 37 °C incubator. At different time points (0 h, 1.5 h, 3 h, 5 h, 12 h, 24 h, 48 h), one unit was withdrawn from each bath. The particle solution was recovered from the units and each unit was washed with 75 μL of PBS. The wash was combined with recovered particle solution and appropriate amount of PBS was added to achieve a total mass of 200 mg. The solution was centrifuged at 14000 rpm for 10 min. The supernatant was measured for

fluorescence (excitation 545 nm, emission 575 nm) by a SpectraMax M5 plate reader (Molecular Devices). The fluorescence from PBS was used as background and the fluorescence from un-cross-linked particles (0.5 mg/mL in PBS) was used as a 100% control.

2.5.2.5 Albumin binding activity after particle dissolution

The BSA particles were cross-linked at 4.4 mM of DIC for 24 h at 40°C and incubated in PBS containing 5mM GSH for 5 h. The solution was then dialyzed against water for 2 h to remove GSH. The concentration of BSA was quantified by BCA assay and standard sandwich ELISA assays for BSA (Bethyl Laboratories, Montgomery, TX) were conducted following the protocol provided by the vendor. Absorbance was measured with a SpectraMax M5 plate reader (Molecular Devices) at 450 nm.

2.5.2.6 Study of the depth of cross-linking reaction on particles

The cross-linking of the particles was performed after PRINT process. The goal of this study is to determine if the cross-linking also occurs in the center of the particles. A macroscopic film that is prepared on PET sheet from 36.5 wt% of BSA, 1 wt% of Alexa fluor 555 labeled BSA, 37.5 wt% of lactose and 25 wt% of glycerol, the same composition as the PRINT particles used in this study. The film is shown in orange and PET is shown in gray. The film was washed with isopropanol three times in order to mimic the particle fabrication process and then reacted with DIC at 4.4 mM of cross-linker concentration for 24 h at 40 ℃. Then the film was collected with PBS using cell scraper. The solution was vortexed for 1 h and centrifuged down for 10 min at 14000 rpm to remove the

cross-linked material. The supernatant was analyzed using fluorescence spectrometry for the amount of free protein and the percentage of free protein was calculated using un-cross-linked film as 100% control.

2.5.3 Results and discussion

The stabilization of PRINT albumin particles in aqueous solutions was achieved by introducing DIC which reacts with the amine groups on the surface of protein molecules (Figure 2.8 A). Particles cross-linked with this disulfide cross-linker can take advantage of the high concentration of intracellular GSH and selectively release encapsulated cargo when they reach cytoplasm. As a control, a non-disulfide non-degradable cross-linker, 2,2'-oxybis(ethane-2,1-diyl) bis(1H-imidazole-1-carboxylate) (OEDIC) was also synthesized and used as a control (Figure 2.8 B).

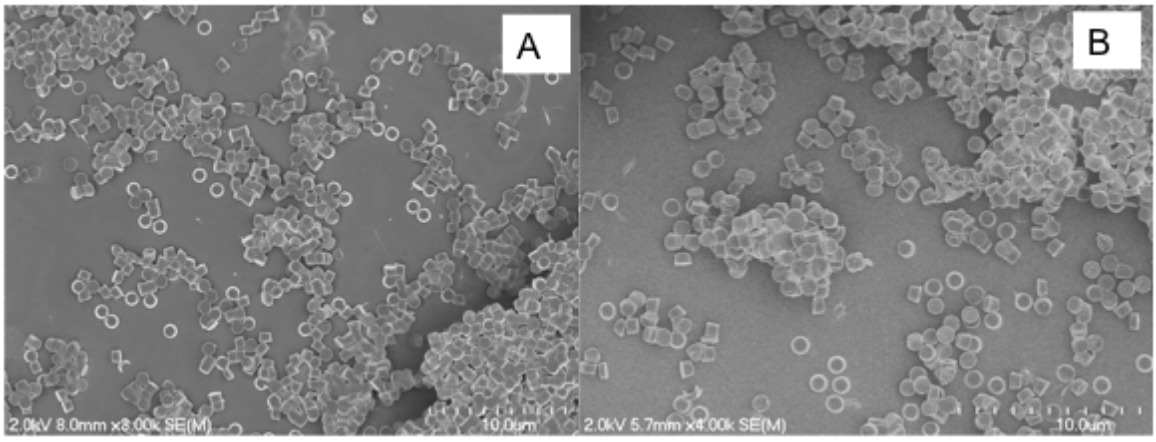

Figure 2.8 SEM images of BSA particles after incubation with water. (A) Particles were cross-linked at 4.4 mM of DIC, (B) particles were cross-linked at 4.4 mM of OEDIC.

BSA particles were crosslinked with DIC and OEDIC at different cross-linker concentrations (based on a constant particle concentration). The cross-linked PRINT protein particles were characterized by dynamic light scattering (DLS) and ζ-potential analyzer. The particles displayed a hydrodynamic diameter around 1 micron and a narrow polydispersisity (Table 2.5). Because the isoelectric point of BSA is around 4.75, crosslinked BSA particles showed a slightly negative ζ-potential. Particles cross-linked at higher cross-linker concentrations showed more negative ζ-potentials due to less free amino groups on the particle surface.

Table 2.5 Characterization of cross-linked BSA particles [a]

	Diameter, [b] nm	**PDI [c]**	**ζ-Potential, [d] mV**
DIC-4.4 mM	1201 ± 152	0.016	-13.6 ± 0.5
DIC-6.6 mM	1164 ± 393	0.114	-16.3 ± 1.0
DIC-9.9 mM	1069 ± 346	0.105	-23.1 ± 0.4
OEDIC-4.4 mM	1069 ± 362	0.114	-10.9 ± 0.3

[a] The particles fabricated for dissolution study. DIC-4.4 mM: particles cross-linked with DIC at 4.4 mM. DIC-6.6 mM: particles cross-linked with DIC at 6.6 mM. DIC-9.9 mM: particles crosslinked with DIC at 9.9 mM. OEDIC-4.4 mM: particles cross-linked with OEDIC at 4.4 mM. [b] Hydrodynamic diameter measured by dynamic light scattering. The average hydrodynamic diameters were obtained from three measurements. The error bars are the half-width of the effective diameters. [c] Polydispersity index from the dynamic light scattering measurements. [d] ζ-potential was measured in 1mM KCl by Zetasizer. The error bars are standard deviations from three measurements.

A quantitative study of particle dissolution was performed. The GSH concentration in cytoplasm of cells ranges from 1 to 15 mM.[23] In this study, PBS containing 5 mM GSH and PBS only were used to simulate intracellular and extracellular environment, respectively. In order to monitor the degradation of

albumin particles, 1 wt% of BSA Alexa Fluor® 555 conjugate was incorporated into the particles and the amount of this dye-conjugated protein released from particles upon particle dissolution was measured using fluorescence spectroscopy (Figure 2.9). A plot of Alexa Fluor® 555 conjugate release versus time for particles cross-linked with DIC at 4.4 mM showed an accelerated rate of dissolution when dispersed in PBS with 5 mM GSH. The same particles dispersed in PBS only showed minimal dissolution at 48 h. Under identical conditions, particles cross-linked with OEDIC showed no noticeable difference in PBS with and without GSH. Particles cross-linked with the DIC at 6.6 mM also dissolved preferentially in PBS with GSH, but the rate was noticeably slower than particles cross-linked using 4.4 mM of DIC. When particles were cross-linked with the DIC cross-linker at 9.9 mM, very minimal dissolution of particles was observed both in PBS with GSH and PBS only during a 48-h time frame.

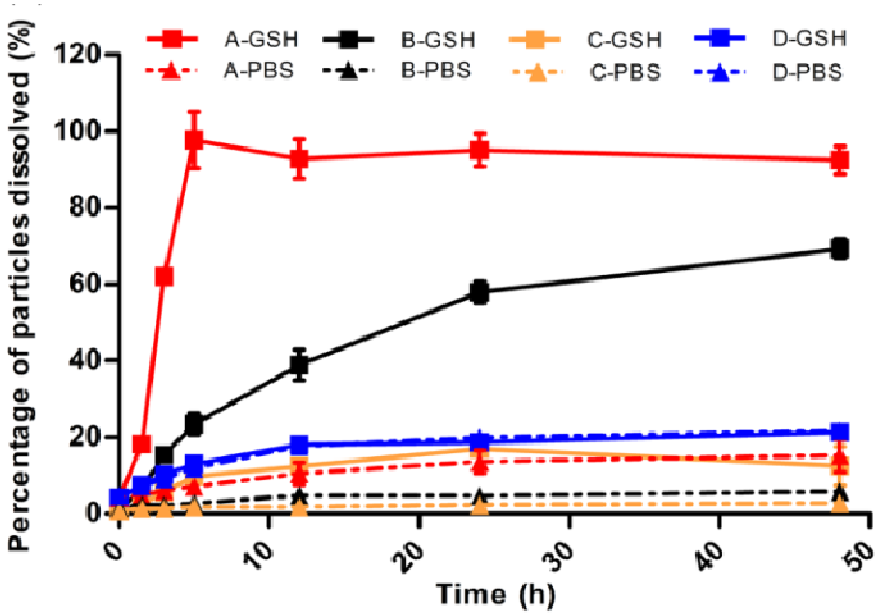

Figure 2.9 Dissolution profile of cross-linked BSA particles in PBS containing 5 mM GSH (GSH) and PBS only (PBS), A: particles cross-linked at 4.4 mM of DIC,

B: particles cross-linked at 6.6 mM of DIC, C: particles cross-linked at 9.9 mM of DIC, D: particles cross-linked at 4.4 mM of OEDIC. Squares with solid lines represent 5 mM GSH containing PBS and triangles with dotted lines represent PBS only. The error bars stand for the standard deviation calculated from three wells.

Fluorescence microscopy was also used to further investigate the integrity of particles cross-linked with DIC and OEDIC at 4.4 mM of cross-linker concentration (Figure 2.10).

From these data, it was apparent that the particles cross-linked with the disulfide linker DIC preferentially dissolved under reducing conditions and the rate of particle dissolution can be effectively modulated by changing the cross-linker concentration used. Alternatively, the cross-linking reaction time can also be used as a parameter to fine tune the particle cross-linking densities and release profiles.

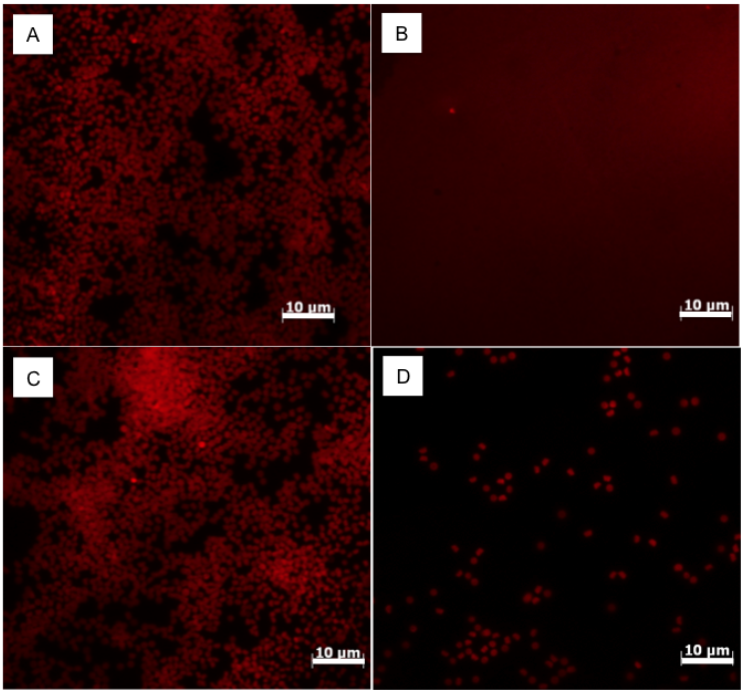

Figure 2.10 Particle dissolution by microscopy image at 5-h time point. (A) Particles cross-linked with 4.4 mM of DIC, in PBS, (B) Particles cross-linked with 4.4 mM of DIC, in PBS containing 5 mM of GSH, (C) Particles cross-linked with

4.4 mM of OEDIC, in PBS (D) Particles cross-linked with 4.4 mM of OEDIC, in PBS containing 5 mM of GSH

In this proof-of-concept study, we are also interested in the integrity of BSA after fabrication and crosslinking process, because it may lead to the delivery of therapeutic proteins of interest using this strategy. To evaluate the biological integrity of the protein after dissolution of the DIC cross-linked particles, enzyme-linked immunosorbent assays (ELISA) were performed on native BSA and BSA released from DIC-cross-linked PRINT BSA particles in PBS with 5mM glutathione, as well as heat denatured BSA. Several concentrations were compared over the sampling range of the assays (Figure 2.11). The results of the assay indicated that the albumin dissolved from the cross-linked particles (squares) had very similar absorbance in the ELISA assay as the native albumin (triangles). The denatured free protein (tilted squares) showed significantly less total absorbance compared to free protein and dissolved particles. ELISA relies upon protein-protein interactions, thus providing insight into the preservation of the protein's binding motifs. The ELISA data illustrated that antibody recognition and protein binding ability of BSA are minimally affected in the PRINT and cross-linking process for albumin.

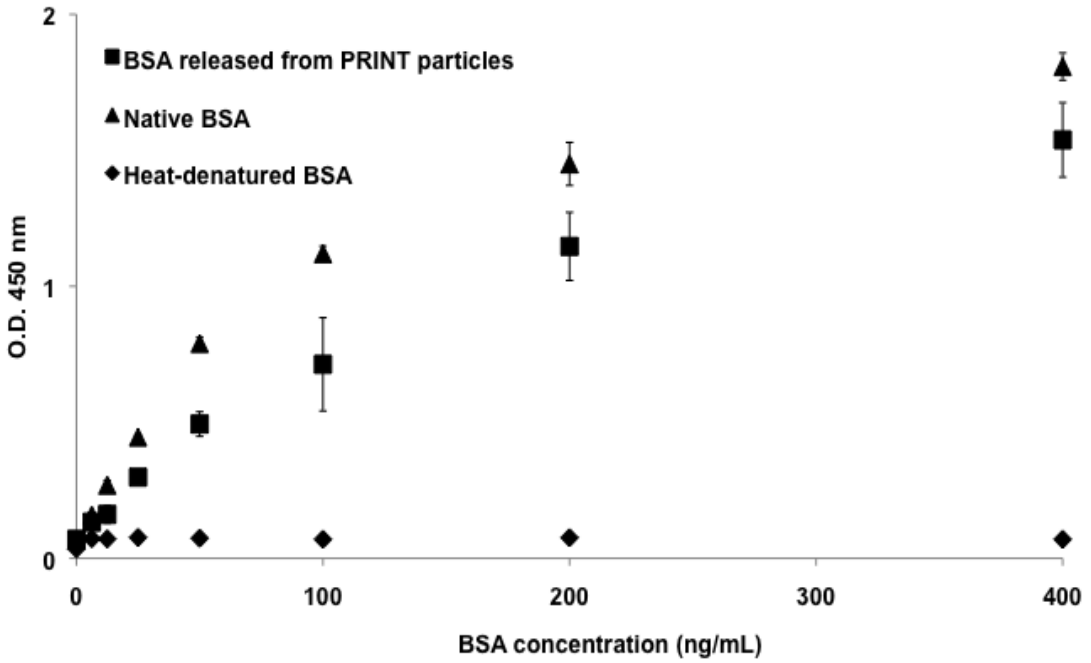

Figure 2.11 The BSA activity measured by ELISA. Square represents BSA released from DIC-cross-linked PRINT particles, triangle represents untreated BSA, and tilted square represents heat-denatured BSA.

The cross-linking depth in one dimension can be determined. If the cross-linking occurs close to the bottom of the a macroscopic film, minimal of free protein can be released after the cross-linking reaction. If the cross-linking reaction only occurs at the surface of the film, the free protein in the center will instantaneously dissolve upon exposure to PBS.

Films with thicknesses of 200 nm, 500 nm and 1.6 µm after 24 h of cross-linking reaction and films with a thickness of 500 nm for 4 h and 14 h of cross-linking reaction were examined. Each experiment was done in triplicate.

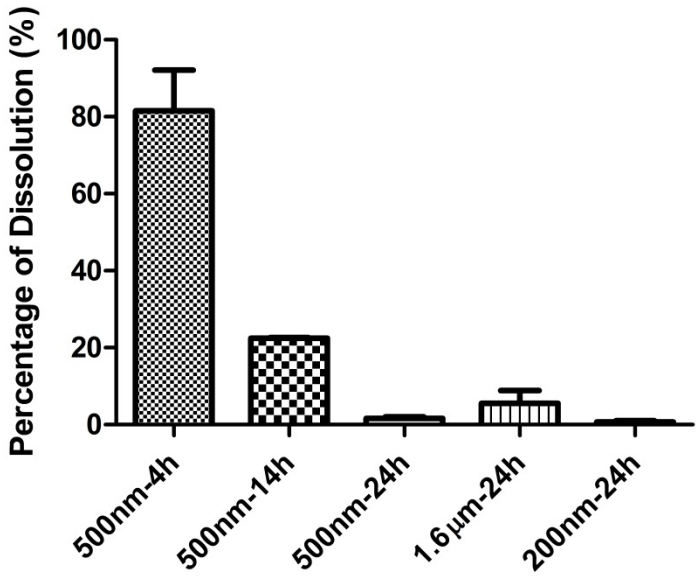

Figure 2.12 Percentage of dissolution of macroscopic films of different thickness and cross-linked for different length of times

Figure 2.12 showed that after 24 hour of cross-linking reaction, the films with thicknesses from 200nm to 1.6 μm all showed minimal dissolution, indicating that the film was cross-linked at the bottom of the film and the cross-linking reaction can penetrate at least 1.6 μm in one dimension. At 4-h and 14-h, the 500nm film was only partially cross-linked.

Based these results, we can come to the conclusion that the cross-linking reaction occurs at the center of the 1-micron cylindrical particles.

2.5.4 Conclusions

From these data, it was apparent that the particles cross-linked with the disulfide linker DIC preferentially dissolved under reducing conditions and the rate of particle dissolution can be effectively modulated by changing the cross-linker concentration used. Alternatively, the cross-linking reaction time can also

be used as a parameter to fine tune the particle cross-linking densities and release profiles. The ELISA data showed that antibody recognition and protein binding ability of BSA are minimally affected in the PRINT and cross-linking process for albumin.

2.6 Summary of conclusions and recommendation for future work

In summary, a novel method for the fabrication of protein (BSA) particles that uses a novel cross-linker strategy was able to effectively render the particles transiently insoluble in aqueous solutions. This particle fabrication method built on PRINT technology platform allows for the fabrication of particles of controlled sizes and shapes. A disulfide cross-linker for the stabilization of the particles was synthesized and applied on the particles. The particles cross-linked with the cross-linker preferentially dissolved under reducing conditions and the rate of particle dissolution can be controlled by adjusting the cross-linker concentration used. These results suggested that these precisely engineered protein particles can be used as carriers for nucleic acids like RNA replicon. In addition, the antibody recognition and protein binding ability of BSA were minimally affected in the PRINT and cross-linking processes, indicating that this method could be applied to delivery of functional proteins to the cytoplasm of cells.

REFERENCES

1. Hawkins, M. J.; Soon-Shiong, P.; Desai, N., Protein nanoparticles as drug carriers in clinical medicine. Advanced Drug Delivery Reviews 2008, 60 (8), 876-885.

2. MaHam, A.; Tang, Z.; Wu, H.; Wang, J.; Lin, Y., Protein-Based Nanomedicine Platforms for Drug Delivery. Small 2009, 5 (15), 1706-1721.

3. Vandelli, M. A.; Rivasi, F.; Guerra, P.; Forni, F.; Arletti, R., Gelatin microspheres crosslinked with D,L-glyceraldehyde as a potential drug delivery system: preparation, characterisation, *in vitro* and *in vivo* studies. Int J Pharm 2001, 215 (1-2), 175-84.

4. Muller, B. G.; Leuengerger, H.; Kissel, T., Albumin nanospheres as carriers for passive drug targeting: an optimized manufacturing technique. Pharmaceutical Research 1996, 13, 32-37.

5. Chen, L.; Remondetto, G. E.; Subirade, M., Food protein-based materials as nutraceutical delivery systems. Trends in Food Science & Technology 2006, 17 (5), 272-283.

6. Fischer, D.; Bieber, T.; Bru¨sselbach, S.; Elsa¨sser, H.-P.; Kissel, T., Cationized human serum albumin as a non-viral vector system for gene delivery? Characterization of complex formation with plasmid DNA and transfection efficiency. International Journal of Pharmaceutics 2001, 25, 97-111.

7. Abbasi, S.; Paul, A.; Prakash, S., Investigation of siRNA-Loaded Polyethylenimine-Coated Human Serum Albumin Nanoparticle Complexes for the Treatment of Breast Cancer. Cell Biochemistry and Biophysics 2011, 61 (2), 277-287.

8. Yan, H.-B.; Zhang, Y.-Q.; Ma, Y.-L.; Zhou, L.-X., Biosynthesis of insulin-silk fibroin nanoparticles conjugates and *in vitro* evaluation of a drug delivery system. Journal of Nanoparticle Research 2008, 11 (8), 1937-1946.

9. Iida, A.; Hasegawa, M., SeV RNA Replicon Vector: An Efficient Cytoplasmic Expression System Derived from Sendai Virus Self_Replicating Ribonucleoprotein Complexes. Molecular Therapy 2004, 9, 275.

10. Weber, C.; Coester, C.; Kreuter, J.; Langer, K., Desolvation process and surface characterisation of protein nanoparticles. Int J Pharm 2000, 194 (1), 91-102.

11. Patil, G. V., Biopolymer albumin for diagnosis and in drug delivery. Drug Development Research 2003, 58 (3), 219-247.

12. Maa, Y.-F.; Nguyen, P.-A.; Sweeney, T.; Shire, S. J.; Hsu, C. C., Protein Inhalation powders: Spray drying vs spray freeze drying. Pharmaceutical Research 1999, 16, 249-254.

13. Whitaker, M. J.; Hao, J.; Davies, O. R.; Serhatkulu, G.; Stolnik-Trenkic, S.; Howdle, S. M.; Shakesheff, K. M., The production of protein-loaded microparticles by supercritical fluid enhanced mixing and spraying. J Control Release 2005, 101 (1-3), 85-92.

14. Han, Y.; Tian, H.; He, P.; Chen, X.; Jing, X., Insulin nanoparticle preparation and encapsulation into poly(lactic-co-glycolic acid) microspheres by using an anhydrous system. Int J Pharm 2009, 378 (1-2), 159-66.

15. Wang, Y.; Caruso, F., Nanoporous Protein Particles Through Templating Mesoporous Silica Spheres. Advanced Materials 2006, 18 (6), 795-800.

16. Kelly, J. Y.; DeSimone, J. M., Shape-specific, monodisperse nano-molding of protein particles. J Am Chem Soc 2008, 130 (16), 5438-9.

17. Desai, N.; Trieu, V.; Yao, Z.; Louie, L.; Ci, S.; Yang, A.; Tao, C.; De, T.; Beals, B.; Dykes, D.; Noker, P.; Yao, R.; Labao, E.; Hawkins, M.; Soon-Shiong, P., Increased antitumor activity, intratumor paclitaxel concentrations, and endothelial cell transport of cremophor-free, albumin-bound paclitaxel, ABI-007, compared with cremophor-based paclitaxel. Clin Cancer Res 2006, 12 (4), 1317-24.

18. Chatterjee, J.; Haik, Y.; Chen, C.-J., Synthesis and characterization of heat-stabilized albumin magnetic microspheres Colloid and Polymer Science 2001, 279, 1073-1081.

19. Arshady, R., Albumin microspheres and microcapsules: methodology of manufacturing techniques. Journal of Controlled Release 1990, 14, 111-131.

20. Wu, L. N. Y.; Fisher, R. R., Subunit structure of submitochondrial particle membrane transhydrogenase. The Journal of Biological Chemistry 1983, 258, 7847-7851.

21. Yu, M.; Ng, B. C.; Rome, L. H.; Tolbert, S. H.; Monbouquette, H. G., Reversible pH lability of cross-linked vault nanocapsules. Nano Lett 2008, 8 (10), 3510-5.

22. Yan, M.; Du, J.; Gu, Z.; Liang, M.; Hu, Y.; Zhang, W.; Priceman, S.; Wu, L.;

Zhou, Z. H.; Liu, Z.; Segura, T.; Tang, Y.; Lu, Y., A novel intracellular protein delivery platform based on single-protein nanocapsules. Nat Nanotechnol 2010, 5 (1), 48-53.

23. Saito, G.; Swanson, J. A.; Lee, K.-D., Drug delivery strategy utilizing conjugation via reversible disulfide linkages: role and site of cellular reducing activities. Advanced Drug Delivery Reviews 2003, 55, 199-215.

24. Dubikovskaya, E. A.; Thorne, S. H.; Pillow, T. H.; Contag, C. H.; Wender, P. A., Overcoming multidrug resistance of small-molecule therapeutics through conjugation with releasable octaarginine transporters. Proceedings of the National Academy of Sciences 2008, 105 (34), 12128-12133.

25. Jones, L. R.; Goun, E. A.; Shinde, R.; Rothbard, J. B.; Contag, C. H.; Wender, P. A., Releasable luciferin-transporter conjugates: tools for the real-time analysis of cellular uptake and release. J Am Chem Soc 2006, 128 (20), 6526-7.

26. Namanja, H. A.; Emmert, D.; Davis, D. A.; Campos, C.; Miller, D. S.; Hrycyna, C. A.; Chmielewski, J., Toward Eradicating HIV Reservoirs in the Brain: Inhibiting P-Glycoprotein at the Blood–Brain Barrier with Prodrug Abacavir Dimers. Journal of the American Chemical Society 2012, 134 (6), 2976-2980.

27. Pires, M. M.; Chmielewski, J., Fluorescence Imaging of Cellular Glutathione Using a Latent Rhodamine. Organic Letters 2008, 5, 837-840.

28. Li, C.; Wu, T.; Hong, C.; Zhang, G.; Liu, S., A General Strategy To Construct Fluorogenic Probes from Charge-Generation Polymers (CGPs) and AIE-Active Fluorogens through Triggered Complexation. Angew Chem Int Ed Engl 2011.

CHAPETER 3

RNA REPLICON DELIVERY VIA PROTEIN-BASED PRINT PARTICLES: IMPLICATIONS FOR NUCLEIC ACID VACCINE

3.1 Introduction

The use of RNA replicons for vaccines, as previously mentioned, is a nucleic acid-based method to express antigens in the cytoplasm of host cells and has great promise to trigger effective immune responses against a variety of diseases. To test the efficacy of the protein-based particles that can be rendered transiently insoluble in extracellular environment and preferentially dissolve in intracellular environment, RNA replicons were explored as the active cargo for intracellular delivery.

The delivery of RNA replicons require that the cargos be delivered to the cytoplasm of host cells and the drug delivery system faces both anatomical and cellular barriers. Depending on the administration route, the delivery vector may encounter serum proteins, nucleases, macrophages and clearance by the reticuloendothelial system (RES) that will disable the vector from reaching their target. Once at the tissue of interest, the delivery vector must enter the cell through endocytosis pathways or protein transduction domains such as TAT peptides.[1] And depending on the cell uptake mechanism, the vector may have to

follow the endo-lysosomal pathways and the vector has to escape the endosomal compartment and get into the cytoplasm before being degraded in a lysosome.

Particles have to be designed to meet all the aforementioned criteria to successfully deliver the RNA replicon *in vivo*. Frequently a cationic component was introduced into the particle to: 1) facilitate cell uptake through electrostatic interactions between positively charged particles and negatively charged cell membrane, 2) promote endosomal escape and particle transfection through the "proton sponge effect" or destabilization of endosomal membranes.

Protein-based particles have been used for gene delivery. Several groups reported the strategy to incorporate poly (ethylene imine) (PEI) into protein-based particles, which achieved successful delivery of siRNA[2] and plasmid DNA[3,4]. Another strategy reported was to prepare particles from cationized protein which may function the same way as other cationic polymers do in facilitating cell uptake and endosomal escape.[5] However, some research groups reported successful transfection of cationized protein particles and delivery of gene cargos [6, 7, 8, 9] while some groups reported that the cationized protein achieved only low transfection efficiencies and cells needed to be treated with choloroquine to achieve endosomal escape.[5]

A RNA replicon is, by nature, a piece of messenger RNA (mRNA) with replication features. The non-viral delivery of mRNA using cationic lipids including 1,2-di-O-octadecenyl-3-trimethylammonium propane (DOTMA),[10] N-[1-(2,3-dioleoloxy)propyl]-N,N,N-trimethyl ammonium chloride (DOTAP)[11, 12, 13, 14] etc. has been described. The DOTAP-based lipoplexes were the most effective

one in delivering mRNA and so far showed the highest activity according to most published reports. Enhancement of protein expression of the DOTAP-mRNA system was also achieved through incorporation of an inorganic nano-apatite,[15] and modification of the mRNA structure.[13] The use of polycations for delivery of mRNA, however, is not as widely studied as compared with plasmid DNA and siRNA. Only several cationic polymers including DEAE-dextran,[10] poly(L-lysine) (PLL)[16] and dendrimers[17] have been used to complex and deliver mRNA. Bettinger T. et al. compared several synthetic vectors including PEI (25 kDa and 2 kDa), PLL (54 kDa and 3.4 kDa), and a short polycation melittin in mRNA transfection. [14] The results indicated that PEI 25 kDa and PLL 54 kDa were not able to mediate protein expression in a cell-free translation assay following cytoplasmic injection into cells, probably due to binding that was too strong between the mRNA and the polycations and free mRNA could not be released to enable the expression of protein (Figure 3.1). In contrast, PEI 2 kDa and PLL 3.4 kDa could give high protein expression but were dependent on chloroquine for successful transfection. And when a melittin peptide was conjugated to PEI 2 kDa, the lipoplex formed with mRNA mediated efficient translation of mRNA in cells. The issue of effective transfection and release of mRNA by polycations was also accessed by cross-linking low Mw polycations using a reducible linker which can be cleaved by the intracellular reducing environment.[18] Instead of complexing the mRNA with cationic polymers, Su X. et al. developed a strategy to complex mRNA to the surface of cationic, core-shell structured nanoparticles with a poly(β-amino ester) (PBAE) core enveloped by a phospholipid bilayer

shell.[19] This system achieved delivery of mRNA both *in vitro* and *in vivo* with minimal toxicity and demonstrated the advantage of particles in mRNA delivery.

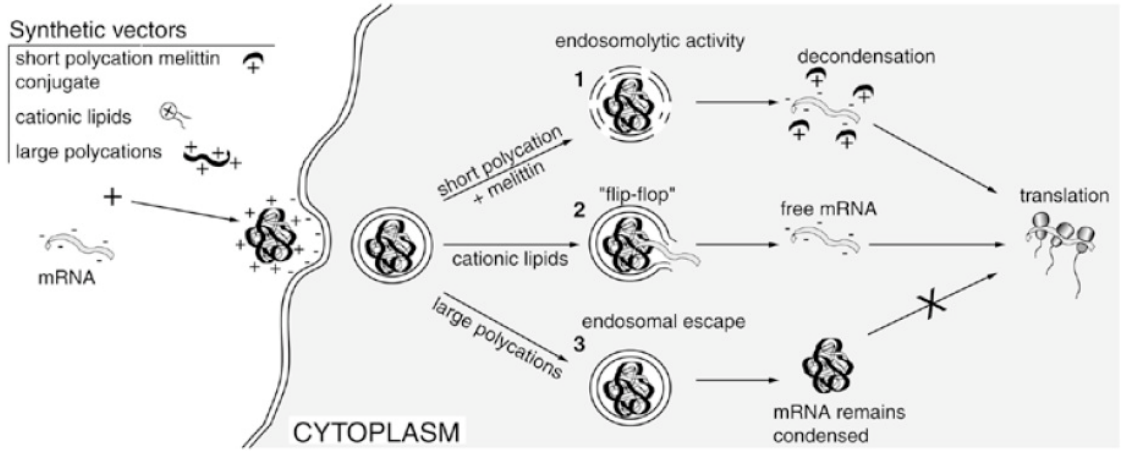

Figure 3.1 Proposed intracellular fate of delivered mRNA, adapted from [14].

Based on the aforementioned studies of protein-based particles for gene delivery and non-viral vectors for mRNA delivery, we designed two strategies to deliver an RNA replicon with the PRINT protein particle.

1) Cationized BSA (cBSA) was used as the particle matrix. The cationic protein may be able to facilitate internalization of particles in the cells and transfection of particles, potentially releasing the cargo once in the cytoplasm of cells.

2) Normal BSA was used as the particle matrices. The negative-charged particles could then be decorated with the cationic agents that can facilitate cell uptake and particle transfection.

Model RNA replicon encoding for chloramphenicol acetyl transferase (CAT), green fluorescence protein (GFP), and Luciferase protein were chosen in this study because CAT, GFP and Luciferase proteins are exogenous for mammalian cells and the assays to quantify the activity of those three proteins

have been well established. CAT is a bacterial enzyme and Luciferase is an enzyme that catalyzes luminescent reactions and has been widely used in non-invasive bioluminescence imaging research. RNA replicons endcoding for the GFP protein was chosen due to the fact that GFP protein exhibits bright green fluorescence when exposed to ultraviolet blue light, which can be easily visualized with fluorescent microscope.

3.2 Incorporation of RNA Replicon into BSA Particles

3.2.1 Introduction

Normal BSA was chosen as the particle matrix since the RNA replicon and BSA are both readily soluble in aqueous solutions and negative-charged molecules in water. RNA replicon and protein appear to be perfectly miscible and could subsequently be molded into particles utilizing PRINT technology when appropriate plasticizers and process aids (lactose and glycerol) were used. Based on previous studies, DCs, the target cell for RNA replicon based vaccines, were found to preferentially take up micron-sized particles.[20, 21] In this study, cylindrical particles with both diameter and height as 1 μm were fabricated.

3.2.2 Experiment Section

3.2.2.1 Materials and cell culture

Bovine serum albumin was from Calbiochem. BCA protein assay reagent was from Thermo Scientific. Quant-iT ™ RNA assay kit was purchased from invitrogen. Lactose assay kit was purchased from Abcam. TransIT®-mRNA transfection kit was purchased from Mirus. α-D-Lactose and glycerol were purchased from Acros.

Vero cells were maintained at 37 ℃ in an atmosphere containing 5% CO_2. The cells were grown in Minimum Essential Medium (MEM; Invitrogen, Carlsbad, CA) supplemented with 5% fetal bovine serum (FBS, HyClone, Logan, UT), MEM non-essential amino acid solution (Invitrogen) and antibiotic–antimycotic (Invitrogen).

Replicon Plasmid Construction: Plasmids containing the reporter genes chloramphenicol acetyltransferase (CAT), Fire Fly Luciferase (Luc2), and Green Fluorescent protein (GFP) were purchased from Promega (CAT # E187A, Luc2 #E6651, GFP #E642). These genes were PCR amplified using iProof™ HF Master Mix Taq polymerase (BioRad), and gene specific primers containing AscI and PacI restrictions sites for sub-cloning. The PCR products were cloned into an intermediate vector for nucleotide sequence verification, pCR®4 Blunt-TOPO (Life Technologies # K2875-40). Upon sequence confirmation the PCR fragments were sub-cloned into an DNA plasmid constructed to contain the following elements: a T7 RNA polymerase promoter for *in vitro* RNA transcription; the 5' untranslated region, nonstructural protein genes, 26S promoter, and the 3' untranslated region of Venezuelan Equine Encephalitis Virus (VEE). Specifically the PCR products and the replicon plasmid base vector were digested with AscI and PacI restriction enzymes. The PCR products were ligated using T4 DNA Ligase into the AscI and PacI restriction enzyme sites contained in the multiple cloning site of the replicon plasmid.

RNA production: the replicon plasmid was linearized with Not I restriction enzyme and used as template for *in vitro* transcription of capped replicon RNA

utilizing the T7 RiboMAX™ Express Large Scale RNA Production System (Promega #P1320) supplemented with 7.5 mm methyl G CAP analog (Promega #P1711). Replicon RNA was purified using the SV Total RNA Isolation System (Promega #Z3101) as specified by the manufacturer.

3.2.2.2 Preparation of RNA replicon loaded BSA-based particles

The bovine serum albumin (BSA) PRINT particles were derived from a mixture composed of 37.0 wt% of BSA, 37.0 wt% of lactose, 25.0 wt% of glycerol and 1.0 wt% of RNA replicon. A 7.8 wt% solution of this mixture in water was prepared and then cast as a film onto a poly(ethylene terephthalate) (PET) sheet. Water was removed with a heat gun moving back and forth. The film was laminated onto a piece of PRINT mold (2 × 4 inch, cylindrical, d =1 μm, h = 1 μm, mold No.: MMM-262-090A, MMM-369-070), forming a sandwich structure with the film in the middle. The mold was delaminated by passing the mold and the PET through a heated laminator with a temperature of 60 °C or 148 °C on the top roller and a pressure of 80 psi between the rollers. The filled mold was relaminated onto a sheet of plasdone covered PET. The laminated mold and PET were passed through the heated laminator again. After the particle filled mold cooled down, the mold was removed gently and all the PRINT particles were transferred from the mold to the plasdone-covered PET. The particles were harvested from the PET by dissolving plasdone with isopropanol. The harvested particles were washed with isopropanol for three times by centrifugation to remove plasdone. The particles were finally dispersed in isopropanol and the

particle concentration was determined by Thermal Gravimetric Analysis (TGA) (TA Q5000).

3.2.2.3 Scanning electron microscopy (SEM)

For visualization samples were coated with 2 nm gold palladium alloy using a Cressington 108 auto sputter coater. Images were taken at an accelerating voltage of 2 kV using a Hitachi model S-4700 scanning electron microscope (SEM).

3.2.2.4 Quantification of BSA, lactose and RNA replicon in particles prior to cross-linking

Particles were dissolved in water. BCA assay (Thermo scientific) was used to quantify the amount of BSA in the solution and a lactose quantification kit (Abcam) was used to quantify the amount of lactose in the solution. Quant-iT ^{TM} RNA assay kit (Invitrogen) was used to quantify the amount of RNA in the solution. The assays were performed according to vendor's instructions and each assay was done in duplicate and three independent samples were measured.

3.2.2.5 RNA replicon extraction from un-cross-linked particles particles

For particles prior to cross-linking, 50 μL of PBS was added to dissolve 0.15 mg of particles. A Qiazol-chloroform extraction procedure was used to extract RNA replicon from the RNA replicon-BSA mixture. Typically:

1) Chloroform (200 μL) was added to 50 μL of samples and mixed through inversion and then incubated at room temperature for 5 min.

2) 1 mL of Qiazol (from invitrogen) was added to the vial and mixed through inversion and then incubated at room temperature for 5 min.

3) The vial was centrifuged at 10600 rpm at 4 °C for 15 min.

4) The aqueous phase was taken out and put in a new vial. Then 500 μL of isopropanol and 2 μL of Glycoblue (Ambion) were added and mixed well.

5) The sample was then incubated at room temperature for 10 min and then centrifuged at 10600 rpm at 4 °C for 10 min.

6) The supernatant was removed and the blue pellet was washed with 1 mL of 75% ethanol. The vial was centrifuged at 8600 rpm at 4 °C for 5 min.

7) Ethanol was removed and the blue pellet was dissolved in 20 μL of DEPC-treated water.

3.2.2.6 Agarose gel electrophoresis

Agarose gel was prepared by dissolving agrasose in 1× NorthernMax®-Gly gel preparation and running buffer (Ambion) at 1 wt%. Typically, 5 μL of sample (RNA replicon extracted) was mixed with 5 μL of water and 10 μL of NorthernMax®-Gly load dye (Ambion) and heated at 50 °C for 10 min before loading onto the gel. The gel was then run in 1× NorthernMax®-Gly gel preparation and running buffer (Ambion) at 70 V for 35 min before being imaged by a GE ImageQuant LAS 4000 biomolecular imager.

3.2.2.7 Evaluation of RNA replicon activity through CAT expression

Typically, 2×10^4 Vero cells were plated into 24 well tissue cultured treated plates 18-24 h prior to assay. Vero cells were transfected with CAT RNA replicon utilizing the TransIT® mRNA transfection kit (Mirus Bio, Madison, WI) following the manufacturer's protocol. Typically, for every well on a 24-well plate, the RNA

replicon were mixed with 2 μL of TransIT-mRNA reagent and 1 μL of mRNA Boost reagent and dosed to cells. Cell lysates were prepared 48h post-transfection and CAT ELISA (Roche, Indianapolis) analysis was carried out according to the manufacturer's instructions. The relative absorbance was calculated using following method:

$$Ar = \frac{Aa}{Ac}$$

Where Ar: the relative absorbance

Aa: the absorbance acquired by plate reader at 405 nm for samples dosed with RNA replicon or particles

Ac: the absorbance acquired by plate reader at 405 nm for untreated cells

3.2.3 Results and Discussion

Based on our previous success, RNA replicon was incorporated into the particle by mixing the cargo with BSA, lactose and glycerol (Figure 2.3). Following the aforementioned PRINT process, cylindrical BSA particles with both diameter and height as 1 μm were fabricated with a preparticle composition containing 37 wt% of BSA, 37 wt% of α-D-lactose, 25 wt% of glycerol and 1 wt% of RNA replicon (Figure 3.2).

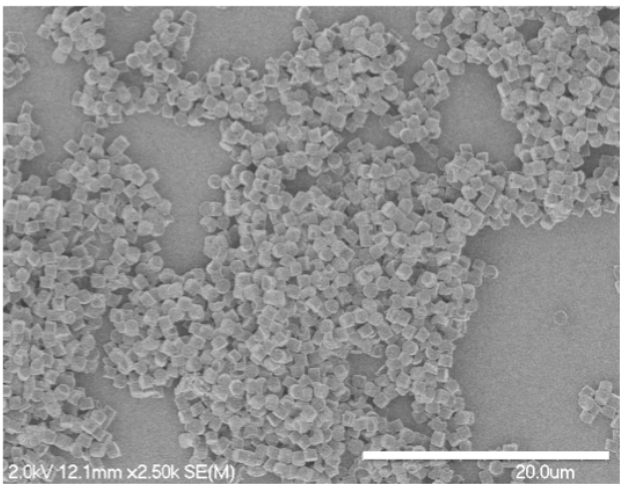

Figure 3.2 PRINT BSA particles loaded with 1 wt% of CAT RNA replicon. Scale bar represents 20 μm

The RNA replicon is a single stranded RNA with low stability. Maintaining its integrity during the PRINT process is essential. We studied the influence of temperature used for particle fabrication on the biological activity of RNA replicon. Typically, 1 wt% of CAT RNA replicon was charged into cylindrical albumin particles (d = 1 μm, h = 1 μm) by using two temperatures on the heated laminator roller: 60°C vs. 148°C. The particles were dissolved in phosphate buffered saline (PBS) and followed by extraction of RNA replicon from the BSA-RNA replicon mixture. It should be noted that the particles used in this experiment did not involve any cross-linking and were readily soluble in water. As a control, the RNA extraction procedure was also performed on the blank particles to rule out any existence of RNA in the BSA used for particle fabrication. The integrity of the extracted RNA replicon was first evaluated using agarose gel electrophoresis, as shown in Figure 3.3. Electrophoresis analysis showed that RNA replicon encapsulated at 60°C displayed a tight band at the same position as the untreated RNA replicon. However, when particles were fabricated at

148°C, only some smears, which were speculated as RNA replicon degradation products, were observed.

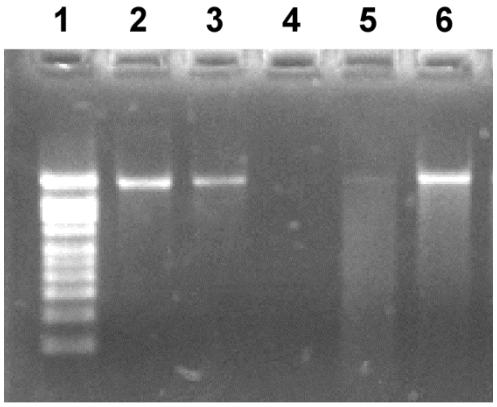

Figure 3.3 Agarose gel of RNA replicon before and after particle crosslinking. 1: RNA ladder, 2: untreated RNA 200 ng, 3: untreated RNA 100 ng, 4: RNA replicon extracted out of blank BSA particles, 5:RNA replicon extracted out of BSA particles fabricated at 148°C, 6: RNA replicon extracted out of BSA particles fabricated at 60°C

The integrity of extracted RNA replicon was further accessed by a CAT ELISA assay after RNA replicon was transfected into Vero cells, a kidney epithelial cell line developed from an African green monkey, using a TransIT®-mRNA transfection reagent (TransIT). The CAT ELISA assay quantifies the amount of CAT protein generated by the cells after RNA replicon transfection. Results showed that RNA replicon encapsulated at 148°C showed very minimal biological activity and RNA extracted from particles fabricated at 60°C produced similar protein expression levels to untreated RNA replicon control (Figure 3.4). The results showed that RNA replicon is very sensitive to the temperature used for particle fabrication and lower temperature is preferred to preserve RNA replicon activity.

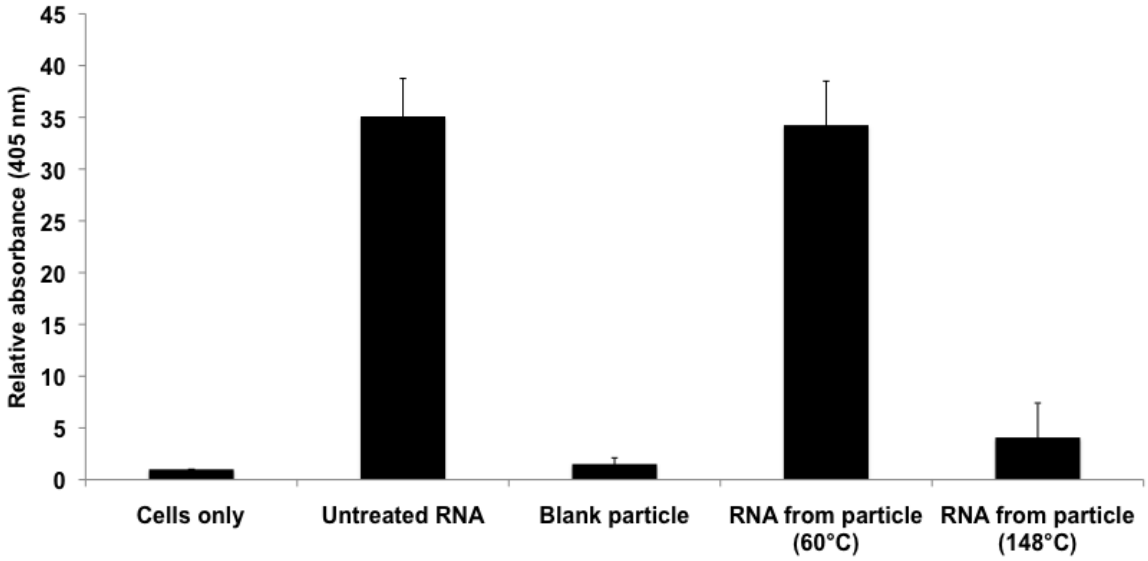

Figure 3.4 Relative absorbance obtained from CAT ELISA. The absorbance from un-treated cells (cells only) were defined as 1. Error bars represent standard deviation calculated from four wells.

After the harvest and purification steps using isopropanol, the particles fabricated at 60°C were determined to contain 1.5±0.1 wt% of RNA replicon after purification step in the final harvested particle composition (Table 3.1). For particles of this size (d = 1 μm, h = 1 μm) this equals to approximately 1500 copies of the RNA replicon per particle (calculated based on a particle density of 0.8 g/mL).

Table 3.1 Composition of RNA replicon-loaded BSA particles

	Charged Composition [a] (wt%)	Final Composition [b] (wt%)
BSA	37.0	81.5±.0.2
Lactose	37.0	10.3± 3.1
Glycerol	25.0	6.7± 2.8
RNA Replicon	1.0	1.5±0.1

[a] The weight percentage of components charged into the preparticle solution that was then drawn into a film on the PET sheet. [b]Final particle composition after

harvest and purification step. The errors stand for standard deviation calculated from three experiments.

3.3 RNA Replicon Integrity in the Process of Cross-linking

3.3.1 Introduction

In order to successfully deliver the RNA replicon, it is essential to retain the bioactivity of this relatively fragile molecule throughout the whole process of fabrication, stabilization, and delivery. The previous results have shown that the fabrication process is RNA-friendly and does not abolish the activity of RNA replicon. The next step is to evaluate the activity of RNA replicon after the cross-linking process.

Dithio-bis(ethyl 1 H-imidazole-1-carboxylate) (DIC) was used as the cross-linker to stabilize the protein particles in aqueous solutions. This cross-linker, compared to DSP, has several advantages for protein particle stabilization for RNA replicon delivery. Imidazoles as the leaving groups enhanced the reaction selectivity for amines over hydroxyl groups compared to NHS esters, which is essential to maintain the integrity of RNA replicon in the cross-linking procedure. Furthermore, DIC is a “traceless” reversible cross-linker, which does not leave any molecular pendants after disulfide. A truly reversible chemistry has many benefits for the delivery of RNA replicon. It releases the amino groups in its original form and avoids the unknown immune response towards novel antigens. Additionally, even if the amine functionalities on nucleobases were cross-linked by DIC, due to the fully reversible nature of the cross-linker, the nucleobases should revert to its original state upon disulfide cleavage if DIC is used. Despite

of all the advantages of the DIC, this cross-linker has to be evaluated for its compatibility with the RNA replicon.

3.3.2 Experimental section

3.3.2.1 Materials

Bovine serum albumin was from Calbiochem. α-D-Lactose, dithiothreitol (DTT) and glycerol were purchased from Acros. DIC was synthesized as described in section 2.3.2.2. Cells were cultured as described in section 3.2.2.1.

3.3.2.2 Cross-linking of CAT RNA replicon loaded particles

The 1 μm cylindrical BSA particle particles containing CAT RNA replicon were prepared as described in section 3.3.2.2. Based on the TGA results, an appropriate amount of isopropanol was added to the particle dispersion to achieve a particle concentration of 1mg/mL. To 850 μL of particle dispersion, cross-linker (1.275 mg, corresponding to 4.4 mM of DIC in the final solution) was added. The resulting dispersion was shaken on a vortex machine for 24 h at 40 °C. The reaction was terminated by centrifuging particles down for 3 minutes using a minicentrifuge (Thermo scientific), followed by removal of the supernatant containing the cross-linker and adding 850μL of isopropanol. The particles were washed three times with 850μL of isopropanol by centrifugation to remove the excess cross-linkers and then aliquoted into 150 μg/vial. The particles were pelleted down through centrifugation and 10 μL of isopropanol was added to the vial to protect the particles from drying out. The particles were stored in -80 °C freezers until further use.

3.3.2.3 Particle imaging

The PRINT particles were incubated in PBS for 4h. The particles were then washed with isopropanol and deposited on glass slide, coated with palladium/gold and imaged by a scanning electron microscopy (Hitachi modelS-4700).

3.3.2.4 RNA replicon extraction from cross-linked particles particles

For particles after cross-linking, 50 μL of PBS containing 10 mM DTT was added to dissolve 0.15mg particles. The particle solution should turn from cloudy to clear in no more than 3 min. After turning clear, the solution was further incubated at room temperature for 4 min before adding 200 μL of chloroform into the vial. A Qiazol-chloroform extraction procedure was then used to extract RNA replicon from the RNA replicon-BSA mixture following the procedures described in 3.2.2.5. The RNA replicon extracted out of particles was evaluated using Agarose gel electrophoresis and CAT ELISA assay as described in sections 3.2.2.6 and 3.2.2.7.

3.3.3 Results and discussion

The stabilization of PRINT albumin particles in aqueous solutions was achieved by introducing DIC as the cross-linker (Figure 3.8). To assess the integrity of RNA replicon after cross-linking reaction, particles were dissolved in 10mM DTT solution and the RNA replicon extracted from the mixture was evaluated by agarose gel electrophoresis (Figure 3.9). The agarose gel results showed that after the cross-linking reaction the RNA replicon inside protein particles was minimally affected. The RNA replicon integrity was also confirmed

by induced expression of CAT protein after transfection to Vero cells (Figure 3.10). Compared with untreated RNA replicon, the RNA replicon extracted out of cross-linked particles showed slight decrease in activity possibly due to the condition used to degrade particles, but a significant amount of intact and viable RNA was still present in the particles.

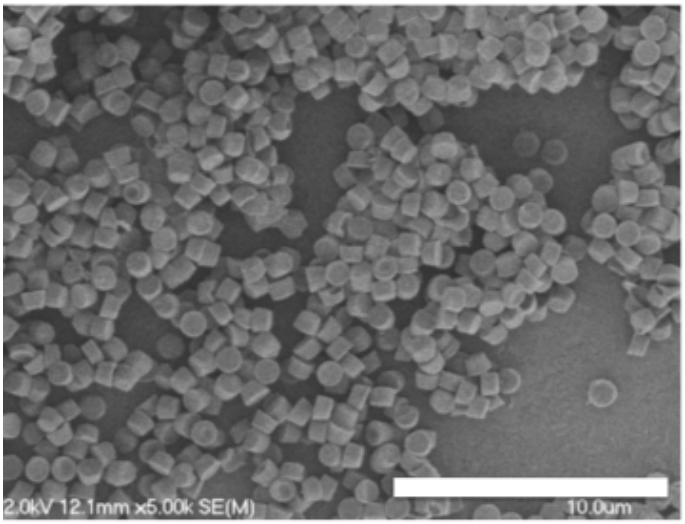

Figure 3.5 SEM image of DIC-cross-linked particles containing CAT RNA replicon, image was taken after incubation with PBS, scale bar stands for 10 μm.

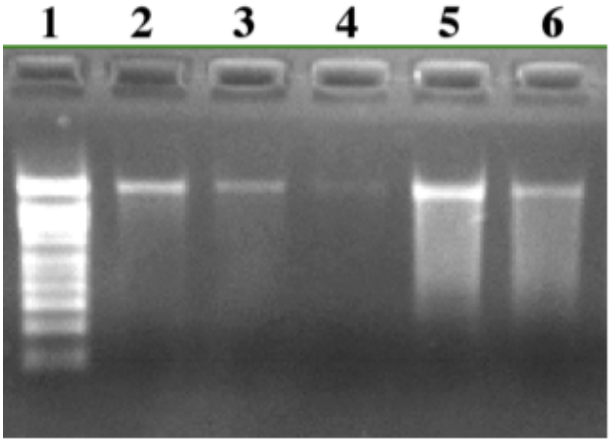

Figure 3.6 RNA replicon characterization using Agarose gel before and after particle cross-linking: lane 1: RNA marker, 2: untreated RNA replicon 200ng, 3: untreated RNA replicon 100ng, 4: untreated RNA replicon 50ng, 5: RNA replicon extracted out of BSA particles before cross-linking reaction, 6: RNA replicon extracted out of BSA particles after cross-linking reaction.

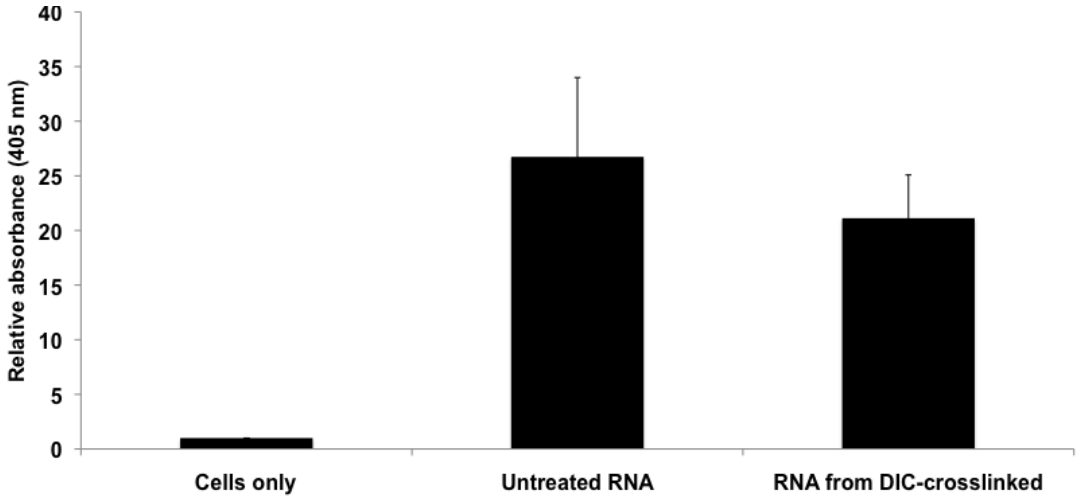

Figure 3.7 RNA replicon integrity after crosslinking reaction evaluated by CAT ELISA. The absorbance from un-treated cells (cells only) was defined as 1. Error bars stand for standard deviation calculated from four wells.

3.4 CBSA-Based particles for Delivery of RNA Replicon

3.4.1 Introduction

The cargo incorporation was optimized with normal un-modified BSA and the results indicated that lower temperature on the heated laminator is the key to maintaining the RNA integrity. The previous results also indicated that the cross-linking using DIC do not harm the activity of RNA replicons. However, the negatively charged normal BSA particles could not be internalized and transfected by cells. As previously mentioned, cationized BSA is one of the strategies used to overcome these issues. The main issue with making cBSA-RNA replicon particle is that the polycation and the polyanionic RNA replicons tend to form strongly binded complexes which will be difficult to fill into the cavities. Base on the study by Fischer D. et al., the pH of the complexation medium can greatly affect the complex sizes and at high pHs above 9, there was no complex formation between the plasmid DNA and the cBSA.[5] Herein, a high

pH solution strategy could be used to break the complexation between cBSA and RNA replicon.

3.4.2 Experimental Section

3.4.2.1 Materials

CBSA was purchased from Thermo Scientific. TransIT®-mRNA transfection kit was purchased from Mirus. α-D-Lactose and glycerol were purchased from Acros. DIC was synthesized as described in section 2.3.2.2.

3.4.2.2 Fabrication of cBSA/RNA replicon particles

The cBSA PRINT particles were derived from a mixture composed of 37.0 wt% of cBSA, 37.0 wt% of lactose, 25.0 wt% of glycerol and 1.0 wt% of RNA replicon (CAT). A 7.8 wt% solution of this mixture in a mixed medium (45% of water, 45% of trifluoroethanol and 10% of ammonium anhydride) was prepared and then cast a film onto a poly(ethylene terephthalate) (PET) sheet. Water was removed with a heat gun moving back and forth. The film was laminated onto a piece of PRINT mold (2 × 4 inch, cylindrical, d =1μm, h = 1μm), forming a sandwich structure with the film in the middle. The mold was filled and the particles were harvested following procedures described in section 2.3.2.2. The particles were finally dispersed in isopropanol and the particle concentration was determined by Thermal Gravimetric Analysis (TGA) (TA Q5000). RNA replicon loaded Alexa fluor 555® labeled BSA particles were derived from a mixture composed of 36.7 wt% of cBSA, 37.0 wt% of lactose, 25.0 wt% of glycerol, 1.0 wt% of RNA replicon and 0.3 wt% of Alexa-fluro-555 labeled BSA.

3.4.2.3 Cross-linking of the cBSA particles

The particles were cross-linked following the procedures described in section 2.4.2.2 using a DIC cross-linker concentration of 4.4 mM in the final solution. The reaction was carried out for 24 h at 40 °C.

3.4.2.4 Alexa fluor 488® labeled BSA particles for Confocal imaging

Typically, 2×10^4 Vero cells were plated into 24 well tissue cultured treated plates 18-24 h prior to assay. The cells were dosed with cross-linked cBSA particles at 1 mg/mL concentration. After 4 h, Confocal images were acquired using a Ziess 710 laser scanning confocal imaging system (Olympus) fluorescence microscope fitted with a PlanApo 60× oil objective (Olympus). The final composite images were created using Adobe Photoshop CS (Adobe Systems, San Jose, CA).

3.4.2.5 Evaluation of cargo loading using agarose gel electrophoresis

An agarose gel was prepared by dissolving agrasose in 1× NorthernMax®-Gly gel preparation and running buffer (Ambion) at 1 wt%. Typically, 5 μL of sample (particle solution without extraction) was mixed with 5 μL of water and 10 μL of NorthernMax®-Gly load dye (Ambion) and heated at 50 °C for 10 min before loading onto the gel. The gel was then run in 1× NorthernMax®-Gly gel preparation and running buffer (Ambion) at 70 V for 35 min before being imaged by a GE ImageQuant LAS 4000 biomaolecular imager.

3.4.2.6 Evaluation of RNA replicon activity through CAT expression

Typically, 2×10^4 Vero cells were plated into 24 well tissue cultured treated plates 18-24 h prior to assay. Vero cells were transfected with CAT RNA replicon utilizing the TransIT® mRNA transfection kit (Mirus Bio, Madison, WI) following the manufacturer's protocol. Cell lysates were prepared 48h post-transfection and CAT ELISA (Roche, Indianapolis) analysis was carried out according to the manufacturer's instructions.

3.4.3 Results and Discussions

To determine replicon RNA encapsulation in cBSA particles and its subsequent release upon reducing reagents and salts, un-crosslinked and DIC cross-linked particles were tested by gel electrophoresis (Figure 3.8). For all cBSA RNA replicon-containing particles tested, no free RNA was detected indicating that RNA replicon was not released in its free form under reducing conditions (lane 5, Figure 3.8). This result suggested that the electrostatic interaction between the cationic BSA and RNA replicon is problematic and does not allow the release of the cargo.

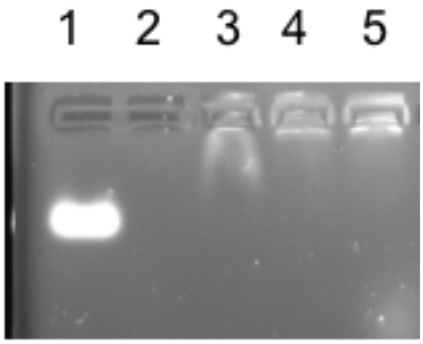

Figure 3.8 Agarose gel of RNA replicon in cBSA particles. Lane 1: CAT RNA replicon standard 1 μg, 2: blank cBSA particle, 3: un-cross-linked cBSA particle loaded with RNA replicon, 4: cross-linked cBSA particle loaded with RNA replicon, 5: cross-linked cBSA particle loaded with RNA replicon treated with 10 mM DTT and $CaCl_2$ (500 mM)

The internalization of cBSA particles by Vero cells was evaluated using Confocal imaging (Figure 3.9) The results indicated that normal BSA particles could not be taken up by cells whereas cBSA particles showed high internalization efficiency.

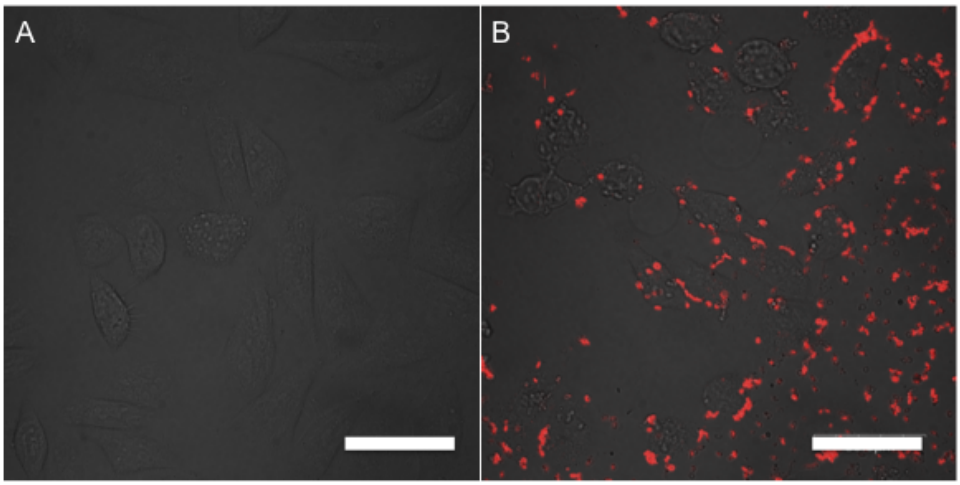

Figure 3.9 Internalization of Alexa fluor 555® labeled BSA particles (A) and cBSA particles (B), red: Alexa fluor 555® labeled particles, scale bars represent 30 μm

The RNA replicon-loaded cBSA particles were then dosed to Vero cells and RNA replicon mixed with a mRNA transfection reagent TransIT® were used as positive controls (black bar in Figure 3.10). The amount of CAT protein generated by cells was measured using CAT ELISA. The CAT proteins were used as standards on ELISA (red bars in Figure 3.10). The results indicated that there was no protein expression associated with cBSA particles loaded with CAT RNA replicon (orange bars in Figure 3.10). The failure could be due to 1) the integrity of the RNA replicon was disrupted by the high pH solution used to prepare pre-particle material, 2) complexation between RNA replicon and cBSA was too strong, 3) the inability of the particles to escape the endosome. This

method was also accompanied by the difficulty of analyzing the RNA replicon integrity after incorporation into the cBSA particles.

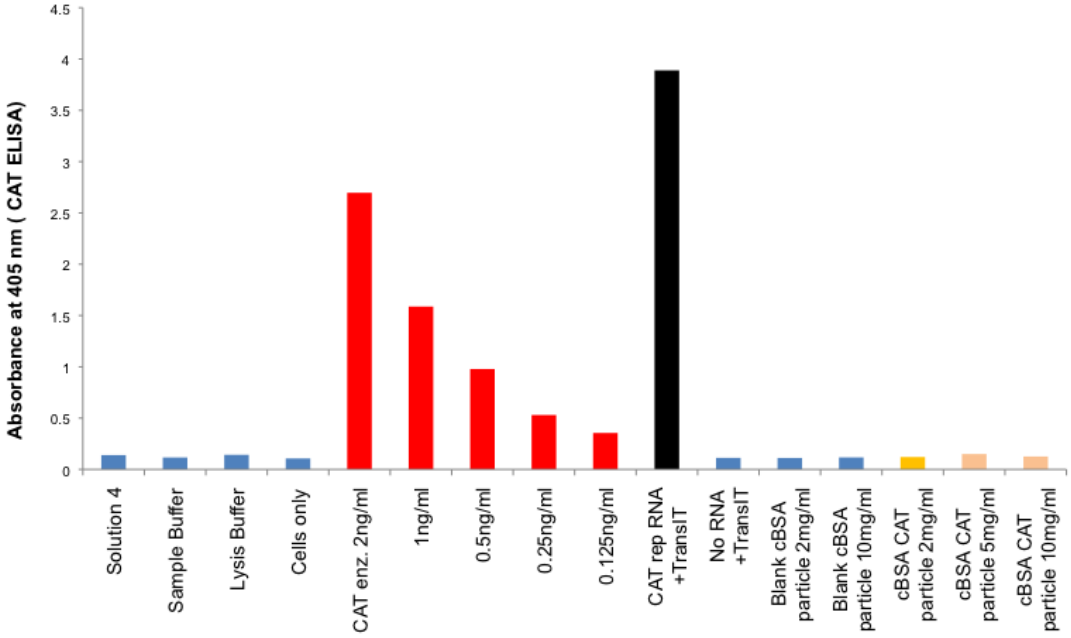

Figure 3.10 Absorbance obtained from CAT ELISA on cBSA particles

3.5 Delivery of RNA Replicon via PRINT Protein-based Particles

3.5.1 Introduction

The previous results indicate that both the particle preparation from un-modified BSA and cross-linking using DIC do not harm the RNA replicon activity. But the cBSA-based particles could not deliver RNA replicons to Vero cells and that method was accompanied by difficulties to analyze the integrity of RNA replicons. Based on these results, we pursued the coating strategy to deliver the particles derived from normal BSA to cells. We first tried TransIT, the commercially available transfection reagent for mRNA, which we used to deliver RNA replicon as a positive control.

3.5.2 Experiment section

3.5.2.1 Materials

Bovine serum albumin and FluorsaveTM reagent were from Calbiochem. Alexa fluor 488® labeled Bovine serum albumin, Alexa Fluor® 546 goat anti-rabbit IgG (H+L) was purchased from invitrogen. Anti-Chloramphenicol Acetyltransferase antibody was purchased from Abcam. TransIT®-mRNA transfection kit was purchased from Mirus. α-D-Lactose and glycerol were purchased from Acros. DIC and OEDIC were synthesized as previously described. Cells were cultured as previously described and CAT, GFP and Luciferase RNA replicons were prepared as previously described.

3.5.2.3 Preparation of RNA replicon loaded particles

CAT and Luciferase RNA replicon loaded Alexa fluor 488® labeled BSA particles were derived from a mixture composed of 36.7 wt% of BSA, 37.0 wt% of lactose, 25.0 wt% of glycerol, 1.0 wt% of CAT or Luciferase RNA replicon and 0.3 wt% of Alexa-fluro-488® labeled BSA. GFP RNA replicon loaded particles were derived from a mixture composed of 37.0 wt% of BSA, 37.0 wt% of lactose, 25.0 wt% of glycerol and 1.0 wt% of RNA replicon.

3.5.2.4 Stabilization of RNA replicon loaded particles

The stabilization of particles with the DIC cross-linker was performed as previously described in section 3.4.2.2.

The particles were cross-linked with OEDIC by following similar procedures: Based on the TGA results, an appropriate amount of isopropanol was added to the particle dispersion to achieve a particle concentration of

1mg/mL. To 850 μL of particle dispersion, 1.096 mg of OEDIC (corresponding to 4.4 mM in the final solution) was added. The resulting dispersion was shaken on a vortex machine for 24 h at 40 °C. The reaction was terminated and the particles were washed, aliquoted and stored as described in section 3.4.2.2

3.5.2.5 Size and ζ potential characterization of the PRINT protein particles

For ζ potential measurements, the particles were dispersed in 1 mM potassium chloride at a concentration of 4 μg/ml. For particles coated with TransIT, to 10 μL of Opti-MEM® I Reduced-Serum Medium, 2 μg of particles, 2 μL of TransIT and 2 μL of boost were added and mixed through pipetting. The hydrodynamic diameters of the PRINT particles were measured by dynamic light scattering (Brookhaven Instruments Inc., 90Plus) and a Zetasizer Nano Analyzer (Malvern Instruments Inc., Nano Zetasizer).

3.5.2.6 Analysis of CAT expression of PRINT BSA particles

The expression of CAT protein from CAT replicon RNA or 1 μm BSA PRINT particles containing 1wt% CAT replicon RNA as cargo was compared. Typically, 2×10^4 Vero cells were plated into 24 well tissue cultured treated plates 18-24 h prior to assay. Vero cells were transfected with CAT RNA replicon or PRINT BSA particles containing 1wt% CAT replicon RNA utilizing the TransIT® mRNA transfection kit (Mirus Bio, Madison, WI) following the manufacturer's protocol. Briefly, to 100 μL of Opti-MEM® I Reduced-Serum Medium, particle solution containing 50 μg, 10 μg, 5 μg, 2 μg, 1 μg, 500 ng, 250 ng of particles, 2 μL of TransIT and 1 μL of boost were added and mixed through pipetting. The

mixture was subsequently incubated with Vero cells for 4 h at 37 ℃ and the non-internalized particles were removed. The cells were further incubated for another 48 h at 37 ℃ to allow CAT protein to express. Cell lysates were prepared 48h post-transfection and CAT ELISA (Roche, Indianapolis) analysis was carried out according to the manufacturer's instructions. The amount of CAT protein generated was calculated based on a standard curve from 2, 1, 0.5, 0.25, 0.125 and 0 ng/mL of CAT protein.

3.5.2.7 Immunofluorescence Microscopy

Vero cells plated at on cover slips in 6-well dishes and grown for 24 hours. Cells were treated with particles for 48 h. Cells were then washed with PBS and fixed with 4% Para formaldehyde in PBS for 10min at room temperature. Cells were permeablized with 0.1% triton –X100 in PBS for 3min and incubated and washed in PBS for 3 times. Samples were then blocked in 5% normal serum in 1%BSA/ 0.2% triton X -100/ PBS overnight at 4 °C. Cells were then incubated in primary antibody abcam (CAT#ab50151) for 1 hr at room temperature, cells were then washed with PBS and incubated in secondary Alexa Fluor® 546 goat anti-rabbit IgG (H+L) (A11010, invitrogen) for 1hr at RT in dark. Washed twice in PBS and mounted with Fluorsave™ reagent. Samples were then analyzed by confocal microscopy. Confocal images were acquired using a Ziess 710 laser scanning confocal imaging system (Olympus) fluorescence microscope fitted with a PlanApo 60× oil objective (Olympus). The final composite images were created using Adobe Photoshop CS (Adobe Systems, San Jose, CA).

3.5.2.8 Analysis of Luciferase expression and GFP expression

Typically, 2×10^4 Vero cells were plated into 24 well tissue cultured treated plates 18-24 h prior to assay. Vero cells were transfected with Luciferase or GFP RNA replicon or PRINT BSA particles containing Luciferase or GFP replicon RNA utilizing the TransIT® mRNA transfection kit (Mirus Bio, Madison, WI) following the manufacturer's protocol. Briefly, to 100 μL of Opti-MEM® I Reduced-Serum Medium, 2 μg, 1 μg, 500 ng or 250 ng of particles, 2 μL of TransIT and 1 μL of boost were added and mixed through pipetting. The mixture was subsequently incubated with Vero cells for 4 h at 37 ℃ and the non-internalized particles were removed. The cells were further incubated for another 24 h at 37 ℃ to allow Luciferase or GFP protein to e xpress. Cell lysates were prepared 24h post-transfection and Luciferase assay was carried out according to the manufacturer's instructions. Cells expressing GFP were imaged using a Ziess 710 laser scanning confocal imaging system (Olympus) fluorescence microscope fitted with a PlanApo 60× oil objective (Olympus).

3.5.3 Results and discussion

Due to the isoelectric point of BSA (*p*I = 4.75), the cross-linked BSA particles with RNA replicons were found to be negatively charged (ζ potential = -15.4 ± 1.0 mV). Based on the previous studies from our group and other groups, cells generally preferentially internalize positively charged particles through a non-specific electrostatic interactions between the positively charged particles and the negatively charged cell membrane.[22] Our confocal microscopy studies confirmed that negatively charged BSA particles did not show significant cell

uptake (Figure 3.6). In order to introduce positive charges to BSA particle surface to enhance cell uptake, a certain amount of TransIT was mixed with BSA particles. The introduction of TransIT is also expected to enhance the endosomal escape of BSA particles, which is the major roadblock for RNA replicon delivery. The cross-linked particles mixed with TransIT achieved a positively charged particle surface (ζ potential = + 0.8 ± 0.3 mV) and were subsequently incubated with Vero cells for 4 h at 37 ℃ and the non- internalized particles were removed. (Table 3.2) Confocal microscopy studies showed that particles coated with TransIT were internalized by Vero cells (Figure 3.11).

Table 3.2 [a]Characterization of cross-linked particles with and without TransIT

	Diameter, nm	**PDI**	**ζ-Potential, mV**
Without TransIT	1214 ± 483	0.159	-15.4 ± 1.0
With TransIT	1179 ± 721	0.374	+ 0.8 ± 0.3

[a] The particles charged with 1 wt% of CAT RNA replicon. The particles (2 μg) were added into 10 μL (Opti-MEM® I Reduced-Serum Medium), and then 1 μL of boost and 2μL of TransIT were added subsequently. The reaction went for 5 min before measurements were taken.

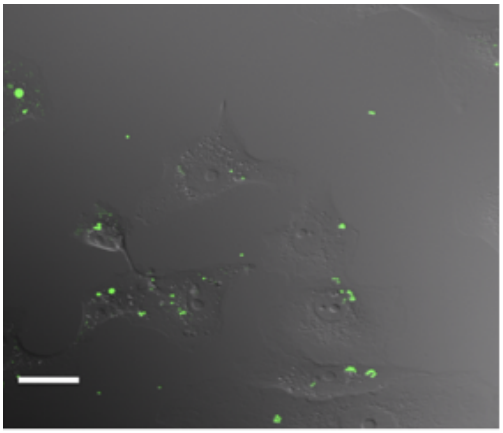

Figure 3.11 Confocal microscopy of Vero cells dosed with PRINT protein particles, RNA replicon-containing BSA particles with TransIT, scale bar represents 30 μm.

The cells were further incubated for another 48 h at 37 ℃ to allow CAT protein to express. The CAT protein generated via delivery of PRINT particles was comparable to the same amount of RNA replicon directly delivered by TransIT (Figure 3.12). As a negative control, blank particles with no RNA replicon encapsulated didn't induce any protein expression. However, it was possible that the protein expression might be induced by RNA replicon that passively released from protein particles through diffusion and transfected by TransIT. To investigate this possibility, DIC-cross-linked BSA particles containing CAT RNA replicon were incubated in PBS for 4 h at 37 °C, which is the dosing condition for the RNA replicon delivery studies, and pelleted down through centrifugation. The supernatant was dosed to cells with TransIT and no protein expression was observed. This result confirmed that RNA replicon was physically entrapped in the BSA particles and was released in the cytoplasm of Vero cells, where CAT protein was expressed.

To study the necessity of a disulfide cross-linker in the delivery of RNA replicon via protein particles, particles cross-linked with the non-degradable linker 2,2'-oxybis(ethane-2,1-diyl) bis(1H-imidazole-1-carboxylate) (OEDIC) under the same reaction condition as DIC was also investigated (Figure 3.13). Because both DIC and OEDIC have imidazoles as the leaving groups and the concentrations of crosslinkers and the reaction time are the same, we expect BSA particles crosslinked with DIC and OEDIC have similar cross-linking density. It was observed that very minimal protein was expressed with particles cross-linked by OEDIC compared to particles cross-linked by the disulfide cross-linker

DIC. This result demonstrated that 1) a disulfide linker is important to achieve cytoplasm release of RNA replicon; 2) the intracellular protease were not responsible for the BSA particle degradation and RNA replicon release at least during the 48-h time frame of our assay; and 3) passive release of RNA replicon through diffusion contributed little to the observed biological activity. Therefore, the disulfide linker DIC can not only stabilize particles in the process of delivery, but also efficiently release RNA replicon at the ultimate site of action.

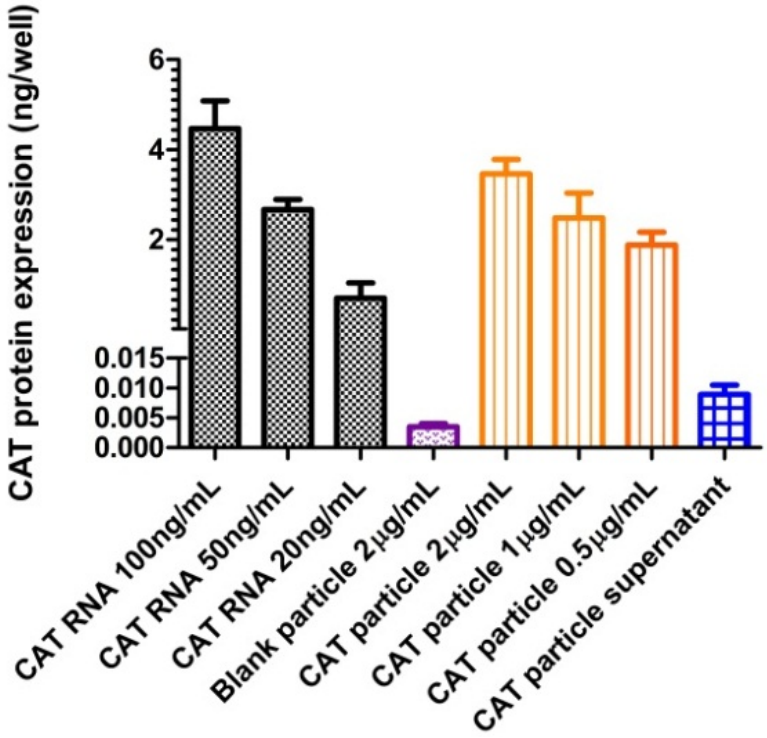

Figure 3.12 CAT protein generated from Vero cells (2×10^4 cells per well) measured by ELISA. Black: CAT RNA standards with TransIT, purple: blank particles with TransIT, orange: CAT RNA containing BSA particles with TransIT, 2, 1 and 0.5 μ g/mL of particles corresponds to 30, 15 and 7.5 ng/mL of RNA (SI), blue: supernatant from particles incubated in PBS for 4 h at 37℃ with TransIT. Error bars represent standard deviation calculated from four wells.

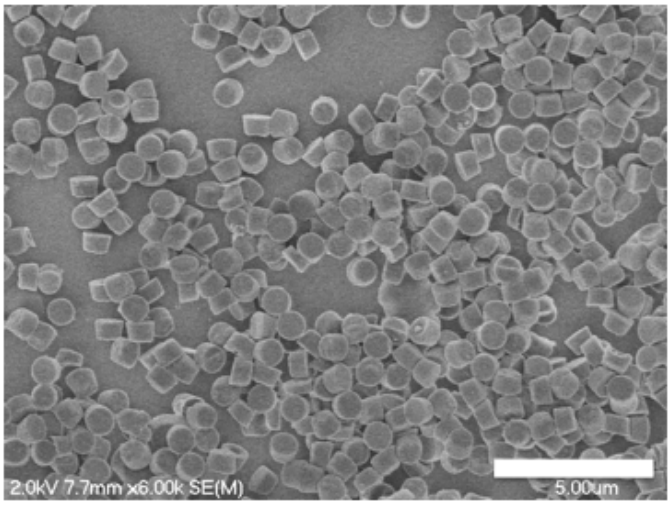

Figure 3.13 SEM image of OEDIC-crosslinked particles containing CAT RNA replicon, scale bar represents 5 μm.

Analysis using confocal microscopy was carried out to visually confirm the generation of CAT protein. Vero cells treated with BSA particles containing RNA replicon were further treated with a primary antibody that binds specifically to CAT protein, and further treated with dye-labeled secondary antibody. Compared to untransfected cells, cells transfected with DIC-cross-linked RNA replicon-containing particles showed intense fluorescence, indicating for high levels of expression of CAT proteins in those cells (Figure 3.14). Blank particles as a negative control showed no trace of CAT protein.

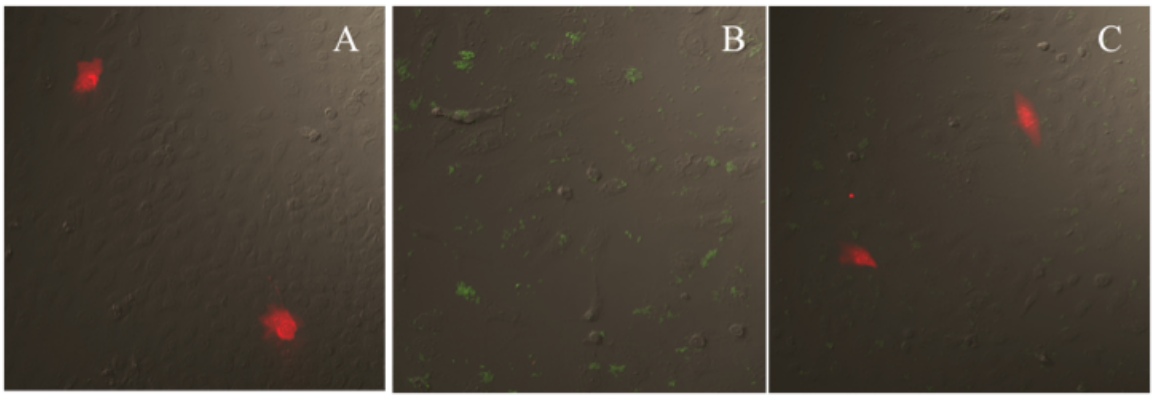

Figure 3.14 Confocal image of CAT protein (40×). (A) 100 ng of CAT RNA replicon with TransIT, (B) blank particles, 2 μg/mL. (C) BSA particles containing CAT RNA replicon cross-linked with DIC, 2 μg/mL.

An issue with the TransIT coated particles is the lack of dependence of protein expression on particle amount. At particle concentrations higher than 2 μg/mL, protein expression drops with increased particle concentration (Figure 3.15) The particle uptake by Vero cells was evaluated using flow cytometry and Confocal imaging. The internalization efficiency started to drop at higher particle concentrations and the confocal imaging study indicated that particles showed aggregation at a particle concentration of 50 μg/mL.

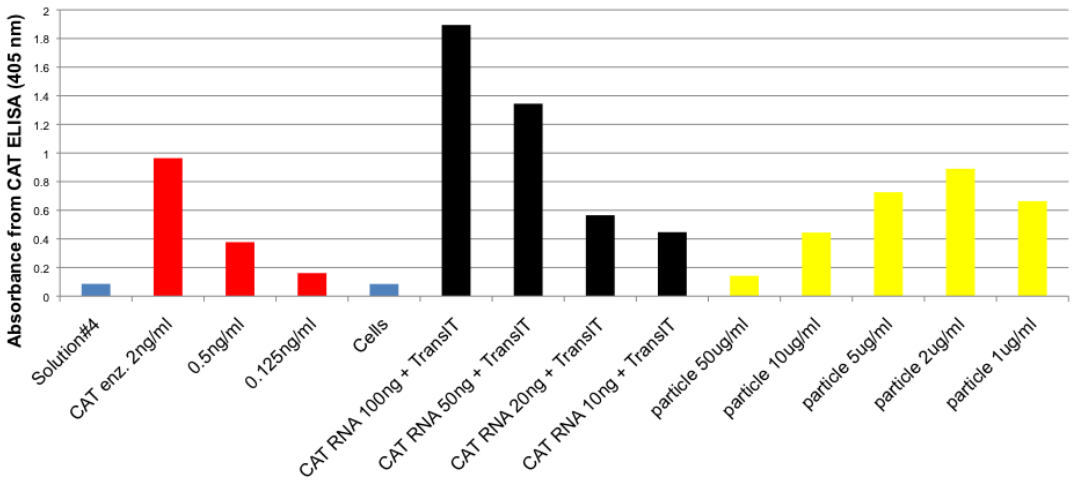

Figure 3.15 Absorbance from CAT ELISA. Black: CAT RNA replicon standards delivered by TransIT, purple: blank particles, yellow: DIC-cross-linked BSA particles containing CAT RNA replicon, red: CAT protein standards, blue: solution only and cells only

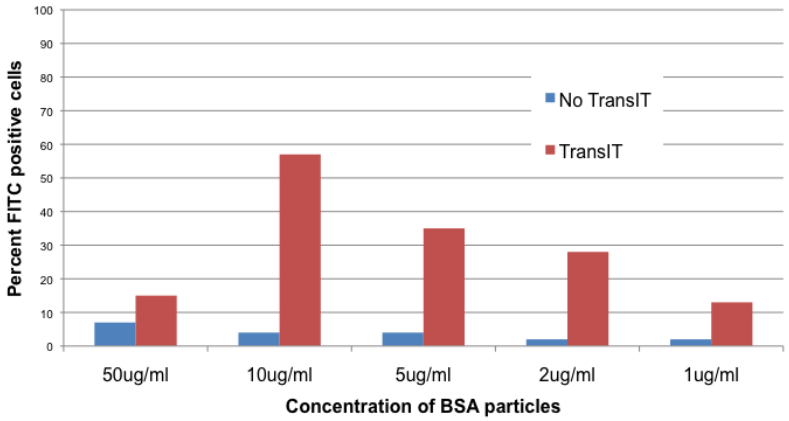

Figure 3.16 Particle internalization characterized by flow cytometry

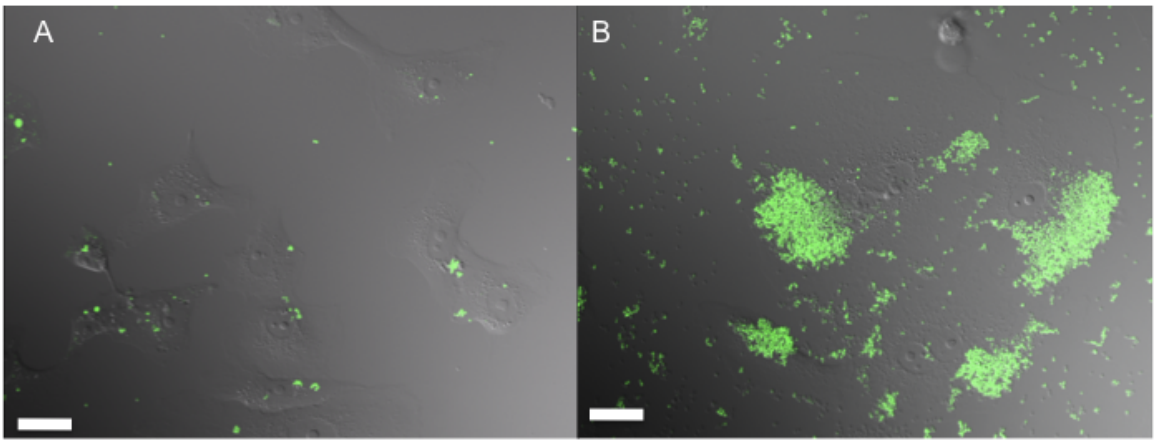

Figure 3.17 Particle internalization after 24 h, characterized by Confocal imaging (A) 2 μg/mL, (B) 50 μg/mL, green: Alexa fluoro 488 labeled particles

To show that RNA replicons encoding different proteins can be encapsulated and delivered within the same PRINT protein particle, RNA replicons encoding Luciferase and GFP were incorporated into BSA-based particles and delivered to Vero cells with TransIT. The Luciferase protein generated via delivery of PRINT particles was comparable to the same amount of RNA replicon directly delivered by TransIT (Figure 3.18). The green fluorescence generated by PRINT particles containing GFP RNA replicons was observed with fluorescent microscope, indicating successful delivery of GFP RNA replicon to the Vero cells (Figure 3.19). These results suggested that PRINT is a platform for molding therapeutics with straightforward incorporation of different cargos and can work in a “plug and play” manner, which is particularly important for development of new vaccines for epidemic diseases.

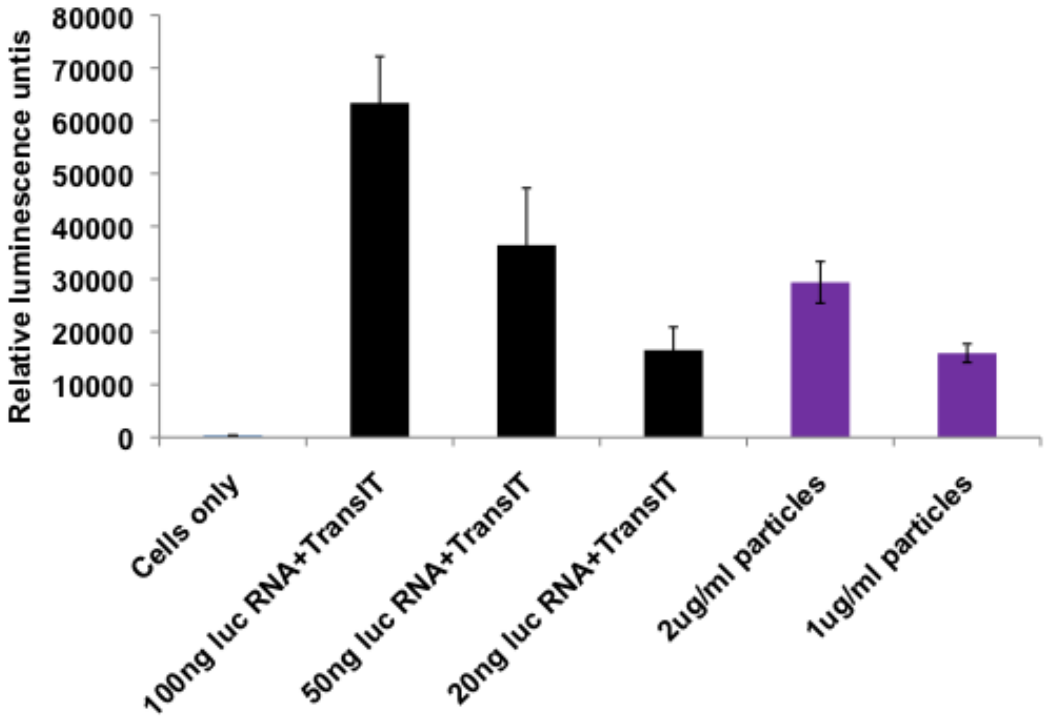

Figure 3.18 Relative Luminesence generated by Luciferase encoded by PRINT particles. Blue: cells only, Black: CAT RNA replicon standards delivered by TransIT, purple: DIC-crosslinked BSA particles containing Luciferase RNA replicon, Error bars represent standard deviation calculated from four wells.

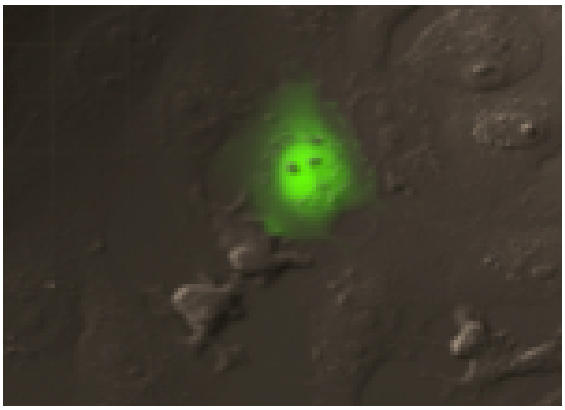

Figure 3.19 Fluorescence generated from GFP encoded by RNA replicon delivered by PRINT particles. GFP RNA replicon delivered by PRINT particles.

3.6 *In vivo* efficacy of PRINT Particles for Luciferase RNA Replicon Delivery

3.6.1 Experiment section

3.6.1.1 Materials

Bovine serum albumin was from Calbiochem. Alexa fluor 488® labeled Bovine serum albumin was purchased from invitrogen. TransIT®-mRNA transfection kit was purchased from Mirus. α-D-Lactose and glycerol were purchased from Acros. DIC was synthesized as previously described. Luciferase RNA replicons were prepared as previously described.

All mice were handled in accordance with the University of North Carolina's Institutional Animal Care and Use Committee (IACUC) protocols. Balb/c Nude mice were purchased from Harlan Labs and quarantined for two weeks before being treated with naked Luciferase RNA replicon or PRINT BSA particles.

3.6.1.2 Preparation of RNA replicon loaded particles

Luciferase RNA replicon loaded Alexa fluor 488® labeled BSA particles were derived from a mixture composed of 36.7 wt% of BSA, 37.0 wt% of lactose, 25.0 wt% of glycerol, 1.0 wt% of Luciferase RNA replicon and 0.3 wt% of Alexa-fluro-488® labeled BSA. The stabilization of particles with cross-linker DIC was performed as previously described in section 3.3.2.2.

3.6.1.3 Injection

All mice were injected through subcutaneous route on the left footpad using syringes (3/10cc insulin syringe U-100 29G ½").

Table 3.3 Dose information for *in vivo* efficacy study

Dose Description	Concentration	Dose Volume for each group
Luci-RNA [a]	0.1 mg/mL	20μL × 3
Luci-RNA with TransIT[b]	0.1 mg/mL	20μL × 3
Luci-RNA Particle with TransIT[c]	10 mg/mL, 5 mg/mL	20μL × 3
Luci-RNA particles[d]	10 mg/mL, 5 mg/mL	20μL × 3

[a] RNA replicon in naked form, [b] 2 μg of RNA replicon dosed with 50 μL of TransIT and 25 μL of boost, [c] For 10 mg/mL of particles, 200 μg of particles were dosed with 50 μL of TransIT and 25 μL of boost and for 5 mg/mL of particles, 100 μg of particles were dosed with 25 μL of TransIT and 12.5 μL of boost , [d] Particles only were dosed to the mice.

3.6.1.4 Imaging

All mice will be imaged at 24-h time point. Imaging of mice followed the same order for injection. Prior to imaging, each mouse was injected i.p. with potassium luciferin substrate, a suggested dose being 200 μL of a 15 mg/mL solution. Imaging of animals took place immediately after luciferin substrate injection. Animals were imaged in both the prone and supine positions using an *IVIS Lumina* imaging system.

3.6.2 Results and discussion

As previously mentioned, *in vivo* immunity has been achieved in mice through direct intramuscular injection.[23] In this study, mice injected with naked RNA replicon in the footpad showed *in vivo* expression of Luciferase protein. However, when the naked RNA replicon is injected with TransIT, there was no protein generated. TransIT as a mRNA transfection reagent has never been reported for use *in vivo* and this results indicated that it may have some inhibiting

effect on the *in vivo* transfection of RNA replicon. The TransIT/particles (10 mg/mL and 5 mg/mL, 5 mg/mL not shown) and particles only particles (10 mg/mL and 5 mg/mL, 5 mg/mL not shown) showed no Luciferase expression, indicating that another transfection reagent different from TransIT is needed to achieve the *in vivo* delivery of these particles. Another disadvantage with TransIT is that it is not possible to find out the detailed information about its structure which is essential to design experiments to further improve the delivery efficacy.

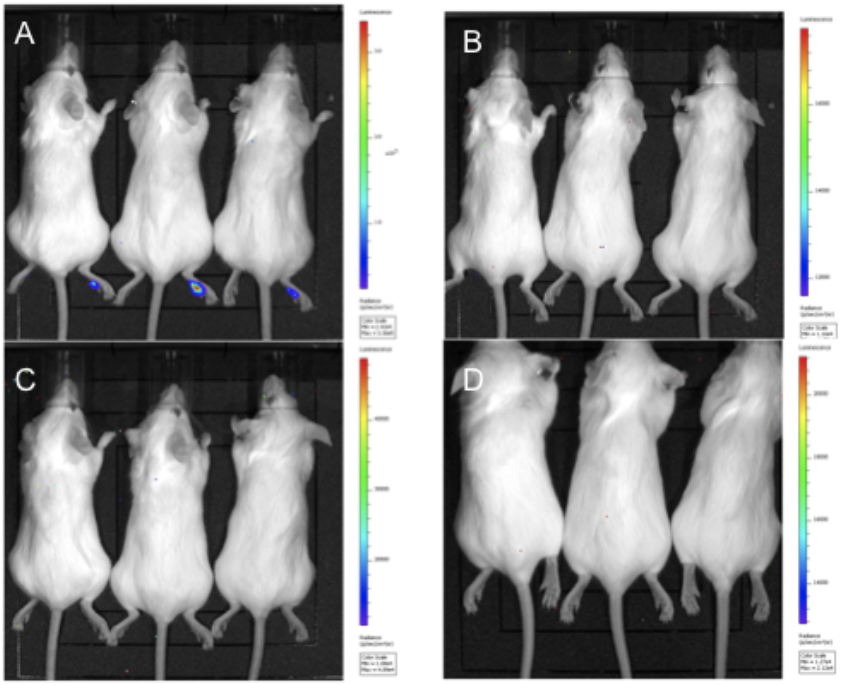

Figure 3.17 Bioluminescence imaging of mice injected with naked luciferase RNA replicon (A), luciferase RNA replicon with TransIT (B), particles with TransIT (C), particles only (D).

3.7 Particle Transfection with Cationic Lipids

3.7.1 Introduction

The aforementioned issues with TransIT as coating agent for the PRINT BSA particles and failure to achieve *in vivo* protein expression motivated us to find another reagent that can facilitate cell uptake and transfection *in vivo*. DOTAP and DOPE have been widely used as transfection reagents for gene delivery and they also enjoy the advantage of being cost-effective and commercially available. [13,14, 24]

3.7.2 Experimental section

3.7.2.1 Materials

1,2-dioleoyl-3-trimethylammonium-propane (chloride salt) (DOTAP), 1,2-dioleoyl-sn-glycero-3-phosphoethanolamine (DOPE), and Transfection Reagent I, contains DOTAP:DOPE (1:1 w/w) in powder forms were from Avanti polar lipids, Inc.

3.7.2.2 Preparation of lipid solutions

Transfection reagent I (5 mg) was first dissolved in 50 μL of trifluoroethanol (TFE) and then 1.616 mL of DEPC-treated water was added to achieve a concentration of 3 mg/mL, which was further diluted with water to achieve concentrations of 2, 1, 0.5, 0.25 and 0.1 mg/mL.

DOTAP solution (3 mg/mL) was prepared by first dissolving DOTAP (1 mg) in 20 μL of TFE and adding 310 μL of water. The 3 mg/mL of DOTAP was further diluted to concentrations of 2, 1, and 0.5 mg/mL.

DOTAP:DOPE (75:25) and DOTAP:DOPE (25:75) were prepared by first dissolving 1 mg of DOTAP and 1 mg of DOPE in 20 μL of TFE separately and mixing the two components according to the above ratio. Then water was added to achieve a concentration of 3 mg/mL which was further diluted to concentrations of 2, 1, and 0.5 mg/mL.

3.7.2.3 Particle complexed with lipids

Particles were prepared and cross-linked as previously described and were resuspended in isopropanol at 1 mg/mL. Particles were pelleted down using a minicentrifuge for 30 seconds. Isopropanol was then removed. Lipid solution were added to the vial to achieve a particle concentration of 1mg/mL and mixed by pippeting. The solution was incubated at room temperature for 1 hour. The particles were pelleted down using a minicentrifuge for 1 minute and then supernatant was removed. The same amount of water was added to the vial to achieve a particle concentration of 1mg/mL and the then dispersed by pippeting.

3.7.2.4 Particle characterization and measurement of luciferase expression

Particles were characterized as previously described in section 3.5.2.4. Luciferase protein expression was analyzed as previously described in section 3.5.2.7.

The amount of lipid comlexed with particles were characterized using HPLC-ELSD method. The amounts of DOTAP and DOPE were measured using HPLC (Agilent Technologies 1260) with a C18 rapid resolution column (Zorbax Eclipse plus, 4.6 × 100 mm, 3.5 micron). A mobile phase of water and methanol on a gradient from 15% of water to pure methanol over 15 minutes with a flow

rate of 0.6 mL/min was employed with a detection temperature of 50 °C on the ELSD (Agilent Technologies 1260). The amount of lipid complexed with particles were calculated by subtracting amount of lipid in the supernatant and washing solutions from the original lipid solution and then comparing to standard curves.

3.7.3 Results and discussion

The cross-linked particles mixed with DOTAP and DOPE lipids achieved a positively charged particle surface (Figure 3. 21). The particle size measured by DLS showed particle aggregation at lower lipid to particle ratios and no aggregation at higher lipid concentrations.

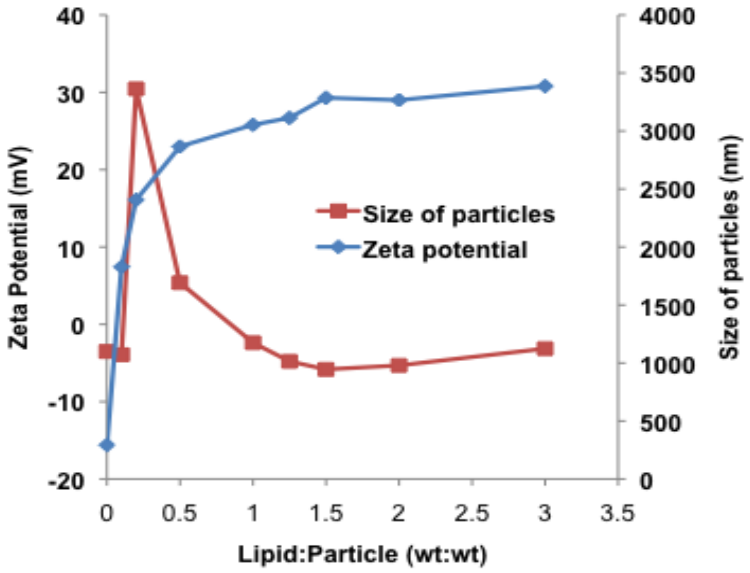

Figure 3.21 Zeta potential and particle size as a function of lipid (DOTAP:DOPE=1:1) to particles ratio (wt:wt)

The particles coated with different lipid formulations (concentration of lipid used to coat particles, lipid composition) were then dosed to Vero cells and Luciferase protein expression was analyzed (Figure 3.22). The results indicated that the TansIT/particle formulation was outperformed by particles incubated with

2 mg/mL and 3 mg/mL of DOTAP solutions, as well as 2 mg/mL and 3 mg/mL of DOTAP:DOPE (75:25) solutions at a particle concentration of 10 μg/mL.

The lipid-complexed particles were further optimized for *in vitro* transfection. It was found that particles incubated with 3 mg/mL of DOTAP:DOPE (75:25) solutions and washed three times to remove residual lipids were the best performing formulation for *in vitro* study and was further analyzed. Based on HPLC-ELSD results, , 0.46 ± 0.06 mg of DOTAP and 0.11 ±0.02 mg of DOPE were associated with 1 mg of these BSA-RNA particles. When these particles were dosed to Vero cells, dose dependence was achieved for up to 60μg/mL of particle concentration. Transfection of up to ~80% of cells was achieved (Figure 3.23 and Figure 3.24).

The *in vivo* transfection of the lipid-complexed particles are now under investigation.

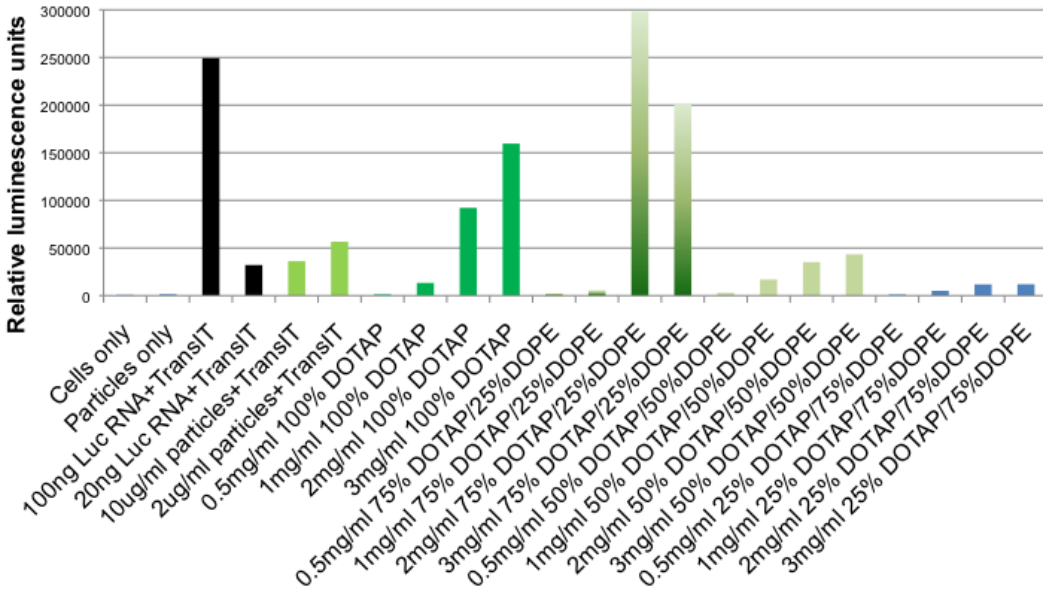

Figure 3.22 Luciferase expression resulting from BSA Luciferase RNA replicon particles utilizing DOTAP and DOPE. For all lipid-coated particles, the particle concentration dosed was 10 μg/mL

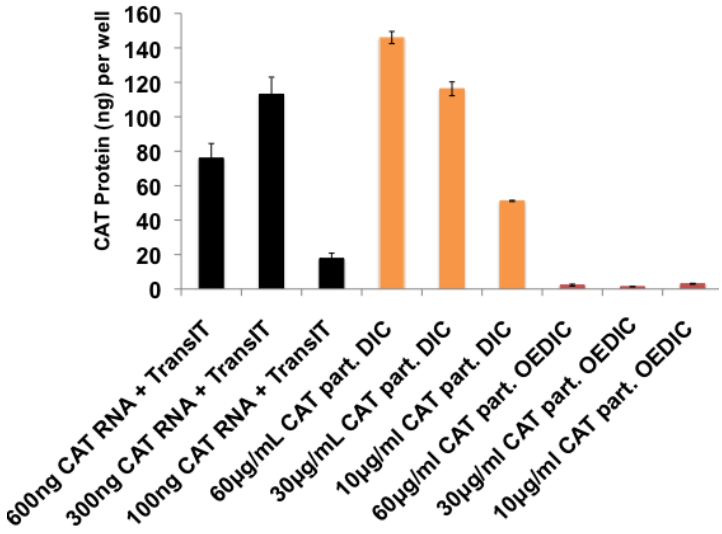

Figure 3.23 Luciferase expression resulting from BSA Luciferase RNA replicon particles inbubated with 3mg/mL of DOTAP:DOPE(75:25)

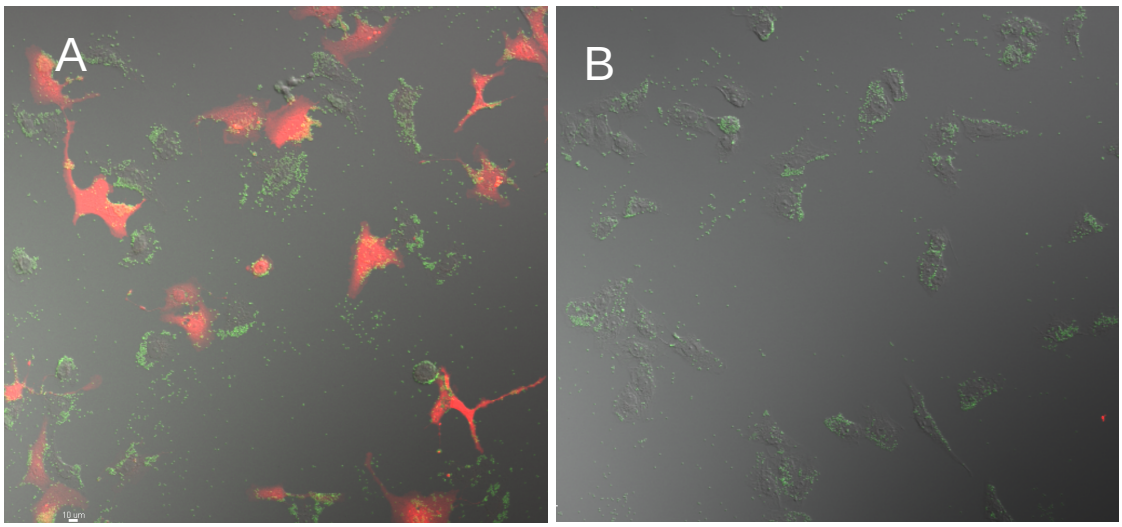

Figure 3.24 Confocal image of CAT protein. (A) 30µg/mL CAT particle DIC, B: 30µg/mL CAT particle OEDIC

3.8 Conclusions and Future Work

Herein, a novel method for the delivery of RNA replicon via protein (BSA) particles was demonstrated. This particle fabrication method, built on PRINT

technology platform, not only allows for the fabrication of particles of controlled sizes and shapes, but also was gentle and RNA replicon could be encapsulated in the particles without abolishing their biological activities. A disulfide cross-linker was used to stabilize the particles in aqueous solutions. The disulfide cross-linker was demonstrated to be RNA-friendly and stabilized the particles without affecting the biological performance of RNA replicons. By coating the particles with TransIT, the particles were delivered to Vero cells and CAT protein was expressed via delivery of PRINT particles. The reversible disulfide linker was demonstrated to play a vital role in the successful delivery of RNA replicon. RNA replicons encoding different proteins including Luciferase and GFP were incorporated into the PRINT particles and delivered using the same strategy. A cationic lipid strategy was also developed to facilitate cell uptake and particle transfection. Investigation of *in vivo* delivery efficiency and immunogenicity is also underway. The future work will focus on RNA replicons encoding proteins that will serve as antigens, trigger production of antibodies and improve immunity towards diseases.

In addition to the cationic lipids which is currently under investigation, the following strategies can also be explored to facilitate the internalization and transfection of protein-based particles:

1) Cell penetrating peptides (CPPs). CPPs such as TAT peptide are short peptides that are able to transport different cargo molecules across plasma membrane and directly to the cytoplasm of cells. This characteristic has been regarded a highly promising strategy to deliver numerous drugs and cargos and

the protein particles with CPPs on the surface may be translocated to the cytoplasm efficiently where the RNA replicon can be released and encode for antigens.

2) Cationic polymer conjugated with fusogenic peptides or histidine-rich peptides, e.g., H5WYG, KALA, ppTG1, etc. The cationic polymer can potentially bind to the surface of the negatively charged particles due to electrostatic interactions and facilitate cell uptake and the peptides may help break the endosome after the particles are internalized.

In summary, the PRINT technology allows for fabrication of protein particles with the ability to encapsulate therapeutics in an easy and gentle way, showing the first non-viral delivery for RNA replicon and great promise as a highly tunable drug delivery system.

REFERENCES

1. Brooks, H.; Lebleu, B.; Vives, E., Tat peptide-mediated cellular delivery: back to basics. *Adv Drug Deliv Rev* 2005**,** *57* (4), 559-77.

2. Abbasi, S.; Paul, A.; Prakash, S., Investigation of siRNA-Loaded Polyethylenimine-Coated Human Serum Albumin Nanoparticle Complexes for the Treatment of Breast Cancer. *Cell Biochemistry and Biophysics* 2011**,** *61* (2), 277-287.

3. Carrabino, S.; Di Gioia, S.; Copreni, E.; Conese, M., Serum albumin enhances polyethylenimine-mediated gene delivery to human respiratory epithelial cells. *The Journal of Gene Medicine* 2005**,** *7* (12), 1555-1564.

4. Rhaese, S.; von Briesen, H.; Rübsamen-Waigmann, H.; Kreuter, J.; Langer, K., Human serum albumin–polyethylenimine nanoparticles for gene delivery. *Journal of Controlled Release* 2003**,** *92* (1-2), 199-208.

5. Fischer, D.; Bieber, T.; Bru¨sselbach, S.; Elsa¨sser, H.-P.; Kissel, T., Cationized human serum albumin as a non-viral vector system for gene delivery? Characterization of complex formation with plasmid DNA and transfection efficiency. *International Journal of Pharmaceutics* 2001**,** *25*, 97-111.

6. Huckett, B.; Ariatti, M.; Hawtrey, A. O., Evidence for targeted gene transfer by receptor-mediated endocytosis. Stable expression following insulin-directed entry of NEO into HepG2 cells. *Biochem Pharmacol* 1990**,** *40* (2), 253-63.

7. Wagner, E.; Zatloukal, K.; Cotten, M.; Kirlappos, H.; Mechtler, K.; Curiel, D. T.; Birnstiel, M. L., Coupling of adenovirus to transferrin-polylysine/DNA complexes greatly enhances receptor-mediated gene delivery and expression of transfected genes. *Proc Natl Acad Sci U S A* 1992**,** *89* (13), 6099-103.

8. Eisele, K.; Gropeanu, R. A.; Zehendner, C. M.; Rouhanipour, A.; Ramanathan, A.; Mihov, G.; Koynov, K.; Kuhlmann, C. R.; Vasudevan, S. G.; Luhmann, H. J.; Weil, T., Fine-tuning DNA/albumin polyelectrolyte interactions to produce the efficient transfection agent cBSA-147. *Biomaterials* 2010**,** *31* (33), 8789-801.

9. Lochmann, D.; Weyermann, J.; Georgens, C.; Prassl, R.; Zimmer, A., Albumin-protamine-oligonucleotide nanoparticles as a new antisense delivery system. Part 1: physicochemical characterization. *Eur J Pharm Biopharm* 2005**,** *59* (3), 419-29.

10. Malone, R. W.; Felgner, P. L.; Verma, I. M., Cationic liposome-mediated RNA transfection. *Proc Natl Acad Sci U S A* 1989**,** *86* (16), 6077-81.

11. Lu, D.; Benjamin, R.; Kim, M.; Conry, R. M.; Curiel, D. T., Optimization of methods to achieve mRNA-mediated transfection of tumor cells *in vitro* and *in vivo* employing cationic liposome vectors. *Cancer Gene Ther* 1994**,** *1* (4), 245-52.

12. Kariko, K.; Kuo, A.; Barnathan, E., Overexpression of urokinase receptor in mammalian cells following administration of the *in vitro* transcribed encoding mRNA. *Gene Ther* 1999**,** *6* (6), 1092-100.

13. Zohra, F. T.; Chowdhury, E. H.; Tada, S.; Hoshiba, T.; Akaike, T., Effective delivery with enhanced translational activity synergistically accelerates mRNA-based transfection. *Biochem Biophys Res Commun* 2007**,** *358* (1), 373-8.

14. Bettinger, T.; Carlisle, R. C.; Read, M. L.; Ogris, M.; Seymour, L. W., Peptide-mediated RNA delivery: A novel approach for enhanced transfection of primary and post-mitotic cells. *Nucleic Acids Research* 2001**,** *29*, 3882-3891.

15. Zohra, F. T.; Chowdhury, E. H.; Nagaoka, M.; Akaike, T., Drastic effect of nanoapatite particles on liposome-mediated mRNA delivery to mammalian cells. *Anal Biochem* 2005**,** *345* (1), 164-6.

16. Fisher, K. J.; Wilson, J. M., The transmembrane domain of diphtheria toxin improves molecular conjugate gene transfer. *Biochem J* 1997**,** *321 (Pt 1)*, 49-58.

17. Strobel, I.; Berchtold, S.; Gotze, A.; Schulze, U.; Schuler, G.; Steinkasserer, A., Human dendritic cells transfected with either RNA or DNA encoding influenza matrix protein M1 differ in their ability to stimulate cytotoxic T lymphocytes. *Gene Ther* 2000**,** *7* (23), 2028-35.

18. Read, M. L.; Singh, S.; Ahmed, Z.; Stevenson, M.; Briggs, S. S.; Oupicky, D.; Barrett, L. B.; Spice, R.; Kendall, M.; Berry, M.; Preece, J. A.; Logan, A.; Seymour, L. W., A versatile reducible polycation-based system for efficient delivery of a broad range of nucleic acids. *Nucleic Acids Res* 2005**,** *33* (9), e86.

19. Su, X.; Fricke, J.; Kavanagh, D. G.; Irvine, D. J., *In vitro* and *in vivo* mRNA delivery using lipid-enveloped pH-responsive polymer nanoparticles. *Mol Pharm* 2011**,** *8* (3), 774-87.

20. Bachmann, M. F.; Jennings, G. T., Vaccine delivery: a matter of size, geometry, kinetics and molecular patterns. *Nature Reviews Immunology* 2010**,** *10* (11), 787-796.

21. O'Hagan, D. T.; Singh, M.; Ulmer, J. B., Microparticle-based technologies for vaccines. *Methods* 2006**,** *40* (1), 10-19.

22. Gratton, S. E. A.; Ropp, P. A.; Pohlhaus, P. D.; Luft, J. C.; Madden, V. J.; Napier, M. E.; DeSimone, J. M., The effect of particle design on cellular internalization pathways. *Proceedings of the National Academy of Sciences* 2008, *105* (33), 11613-11618.

23. Vignuzzi, M.; Gerbaud, S.; van der Werf, S.; Escriou, N., Naked RNA immunization with replicons derived from poliovirus and Semliki Forest virus genomes for the generation of a cytotoxic T cell response against the influenza A virus nucleoprotein. *J Gen Virol* 2001, *82* (Pt 7), 1737-47.

24. Hasan, W.; Chu, K.; Gullapalli, A.; Dunn, S. S.; Enlow, E. M.; Luft, J. C.; Tian, S.; Napier, M. E.; Pohlhaus, P. D.; Rolland, J. P.; DeSimone, J. M., Delivery of multiple siRNAs using lipid-coated PLGA nanoparticles for treatment of prostate cancer. *Nano Lett* 2012**,** *12* (1), 287-92